



UNIVERSITY OF LINCOLN

The Effect of Quinine Products on Tamoxifen Resistant Breast Cancer Cells

By

Jeremiah S Osei-Baidoo

Supervisors

Dr. Issam Hussain

Dr. Mohammed El-Sheemy

Dr. Csanad Bachrati

A thesis submitted to the University of Lincoln in partial fulfilment of the requirements of the degree of Master of Philosophy (M.Phil.)

December 2015

THIS WORK IS DEDICATED TO THE SOUL OF MY FATHER

AND TO MY MOTHER, BROTHERS AND SISTER FOR THEIR

LOVE AND SUPPORT

“VEL PRIMUS VEL CUM PRIMIS”

Acknowledgements

I would like to express my most sincere gratitude to my research project supervisory team, **Dr. Issam Hussain**, **Dr. Mohamed El-Sheemy** and **Dr. Csanad Bachrati** for their guidance with special thanks to **Dr. Issam Hussain** who has proven to be as much a brother and a friend as he has a mentor. I would also like to thank **Prof. Shamus Fagbemi** for his valued support.

I would also like to extend my sincere thanks to **Dr. Saraswati Sukumar** at Johns Hopkins University, USA for kind donation of the MCF7 tamoxifen resistant cell line that served a major role in this study

I am indebted to the steadfast and sure laboratory technicians **Angela** and **Beverly** for their constant support, cheerful demeanor and sage resourcefulness.

I would also like to thank **Adesola Badejo**, **Anastasios Sakis Karountzos**, **Daniel Cosgrove** and **Lewis Quayle** for their companionship and advice and wish them all the best in their future endeavors.

Declaration

The experimental procedures described in this report were carried out by the author in their entirety. I declare that this thesis and the work presented in it has been planned and generated by myself and my supervisors. I have acknowledged all main sources of help.

Research Publications

In Preparation:

- 1.) The Potentiative Effect of Chloroquine on Tamoxifen Resistant Breast Cancers

Table of Contents

Acknowledgements	2
------------------------	---

Declaration.....	3
i Abstract	7
ii List of Abbreviations	9
iii List of Figures	11
1.0 Introduction	16
1.1 Epidemiology of Breast Cancer	16
1.2 Aetiology of Breast Cancer	18
1.3 The Oestrogen Receptor (ER).....	22
1.3.1 ER in Cancer	26
1.3.2 ER Splice Variants	27
1.4 Genetic Risk	28
1.5 Breast Cancer Profiling	30
1.6 Diagnosis of Breast Cancer	33
1.7 Treatment.....	36
1.7.1 Chemotherapy.....	37
1.8 Tamoxifen.....	39
1.8.1 History of Tamoxifen	39
1.8.2 Properties of Tamoxifen	41
1.8.3 Tamoxifen in Cancer Therapy.....	42
1.9 <i>Chloroquine</i>	43
1.9.1 Properties of Chloroquine	44
1.9.2 Quinines in Cancer Therapy.....	45
1.10 <i>Drug Resistance</i>	46
1.10.1 Drug Combination and Resistance	48
1.2 Aims & Objectives.....	49
2.0 Materials and Methods.....	51
2.1 Materials.....	51
2.1.1 Safety Measures	51
2.1.2 General Equipment Required	51
2.1.3 Reagents used for cell culturing	52
2.1.4 Reagents and equipment used for cell counting.....	53
2.1.5 Reagents and equipment used for cryostorage	53
2.2 Methods	54
2.2.1 Safety note	54

2.2.1 Aseptic technique	54
2.2.2 a Culture media preparation	54
2.2.2 b Cell Culture Procedure	54
2.2.2 c Subculture	55
2.2.3 Cell Counting.....	56
2.2.4 Cryostorage and Recovery.....	58
2.2.5 Waste Disposal	59
2.2.6 MTT (3-(4,5-dimethylthiazol-2-yl)-2,5-diphenyltetrazolium bromide) Cytotoxicity Assay.....	59
2.2.7 Neutral Red Assay.....	63
2.2.8 Caspase 3 Colorimetry Assay.....	67
2.2.9 Annexin V ELISA.....	69
2.2.10 Acridine Orange Assay.....	73
2.2.11 Statistical Analysis	74
3.0 Results.....	76
3.0.1 Subculture & Counting	76
3.1 Quantitative Assay.....	78
3.1.1 MTT.....	78
3.1.2 Neutral Red.....	88
3.1.3 Caspase 3 Colorimetry Assay.....	98
3.1.4 Annexin V ELISA.....	100
3.2 Qualitative Assay	102
3.2.1 Neutral Red Microscopy	102
3.2.2 Acridine Orange Assay.....	107
4.0 Discussion	113
4.1 Cell Culture Characteristics.....	114
4.2 The Effect of Tamoxifen on Breast Cancer Cells.....	115
4.3 The Effect of Chloroquine on Breast cancer cells.....	120
4.4 The Combined Effect of Chloroquine and Tamoxifen on Breast Cancer Cells	123
4.5 Conclusion	126
5.0 Further Studies	128
6.0 References.....	132
7.0 Appendices	155

7.1 Appendix 1: 2way ANOVA with Dunnet’s multiple comparisons test for all MTT Assays against Control	155
7.2 Appendix 2: 2way ANOVA with Tukey’s multiple comparisons test for all MTT Assays; cross comparison.....	157
7.3 Appendix 3: 2way ANOVA with Dunnet’s multiple comparisons test for all MTT Assays against Control	164
7.4 Appendix 3: 2way ANOVA with Tukey’s multiple comparisons test for all MTT Assays; cross comparison.....	167
7.5 Appendix 4: Annexin V Standard Curve.....	172
7.6 Preliminary Combination Graphs	173

i Abstract

In the ongoing quest to further expand the repertoire of drugs for cancer therapy, sights have turned on the machinations of the anti-malarial drug, chloroquine as an untapped prospective drug for use in such treatments.

In order to establish the nature of chloroquine diphosphate (CQ) on differing breast cancers subtypes and to explore its relationship with tamoxifen (TAM) both in comparative effect and in conjunction, three phenotypically disparate cell lines were investigated; oestrogen receptor positive (ER⁺) MCF-7 WT, tamoxifen resistant subtype MCF-7 TMX and oestrogen receptor negative (ER⁻) MDA-MD-231. In order to establish a baseline, each cell line was investigated first independently with various concentrations of tamoxifen (2-30 μ M) and chloroquine (10-140 μ M) for 48 hours, the results of which were used to design a combined treatment modality to assay the effect of both drugs on the cells in tandem. The preliminary results showed that response to the initial two single drug treatment studies were dose dependent with lower concentrations of tamoxifen (2-10 μ M) and chloroquine (10-20 μ M) inhibiting growth and increasing vacuolation in all cell lines evidenced by increased uptake in Neutral Red (NR) stain and increased volume of acidic compartments (VAC). Higher treatment concentrations (12-32 μ M TAM, 40-120 μ M CQ) were seen to have a cytotoxic effect on all the cell lines in conjunction with a decrease in NR uptake and VAC. All three cell lines exhibited analogous response to CQ and singular treatment with tamoxifen resulted in similar dose-dependent responses albeit with higher doses of the drug necessary for MCF-7 TAM and MDA-MB-231 to develop any significant ($P \leq 0.05$, $n=3$) cytotoxic deviation. This effect on the ER⁻ and oestrogen resistant cell lines imply exogenous cytotoxic pathways independent of the oestrogen receptor. Combination treatment, using the same range of TAM with a static dose (10 μ M) Studies combining the two drugs were performed using the preliminary data as rationale for dosage. Using variable concentrations of tamoxifen (2-30 μ M) and keeping that of CQ (10 μ M) saw changes in cell morphology mimicking more closely that of high dose CQ treatment in qualitative NR and acridine orange (AO) staining from relatively low doses of TAM as well as substantially decreasing the ED₅₀ (minimum dosage to kill 50% of cells) in all cell lines. Caspase 3 colorimetry and Annexin V ELISA was used for the quantification of apoptosis and to help determine the mechanism of cell death utilised by these drugs and implied Caspase

dependent apoptosis was occurring alongside the more visible caspase-independent cytotoxic events.

The results suggest that CQ may potentiate cell death of breast cancer cells treated with tamoxifen through the abrogation of autophagy and potentially re-sensitising resistant and ER⁻ cells to hormone therapy treatment.

ii List of Abbreviations

4-OHT	4-Hydroxytamoxifen
Ac-DEVD-pNA	Acetylate-Asp-Glu-Val-Asp p-nitroanilide
AF(1,2)	Activating Function

AO	Acridine Orange
ATCC	American Type Cell Association
BRCA	Breast Cancer Early Onset Gene
CK	Cytokine
CQ	Chloroquine
CSC	Cancer Stem Cells
CT	Computed Tomography
DBD	DNA Binding Domain
DCIS	Ductal Carcinoma <i>in situ</i>
DMSO	Dimethyl Sulfoxide
DNA	Deoxyribonucleic Acid
ED ₅₀	Effective dose necessary to kill 50% of sample population
EGFR	Epidermal Growth Factor
ELISA	Enzyme Linked Immunosorbant Assay
ER ⁺	Oestrogen Receptor Positive
ER ⁻	Oestrogen Receptor Negative
ERE	Oestrogen Responsive Element
FCS	Foetal Calf Serum
HBD	Hormone Binding Domain
HeR1	Human Epidermal Growth Factor 1
HeR2	Human Epidermal Growth Factor 2
IC ₅₀	Inhibitory Concentration 50
IHC	Immunohistochemistry
JAK2	Janus Kinase 2
LDH	Lactate Dehydrogenase
MCF-7	Michigan Cancer Foundation-7 Adenocarcenoma
MDA-MB-231	MD Anderson Metastatic Breast cancer cell line
MDR	Multidrug Resistance
MTS	3-(4,5-dimethylthiazol-2-yl)-5-(3-carboxymethoxyphenyl)- 2-(4-sulfophenyl)-2H-tetrazolium
MTT	3-(4,5-dimethylthiazol-2-yl)-2,5-diphenyltetrazolium bromide
NHS	National Health Service
NR	Neutral Red

PBS	Phosphate Buffered Saline
PDT	Population Doubling Time
PET	Positron Emission Tomography
P-gp	P-glycoprotein
PR	Progesterone Receptor
PS	Phosphatidyl Serine
PTEN	Phosphatase and Tensin homolog
SC	Stem Cells
SERM	Selective Oestrogen Receptor Modulator
STK	Serine-Threonine Kinase
SPSS	Statistical Package for the Social Sciences
TDLU	Terminal Duct Lobular Unit
TMX	Tamoxifen Resistant
UK	United Kingdom
WT	Wild-Type

iii List of Figures

Figure 1.1: The continuum of cancer development (Adapted from Caldas, 2012). The grey circle represents a normal cell, the dotted grey circle represents the initiating somatic mutation and the coloured circles represent accumulative generations with individual characteristics and oncogenotypes. 19

Table 1.1: Epidemiological risk factors for breast cancer, association: ++++ very strong; +++ strong, ++ modest, + weak. 21

(Adapted from Trichopoulos et al, 2008).....	21
Table 1.2: The “Classic” Intrinsic Gene List; illustrating 5 known subtypes of breast cancer with respects to the presence of specific markers. ER, Oestrogen Receptor, PR, Progesterone Receptor; Her2, Human endothelial growth factor receptor 2; CK (Cytokine) 5/6, Cytokeratin 5 and 6; EGFR, Epidermal growth factor (Adapted from Kwan et al, 2009).	22
Fig 1.2 Illustrating the distribution of ER α & ER β in the human body. Adapted from Pearce & Jordan, 2004.	23
Fig. 1.3: The structure and function of oestrogen receptors.....	25
Table 1.3: Characteristics of Molecular Subtypes (Stanford and new subtypes); illustrating 5 known subtypes of breast cancer, (Adapted from Alizart et al., 2012).....	33
Figure 1.4: Comparison of X-ray Mammography vs. MRI (A) Negative X-ray mammogram of 43-year old woman. (B) contrast enhanced MRI of the same breast identifying multifocal carcinoma (C) saggital X-ray mammogram revealing abnormal tissue density. (D) contrast enhanced MRI of same patient identifying (Morrow et al, 2011; Davies, 2012)	34
Figure 1.5: The effect of antitumor antibiotics on different phases of the cell cycle, adapted from Brown et al (2011)	37
Figure 1.6: Oestrogen with antioestrogen competitors, Clemons et al, 2002.	40
Figure 1.7: Mode of action of oestradiol and tamoxifen. Clemons et al, 2002	41
Figure 1.7: Molecular Structure of Chloroquine	43
Figure 1.8: The progress of macroautophagy in mammalian cells (Mizushima, 2007).....	45
Figure 2.1: The gridlines of a haemocytometer chamber. 16 squares make up each corner quadrant (blue) in a chamber. (Abcam 2015)	57
Figure 2.2: Preliminary MTT schematic for tamoxifen schematic. Blue line – dH ₂ O; C – control with complete medium blank, figures – drug concentration (μ M), B- Empty blank	60
Figure 2.3: Plate freshly set up for preliminary MTT testing. Peripheral wells filled with basal medium to protect the central wells from desiccation.	60
Figure 2.4: Typical template for drug combination assay. Blue = dH ₂ O, Black Figures = tamoxifen (μ M) Red Figures = chloroquine (μ M). Note all doses are done in triplicate.....	63
Table 2.1: Illustrating the minimum work required for both MTT and Neutral Red evaluation of the breast cancer cell lines.	63
Figure 2.5: Visual colorimetric difference between seeding densities for chloroquine with MCF-7 WT after 4 hours	65
Figure 2.6: General seeding layout for cells in 6 well plate for c3pNA colorimetry assay	68
Figure 2.7: Showing the plate scheme for the 96 well plate Caspase 3 analysis.	69
Table 2.2: 96 well plate microarray reaction scheme.	69
Figure 2.8: The 12 well microplate cell culture template used in cell culture for the Annexin V ELISA assay.	71
Figure 2.9: The ELISA strip layout for Annexin V assay. This is repeated in duplicate.	71
WT = MCF-7 WT.....	71
TMX = MCF-7 TMX MDA = MDA MB 231	71

Figure 3.1: MCF-7 WT with grape-cluster morphology typical of luminal breast cancer cells after four days of culture. Magnification x10.....	77
Figure 3.3: MDA-MB-231 cell line with characteristic invasive processes, four days after culture. Magnification x10.....	77
Figure 3.2: MCF-7 TMX cell line with four days after culture. Magnification x10	77
Table 3.1: Doubling times of the three cell lines MCF-7 WT, MCF-7 TMX and MDA-MB-231 as extrapolated from proliferation assay (\pm SE, n=3)	78
Table 3.2: ED ₅₀ values for MTT assay of each cell line with drug modalities TAM, CQ & TCQ	78
Figure 3.4: MTT cytotoxicity assay showing the effect of tamoxifen on MCF-7 WT (\pm SE, n=3). ED ₅₀ concentration reads at 15.4 μ M of tamoxifen. Signal fall significantly from 14 μ M onwards. There is near 100% cell death by 22 μ M ...	79
Figure 3.5: MTT cytotoxicity assay showing the independent effect of chloroquine on MCF-7 WT (\pm SE, n=3). The ED ₅₀ concentration reads at 52 μ M of chloroquine.	80
Figure 3.6: MTT cytotoxicity assay showing the combined effect of tamoxifen and chloroquine on MCF-7 WT (\pm SE, n=3 For this assay, the concentration of chloroquine is a static 10 μ M. The ED ₅₀ concentration reads at 12 μ M of tamoxifen.	81
Figure 3.7: MTT cytotoxicity assay showing the independent effect of tamoxifen on MCF-7 TMX (\pm SE, n=3). ED ₅₀ concentration reads at 18 μ M of tamoxifen.	82
Figure 3.8: MTT cytotoxicity assay showing the effect of chloroquine on MCF-7 TMX (\pm SE, n=3). ED ₅₀ concentration reads at 72 μ M of chloroquine.....	83
Figure 3.9: MTT cytotoxicity assay showing the combined effect of tamoxifen and chloroquine on MCF-7 TMX (\pm SE, n=3). ED ₅₀ concentration reads at 11.8 μ M of tamoxifen.	84
Figure 3.10: MTT cytotoxicity assay showing the independent effect of tamoxifen on MDA-MB-231 (\pm SE, n=3). ED ₅₀ concentration reads at 18.5. μ M of chloroquine.	85
Figure 3.11: MTT cytotoxicity assay showing the independent effect chloroquine on MDA-MB-231 (\pm SE, n=3). ED ₅₀ concentration reads at 44 μ M of chloroquine.	86
Figure 3.12: MTT cytotoxicity assay showing the combined effect of tamoxifen and chloroquine on MDA-MB-231 (\pm SE, n=3). Chloroquine kept as a static dose of 10 μ M. The ED ₅₀ concentration reads at 12 μ M of tamoxifen.	87
Figure 3.13: NR viability assay showing the effect of tamoxifen on MCF-7 WT (\pm SE, n=3). Peaking becomes evident at 12 μ M tamoxifen	89
Figure 3.14: NR viability assay showing the effect of Chloroquine on MCF-7 WT (\pm SE, n=3). Peaking becomes evident after the first dose at 10 μ M of Chloroquine.	90
Figure 3.15: NR viability assay showing the effect of variable doses of tamoxifen (μ M) with a static concentration (10 μ M) of chloroquine on MCF-7 WT (\pm SE, n=3). Peaking becomes evident after the first dose at 10 μ M of Chloroquine.	91
Figure 3.16: NR viability assay showing the effect of tamoxifen on MCF-7 TMX (\pm SE, n=3). Signal increases immediately after the first dose at 2 μ M of TAM and peaks at 8 μ M of TAM.....	92

Figure 3.17: NR viability assay showing the effect of chloroquine on MCF-7 TMX (\pm SE, n=3). Signal increases immediately after the first dose at 10 μ M of TAM and peaks at 40 μ M of TAM	93
Figure 3.18: NR viability assay showing the effect of chloroquine on MCF-7 TMX (\pm SE, n=3). Signal increases immediately after the first dose at 10 μ M of TAM and peaks at 40 μ M of TAM	94
Figure 3.19: NR viability assay showing the effect of tamoxifen on MDA-MB-231 (\pm SE, n=3). Signal increases immediately after the first dose at 10 μ M of TAM and peaks at 40 μ M of TAM	95
Figure 3.20: NR viability assay showing the effect of chloroquine on MDA-MB-231 (\pm SE, n=3). Signal increases immediately after the first dose at 10 μ M of TAM and peaks at 40 μ M of TAM	96
Figure 3.21: NR viability assay showing the effect of chloroquine (10 μ M) with a variable dosage of tamoxifen on MDA-MB-231 (\pm SE, n=3). Signal increases immediately to peak after the first dose at 2 μ M of TAM.....	97
Figure 3.22: Relative caspase 3 activity after 48 hours' treatment with the 3 drug modalities on breast cancer cell lines MFC-7 WT, MCF-7 TMX and MDA-MB-231 with their respective ED ₅₀ dosage values. (C: control; T: tamoxifen; CQ: chloroquine; TCQ: tamoxifen/chloroquine combination)	99
Figure 3.23: Relative Annexin V activity after 48 hours' treatment with the 3 drug modalities on breast cancer cell lines MFC-7 WT, MCF-7 TMX and MDA-MB-231 with their respective ED ₅₀ dosage values. (C: control; tamoxifen; CQ: chloroquine; TCQ: tamoxifen/chloroquine combination)	101
Figure 3.24: Neutral Red panel of control samples for MCF-7 WT, TMX and MDA, very low yet present neutral red uptake visible within cells indicating low lysosomal activity. Magnification x10	103
Figure 3.25: Panel illustrating the effect of TAM (A,B,C) CQ (D,E,F) and TCQ (G,H,I) on lysosomal profile of MCF-7 WT cells with Neutral Red. The cells were treated with TAM, 8, 16 and 24 μ M; 10, 40, 80 μ M; and TCQ 8, 16 and 24 μ M TAM with a static dose of 10 μ M Chloroquine. Cell death was most apparent in all rightmost slides with minimal NR retention. The richest lysosomal signal per-cell is visible in the ED ₅₀ (centremost slides) in dead cells are also present. (x10).....	104
Figure 3.26: Panel illustrating the effect of TAM (A,B,C) CQ (D,E,F) and TCQ (G,H,I) on lysosomal profile of MCF-7 TMX cells with Neutral Red. The cells were treated with TAM, 8, 16 and 24 μ M; 10, 40, 80 μ M; and TCQ 8, 16 and 24 μ M TAM with a static dose of 10 including controls (not pictured). Cell death and was most apparent in all rightmost slides with minimal NR retention. The richest lysosomal signal per-cell is visible in the ED ₅₀ (centremost slides) in dead cells are also present. (x10)	105
Figure 3.27: Panel illustrating the effect of TAM (A,B,C) CQ (D,E,F) and TCQ (G,H,I) on lysosomal profile of MDA-MB-231 cells with Neutral Red. The cells were treated with TAM, 8, 16 and 24 μ M; 10, 40, 80 μ M; and TCQ 8, 16 and 24 μ M TAM with a static dose of 10 including controls (not pictured). Cell death and was most apparent in all rightmost slides with minimal NR retention. The richest lysosomal signal per-cell is visible in the ED ₅₀ (centremost slides) in dead cells are also present. (x10)	106
Figure 3.28: Acridine Orange panel of control samples for MCF-7 WT, TMX and MDA, monochromatic appearance of slides indicates low-volume of acidic compartments without drug treatment. Magnification x10	108

Figure 3.29: Panel illustrating the effect of TAM (A,B,C) CQ (D,E,F) and TCQ (G,H,I) on lysosomal profile and nuclear fragmentation of MCF-7 WT cells With Acridine Orange. The cells were treated with TAM, 8, 16 and 24 μM ; 10, 40, 80 μM ; and TCQ 8, 16 and 24 μM TAM with a static dose of 10 including controls (not pictured). Cell death and nuclear fragmentation was apparent in all rightmost slides. The greatest lysosomal signal is visible in the ED₅₀ (centremost slides) and especially in the samples treated with CQ (D-I) in which nuclear fragmentation is also apparent. (x10) 109

Figure 3.30: Panel illustrating the effect of TAM (A,B,C) CQ (D,E,F) and TCQ (G,H,I) on lysosomal profile and nuclear fragmentation of MCF-7 TMX cells with Acridine Orange. The cells were treated with TAM, 8, 16 and 24 μM ; 10, 40, 80 μM ; and TCQ 8, 16 and 24 μM TAM with a static dose of 10 including controls (not pictured). Cell death and nuclear fragmentation was apparent in all rightmost slides. The greatest lysosomal signal is visible in the ED₅₀ (centremost slides) in which nuclear fragmentation is also apparent. (x10). 110

Figure 3.31: Panel illustrating the effect of TAM (A,B,C) CQ (D,E,F) and TCQ (G,H,I) on lysosomal profile and nuclear fragmentation of MDA-MB-231 cells with Acridine Orange. The cells were treated with TAM, 8, 16 and 24 μM ; 10, 40, 80 μM ; and TCQ 8, 16 and 24 μM TAM with a static dose of 10 including controls (not pictured). Cell death and nuclear fragmentation was apparent in all rightmost slides. The greatest lysosomal signal is visible in the ED₅₀ (centremost slides) in which nuclear fragmentation is also apparent. (x10). 111

Figure 7.1: MTT cytotoxicity assay highlighting the difference in response in the combined effect of tamoxifen and chloroquine on MCF-7 WT with different doses of chloroquine ($\pm\text{SE}$, n=3). WTxT – No CQ, WTxTCQ – 10 μM CQ, WTxTCQ40 – 40 μM CQ. The ED₅₀ concentrations read at 16 μM of tamoxifen for WTxT, 12 μM for WTxTCQ and 1 μM for WTxTCQ40. 173

Figure 7.2: MTT cytotoxicity assay highlighting the difference in response in the combined effect of tamoxifen and chloroquine on MCF-7 TMX with different doses of Chloroquine ($\pm\text{SE}$, n=3). WTxT – No CQ, WTxTCQ – 10 μM CQ, WTxTCQ40 – 40 μM CQ. The ED₅₀ concentration reads at 18 μM of tamoxifen for TMXxT, 15 μM for TMXxTCQ and 2.5 μM for TMXxTCQ40. 176

Figure 7.3: MTT cytotoxicity assay highlighting the difference in response in the combined effect of tamoxifen and chloroquine on MDA-MB-231 with different doses of Chloroquine. WTxT – No CQ, WTxTCQ – 10 μM CQ, WTxTCQ40 – 40 μM CQ. The ED₅₀ concentration reads at 19 μM of tamoxifen for MDAXT, 12 μM for MDAXTCQ and 2.5 μM for MDAXTCQ40. 177

Chapter One

Introduction to Breast Cancer

1.0 Introduction

1.1 Epidemiology of Breast Cancer

Although sexually biased in nature, breast cancer has remained the most common cancer in the United Kingdom (UK) since 1997 (CancerResearchUK,

2010), only occurring very infrequently in males (<400/year) yet accounting for 31% of all new cancer incidences in females at a staggering rate of approximately 50,000 new cases *per annum*. This pattern is observed worldwide with 1.3 million annual new diagnoses and 465,000 deaths subsequent to the disease (Lloyd Davies, 2012).

Extensive documentation of the disease has led to suggest a strong correlation with the increased incidence of disease and age; in the UK, 80% of all new diagnoses occur in women over 50 years of age with incidence rates rising steeply up until its peak at the 85+ age group (CancerResearchUK, 2010). This pattern can be observed globally, with 89% of breast cancers diagnosed from the age of 40 onwards with a marked disparity between that of more economically developed countries (95% of cancers >40 years) vs. less economically developed countries (84% of cancers >40 years) which has been attributed to a number of factors, particularly in differences in that of lifestyle; variances in population levels of obesity, alcohol consumption, hormone replacement therapy and age of primary pregnancy and breast feeding status are all taken into consideration (Youlten *et al*, 2012).

Relative breast cancer survival rates for the United Kingdom collated from a 2005-2009 cohort study made available by Breast Cancer Research UK (2010) have shown that 95.8% of women newly diagnosed are expected to survive at least one year. Subsequent 5 and 10 year evaluations show this figure falling to 85.1% and 77.0% respectively due to late recurrences and metastatic disease (Youlten *et al*, 2012)

In conjunction to typical cancer treatment through remedial surgical excision of aberrant tissue, adjuvant care regimes such as hormone therapy, radiation and chemotherapy exist; the purpose of which is to downgrade and downstage (Kaminsky-Forrett *et al*, 1998) existing neoplasia either prior surgery, the 'neoadjuvant' approach (Chuthapisith *et al*, 2006), or post-surgically as a prophylactic measure to ensure the removal of as much aberrant tissue as possible (Cionini *et al*, 1996). Multiple adjuvant therapies can be used concurrently or sequentially for a more positive survival prognosis, the efficacy of which has been recognised and deliberated at length by many researchers (Peters *et al*, 2000; Zhang *et al*, 2009; Bedognetti *et al*, 2011).

A large percentage of patients do not respond well to neoadjuvant chemotherapy, with less than 30% of cancer patients responding completely to treatment (Chuthapisith *et al*, 2006); in 2009 a reported 11,728 patients died in the UK as a result of complications from breast cancer (CancerResearchUK, 2016). Resistance to chemotherapeutic drugs is inevitable in most cases and is corollary with poor treatment response, subsequent remission and death. It is for this reason that most administered treatments are of a combined nature, with several classes of agents used at a time in an attempt to elongate the period between clinical efficacy and resistance (Bhosle & Hall, 2009). For this and other (socioeconomic) reasons, new chemotherapeutic analogues and classes are constantly being investigated to expand and sustain the current repertoire.

Chloroquine (CQ) is one such drug that is now under the spotlight as having potential in chemotherapeutic medicine. Due to the emergence of CQ-resistant *Plasmodium falciparum*, it has been largely discontinued in many countries as an antimalarial drug (Ginsburg, 2005; Gharbi *et al*, 2013) in favour of newer therapies for example, artemisinin-based combination therapy. Understanding and on-going research into the properties of CQ have led us to believe that it may hold some qualitative chemotherapeutic value in the potentiation of existing chemotherapeutic drug action through its unique mechanisms of lysosomotrophy and subsequent autophagy abrogation (Solomon & Lee, 2009).

The pharmacodynamic relationship between the widely used anti-oestrogen chemotherapeutic agent tamoxifen and CQ is largely unknown. It is the purpose of this investigation to test the effect of CQ, if any on hormone-responsive (Levenson & Jordan, 1997) breast cancer cell line MCF-7 and in combination with tamoxifen in order to establish the mechanism of action and to explore whether or not CQ has any ability to potentiate the chemotherapeutic effects of tamoxifen.

1.2 Aetiology of Breast Cancer

The Cell Cycle

Although perhaps not yet understood in its entirety, the aetiological model for breast cancer is one that is constantly evolving as new ideas, concepts and findings have come to light. Studies documented on the aetiology of breast cancer from through by epidemiological studies that govern risk such as gender, age and weight has also contributed greatly to the aetiological model. *Table 1.1* lends a summarized view of many of the known risk factors with indication to relative strength and risk of cancer. The basic understanding on the developmental biology of breast cancer is almost always attributed to the (somewhat ambiguous) somatic mutation of a single cell/group of cells and may be expressed as a singular continuum and has been summarised in **Figure1.1**.

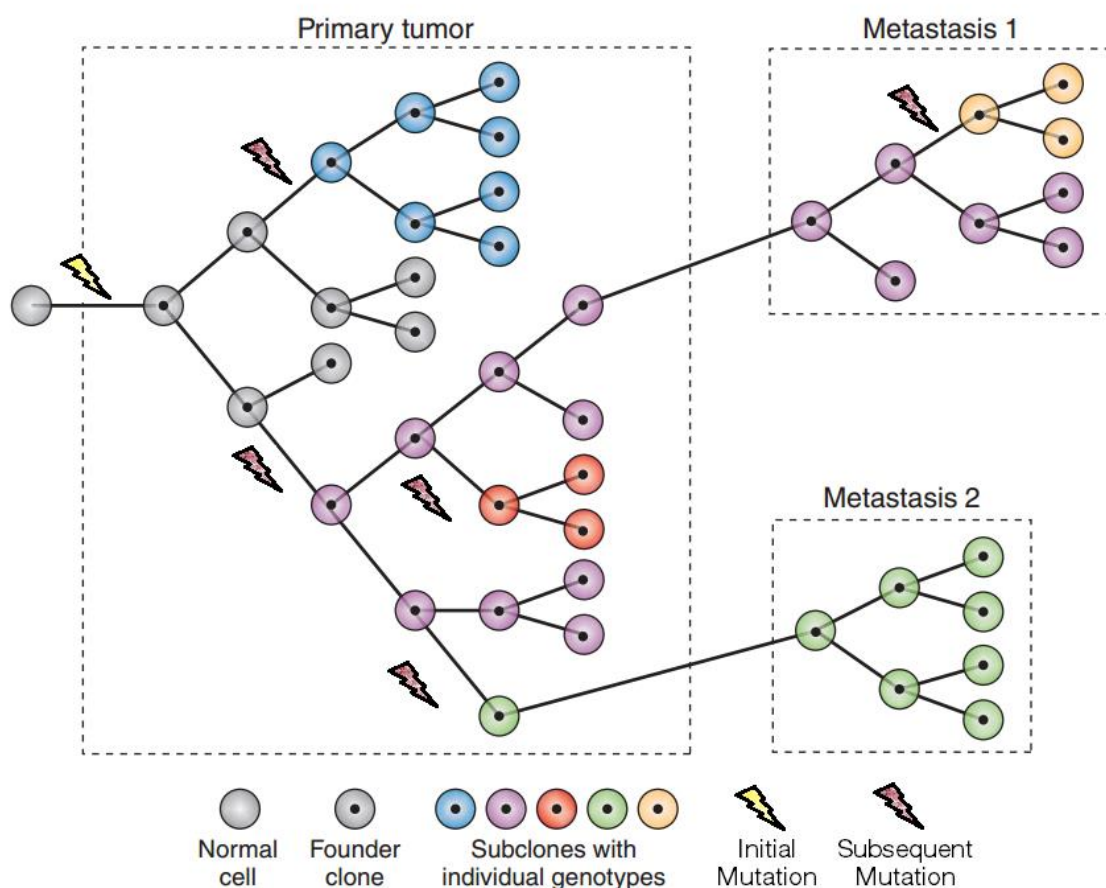


Figure 1.1: The continuum of cancer development (Adapted from Caldas, 2012). The grey circle represents a normal cell, the dotted grey circle represents the initiating somatic mutation and the coloured circles represent accumulative generations with individual characteristics and oncogenotypes.

On brought forward by Adami, Trichopoulos and collaborators in their multiple publications over the past two decades (1995, 1998, and 2008). Their model collates what

we know about the epidemiological factors of breast cancer into three distinct components which emphasise the early life circumstances and determinants of breast cancer, these components include:

- i.) Mammary Gland Mass-** The likelihood of breast cancer depends on the number of mammary tissue-specific cells determined in the intrauterine period of life; the mammographic mass of the mammary glands may infer the total number of mammary cells (Kuchiki *et al*, 2010), this first component can be substantiated by evidence such as the disparity of incidence of the disease between Western and Asian populations (Huang *et al*, 2009) and even between that of man and woman.
- ii.) Growth Hormone levels-** Much investigation has been undergone in ascertaining the roles between growth hormones such as oestrogens and progesterone in breast cancer (Hulka & Moorman, 2001; Da Silva & Lakhani, 2010; Adami *et al*, 1995, 1998, 2008; Gusterson & Stein, 2012). Growth factors and hormones are responsible for the replication of mammary tissue and specific progenitor cells, they increase the likelihood of retaining cells with spontaneous somatic mutations as well as the expansion of initiated clones making marked or atypical levels of such hormones through developmental stages increase the risk of cancer. Growth hormone levels may be directly correlated with the increased risk of breast cancer in taller individuals (Cold *et al*, 1998)
- iii.) Terminal Differentiation-** Pregnancy is known to convey a long-term protection through the differentiation of a large proportion of mammary-tissue specific progenitor cells (Trichopoulos *et al*, 2008; Gusterson & Stein, 2012). It is thought that the later a woman becomes pregnant, the higher the number of cells would have already initiated, thus the less protection she would gain. Additionally, this protection is a double-edged sword due to the natural increase of mammatropic hormones during pregnancy, which as Trichopoulos (2008) put it would overshadow the terminal

differentiation of mammary cells. This could be the reason why the risk women in more developed countries who choose to set up a family later on in life (past the age of 35) is higher than nulliparous individuals.

This model further differentiates the factors of the epidemiological risk previously listed in *Table 1.1* depending on their relationship to general principles of carcinogenesis, number of mammary tissue specific progenitor cells, growth enhancing mammotropic hormones and terminal differentiation of the tissue.

Risk factor	Category/change	Strength
Gender	Women vs. men	++++
Age	Increase	++++
Ethnic group	Caucasian vs. Asian	+++
Family history	Yes vs. no	+++
Specific genes	Yes vs. no	++++
Cancer in other breast	Yes vs. no	+++
Height	Increase	++
Birth weight	Increase	+
Growth in early life	Increase	+
Mammographic density (mammary gland mass)	High vs. low density (increasing mass)	+++
Age at menopause	Later	++
Type of menopause	Natural vs. artificial	++
Age at 1st full term pregnancy	Later	+++
Age at other pregnancies	Later	+
Parity overall	Lower	++
Plant foods and olive oil	Reduced intake	+
Saturated fat	Increased intake	+

Table 1.1: Epidemiological risk factors for breast cancer, association: ++++ very strong; +++ strong, ++ modest, + weak. (Adapted from Trichopoulos et al, 2008)

Further research into the perinatal, infant and adolescent periods and their relationship with the aetiology of breast cancer has been done by other investigators expanding the current base of risk factors. Ruder and colleagues (2008) have collated together scores of cohort studies into the links between factors such as gestational age, birth weight and length along with other

childhood statistics and lifestyle to ascertain their relevance to which they found an inverse correlation in gestational age and a positive correlation in birth weight and length. Research into the clinical and molecular nature of breast cancer utilising cDNA microarrays and immunohistochemical (IHC) assays have been used to classify breast cancer into that of five distinct subtypes based on expression (or lack thereof) of cellular markers:

BC Subtype	ER	PR	HER2	CK 5/6	EGFR
Luminal A	+	+/-	-	-	-
Luminal B	+	+/-	+	-	-
Her2 Overexpressing	-	-	+	-	-
Basal-like	-	-	-	+	+
Normal-like	n	n	N	N	N

Table 1.2: The “Classic” Intrinsic Gene List; illustrating 5 known subtypes of breast cancer with respects to the presence of specific markers. ER, Oestrogen Receptor, PR, Progesterone Receptor; Her2, Human endothelial growth factor receptor 2; CK (Cytokine) 5/6, Cytokeratin 5 and 6; EGFR, Epidermal growth factor (Adapted from Kwan et al, 2009).

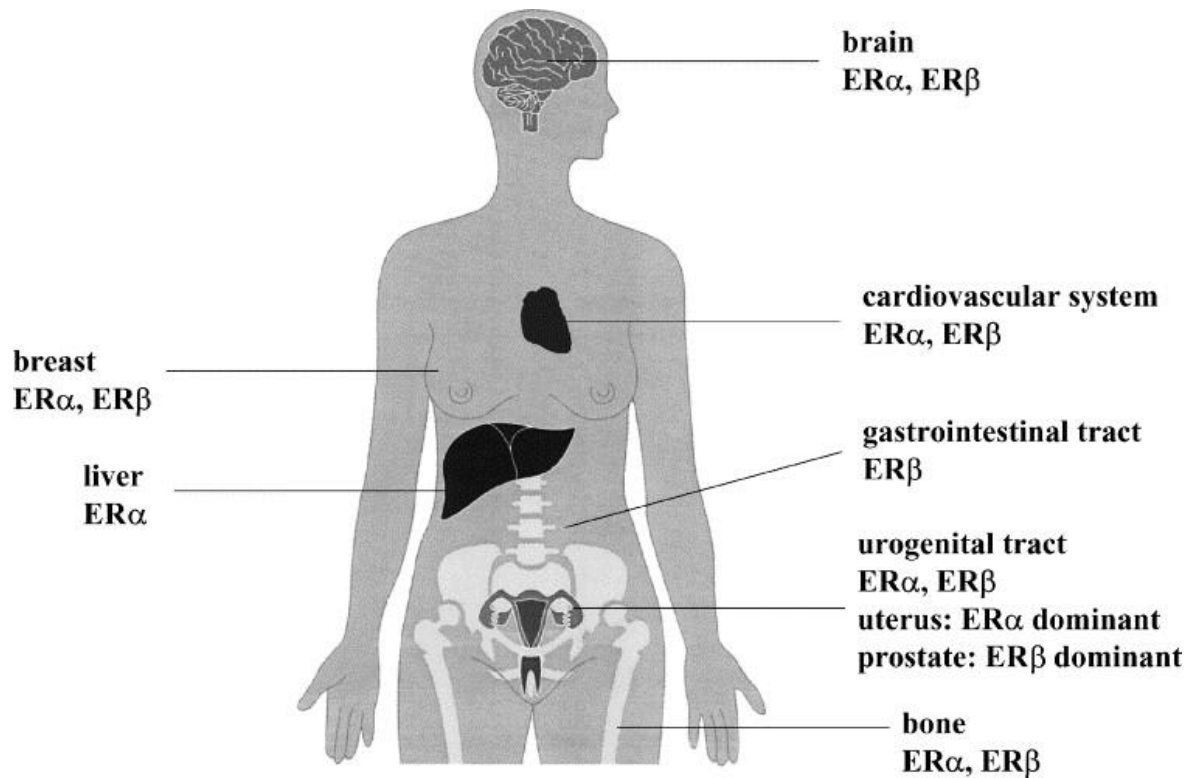
Approximately 70% of ‘triple-negative’ breast cancers express basal markers thus triple negative subtype may often be used as an indicator for the basal-like subtype.

According to the highly accessed epidemiological research article published by Kwan and colleagues (2009), luminal tumours are more often associated with more favourable outcomes to its sister subtypes such as Her2-overexpressing, basal-like and otherwise triple negative tumours which are associated with much poorer prognoses. 15% of all invasive breast cancers in the United States can be attributed to the triple negative subtype, which is often associated with the African-American demographic, patients presenting at younger ages of the disease, more advanced grading and staged cancers, diseases with higher mitotic indices and those with a familial history of breast cancer.

1.3 The Oestrogen Receptor (ER)

Steroid hormone receptors such as oestrogen receptors (ER) and progesterone receptor modulate the transcription of target genes when bound

to their respective ligands to modulate physiological processes such as reproductive organ development and function, and bone density (Pearce & Jordan, 2004).



O

Fig 1.2 Illustrating the distribution of ER α & ER β in the human body.
Adapted from Pearce & Jordan, 2004.

Oestrogen receptors exist as two characteristic subtypes, ER α & ER β ; the abundance and distribution of which, determines the effect of the binding ER ligand on the target tissues. Oestradiol (E₂, the most potent and bioavailable of the three major cholesterol derived naturally synthesised oestrogens), has a large and diverse functional role, not only in female reproductive functions but also in the mediation of many metabolic processes in various tissues of the body (Figure 1.1) such as cell growth, pubescence and epiphyseal plate closure (Weise *et al*, 2001; Janfaza *et al*, 2006), cell differentiation as well as intricate roles in the metabolic processes of the liver, brain, linear bone growth, cardiovascular system and the regulation of male physiology (Ascenzi *et al*, 2006). Target tissues which express a higher level of ER are predicted to produce a greater response to the presence of ER ligands (Pearce & Jordan, 2004). Further plasticity for the cell's response to oestrogens is brought about by the fluid mobility of the oestrogen receptor which is able to migrate spontaneously intracellularly between the membranes of the organelles, for instance, between the nucleus and the plasma membrane allowing for oestrogens to generate different and synergetic signal transduction pathways on both a genomic and non-genomic level (Ascenzi *et al*, 2006; Gouglet *et al*, 2007). Work done with the 'knockout mouse' (KO) model, *i.e.* transgenic mice where the genes pertaining to the protein/molecule of interest (in this case, ER α & β) has been performed to demonstrate the different effects and sensitivities of oestrogen on target tissues and organ systems, including the male and female reproductive tract, mammary gland, bone and the phenotypic changes that it incurs (Couse *et al*, 2000; Curtis Hewitt *et al*, 2000; Pearce & Jordan, 2004).

Through their interplay at the receptor expression and signalling level, oestrogens play an integral part in the modulation of growth hormone (GH) which plays a fundamental role in the regulation of growth and development of the body (Leung *et al*, 2010). Oestrogen and GH levels are tightly correlated during puberty, with increases in oestrogen levels such as those observed during the periovulatory phase resulting in a similar marked increase in GH; the administration of exogenous oestrogen is also seen to cause an increase in circulating GH, however, it has been found that depending on the route of

administration the exogenous E₂ is found to dissociate the growth hormone/insulin-like growth factor-1 (IGF-1) axis, resulting in a marked decrease in the metabolic activity of peripheral tissues as is the case with orally administered oestrogen (Leung *et al*, 2010).

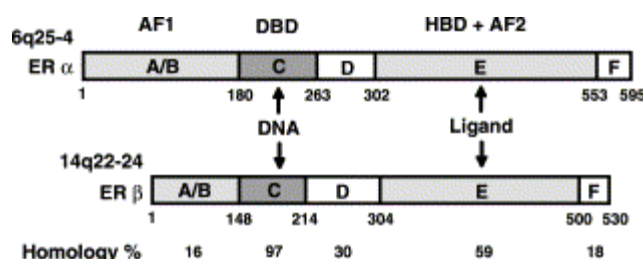


Fig. 1.3: The structure and function of oestrogen receptors

Figure 1.3 highlights the structure of the oestrogen receptors; oestrogen receptors consist of 6 domains (A-F, F being a domain exclusive to the ERs which are members of the nuclear receptor superfamily of which domains A-E are common). Oestrogens bind to the hormone binding domain (HBD) which in turn causes a trans-conformational change of the molecule in which unmasks activating function 1 (AF1) within the A/B domain through the removal of chaperone protein HSP90, receptor dimerization and activation of activating function 2 (AF2) which resides within the C-terminus of the domain. This allows DNA binding domain (DBD) C to then bind to oestrogen-responsive elements (ERE) on target genes. The ERE-bound ER-dimers modulate the transcription of target proteins through the interaction of co-activators and co-expressors. (Platet *et al*, 2004)

The role of ER and its ligands in the development of normal breast tissue have been shown to be crucial from the embryonic state with maternal oestrogen levels governing the degree of development of aforementioned tissue at birth (Gusterson & Stein, 2012). Low levels of oestrogen receptor have been reported in the luminal cells of pre-pubertal/perimenarchal glands of females, however due to available profiles being based on limited, post mortem tissues, may not be representative of ER profile of periadolescent breast tissue status *in vivo*. The work done on ERα & -β knockout mice (αβERKO, βERKO & αERKO models respectively) show that pubertal mammary development does not occur without the presence ERα, thus expressing its importance in

mammary development (Pearce & Jordan, 2004; Gusterson & Stein, 2012), furthermore in these studies, ER β was found to be integral for fertility in female mice, especially follicular maturation, yet extraneous to mammary growth, leaving its role in the physiology of breast in question (Shyamala *et al*, 2000).

1.3.1 ER in Cancer

Due to the aforementioned effects of oestrogens on the facilitation of cell proliferation, ERs thus have a very involved relationship when present in proliferative disease of the breast. It has been long understood that the agonistic interaction of oestrogens with ER α resulting in a direct increase in cell proliferation; increasing the number of G0/G1 cells entering the cell cycle *in-vitro* (Cullen *et al*, 2001; Pearce & Jordan, 2004; Platet *et al*, 2004) and thus is a strong prognostic and predictive marker for endocrine therapy for the clinical management of the disease (Mandusic *et al*, 2012). Understanding the relationship between ER α and breast cancer has led to the development of endocrine treatments as a means of treating hormone responsive breast cancers (Pearce & Jordan, 2004) and will be discussed at length in a later chapter. Conversely, it has been described in recent literature that ER β agonists elicit inhibitory effects on hormone-dependent tumours (Lattrich *et al*, 2013) which has promising implications in future avenues of hormone mediated breast cancer control.

In addition to the discussed wild-type oestrogen receptors, numerous splice variants have been identified for both ER α and ER β and have found to be frequently co-expressed with their wild-type counterparts (Ascenzi *et al*, 2006), moreover, several splice variants of ER α have been found in a variety of tissues and disease states including, intriguingly, ER- classified breast cancer (Herynk & Fuqua, 2004). The most common splice variants of both ERs may exhibit frame deletion mutations, specifically of exons 3, 4 or both although many other truncations and insertions along the coding gene have also been characterised; the mRNA expression of many ER β isoforms are in fact found in

higher quantities in human breast tissues than their wild-type variant with much documented evidence to suggest the possibility of protein expression of several isoforms of ER β *in vivo* (Herynk & Fuqua, 2004, Ascenzi *et al*, 2006). One uniquely characterised ER β splice variant is that of ER β 2, which has been accepted as a naturally occurring isoform of ER β in several species (Froehlicher *et al*, 2009; Davis *et al*, 2010; Mandusic *et al*, 2012) and largely shares the same structural conformation as its wild-type variant, save for an 18 amino-acid disparity as 26 unique amino-acid residues described as 'exon 9' replace exon 8 (Ascenzi *et al*, 2006); the result is a receptor which does not bind ligand characteristically favours heterodimeric bonding to ER α over typical ER β -ER β dimerization, where it actively inhibits the ability of ER α to bind to DNA. It is of note to mention that whilst many ER splice variants have been uncovered the genetic level, there is little supporting evidence as to whether or not all other splice variants are expressed as proteins or further modified nor as to their physiological activity (Ascenzi *et al*, 2006) if any.

1.3.2 ER Splice Variants

It has been posed that due to the antagonistic nature the two ERs present in the breast that the exact nature of oestrogens in breast cancer progression may be dual in nature; affected by the expression ratio of ER α and ER β as opposed to their absolute levels (Platet *et al*, 2004; Mandusic *et al*, 2012). It has been evidenced that as a luminal (ER+) carcinoma progresses from carcinoma in situ to further stages, its ER profile changes significantly, with pre-malignant and normal tissues expressing ER α at a generally lower level (10-20%) and increasing in proliferative ductal carcinoma in situ (DCIS), suggesting a correlation with an increased receptivity of oestrogen with increased risk of tumorigenesis (Travis & Key, 2003). Alongside this increase in expressed cytoplasmic ER α , the cellular concentration of ER β 1 (i.e. Wild-type) is seen to fall from normal tissue through to proliferative ductal hyperplasia and into DCIS. Of note, it has been observed for high-grade DCIS to display a marked decrease in both oestrogen receptors down to negligible or absent levels where once they may have been in abundance (Platet *et al*, 2004); this association allows to make the inference that the presence of estrogens and their receptors may in fact help protect against cancer cell invasiveness; this is

made more plausible due to the fact that overexpression of ER β 2 in advanced disease is found to be associated with better patient outcome (Mandusic *et al*, 2012).

1.4 Genetic Risk

The notion that familial inheritance may play a role in breast cancer susceptibility has been widely accepted and has been evidenced with figures suggesting at least a two-fold increase in the risk of female breast cancer when as little as one first-degree relative is found to suffer the disease (Antoniou & Easton, 2006; Oldenburg *et al*, 2007). A number of high penetrance germline mutations exist such as the BRCA1 (BRCA1 Breast Cancer early onset) and BRCA2 mutations, however, these only account for 15-20% of breast cancers which cluster in families and less than 5% of all reported cases of the disease (Nathanson *et al*, 2001; Antoniou & Easton, 2006; Oldenburg *et al*, 2007).

Germline mutations of the BRCA1 gene, are often oncogenic, displaying a high penetrance; being present in around 15-20% of women with family diagnosed with breast cancer and 60-80% of women who have a family history of both breast and ovarian cancer and is linked with an increased risk of both breast and ovarian cancer within an individual's lifetime (Nathanson *et al*, 2001). BRCA1, located on chromosome 17q21, is a relatively large gene coding for a 220kd protein of 1863 amino acids with implicated functions in DNA repair and cell cycle regulation. Often referred to as a "Caretaker Gene", BRCA1 is a well-known tumour suppressor with multiple interacting partners and a number of functions mentioned herein; it binds to BRCA2, p53 and has an epigenetic role in tumour suppression (Nathanson *et al*, 2001; Chang *et al*, 2011). It also serves as a transcriptional regulator with the ability to bind with several transcriptional regulatory proteins such as ZBRK1, STAT1, Myc, p53 and ER α receptor (MacLachlan & El-Deiry, 2000) and is involved in chromatin remodelling and ubiquitylation (Nathanson *et al*, 2001; Oldenburg *et al*, 2007; Da Silva & Lakhani, 2010) thus, cells without a functioning BRCA1 gene are unable to arrest development in the G2 growth phase after DNA damage and

subsequently cannot undergo other functions such as transcription coupled repair. As of yet it is still not evident as to why germline mutations of BRCA1 have such an affinity to malignancies of the breast and is due to the suggested metabolic importance of its protein not seen as commonly in other cancers, that being said, the relative lifetime risk of other cancers such as of the colon, Mullerian, pancreatic and prostate cancers in BRCA1 carriers and gall bladder, biliary, gastric, bone and pharyngeal cancers in BRCA2 carriers in addition to breast cancer which remains the focal pathology (Oldenburg *et al*, 2006).

BRCA2 germline mutations of chromosome 13q12 carry a similar lifetime risk as BRCA1 from 60-85% with an increased ovarian cancer risk of about 10-20% and a 100 fold increase from the norm in the likelihood of male breast cancer (Ottini *et al*, 2010). Unlike BRCA1 mutations, variants of BRCA2 are also observed in a number of other cancers involving the gastrointestinal system (GIT) (Nathanson *et al*, 2001; Rafnar *et al*, 2004; Karhu *et al*, 2006). The large 3418 amino acid protein (larger than the BRCA1 by 160kd) for which the BRCA2 gene encodes is known to bind to BRCA1 and RAD51 (involved in the homologous recombination of DNA), inferring a relationship in gene repair and chromosome integrity. Research done on rat models have also led to inference of possible involvement in chromosome segregation as well as gene repair (Nathanson *et al*, 2001; NCBI, 2013). Of note it has been documented that whilst multiparity (bearing multiple children) in BRCA1 mutation carriers appears to be protective, it has been observed to have the contrary effect in BRCA2 mutation carriers which are observed to have an overall increased risk of breast cancer (Narod, 2006).

The clinical detection of amplified HER2 (Human Epidermal Growth Factor Receptor 2) (to be discussed in the next section), a cell surface protein present in most is often associated with certain aggressive types of breast cancer.

Other well documented high penetrance gene mutations at risk of causing breast cancer are mostly associated with cancer syndromes and disease states, they include the serine-threonine kinase STK11/LKB1 mutation of Peutz-Jehger syndrome with a 20.3 relative risk compared to normal carriers; Cowden's syndrome's PTEN mutation (of which belies a 20-30% lifetime risk) and mutations of p53 from which Li-Fraumeni syndrome manifests with childhood leukaemias, brain tumors and a 100% breast cancer penetrance past

childhood along with other (Nathanson *et al*, 2001; Antoniou & Easton, 2006; Da Silva & Lakhani, 2010) however such gene mutations are as rare as they are lethal. Although these high penetrance mutations carry a significant risk, they only account for 25% of familial clustered cases, with sporadic, idiopathic breast cancers being the dominant cause, inclining or to the evidence that perhaps other breast cancer susceptibility genes may be in play in mammary oncogenesis; such as the elusive 'BRCA3' or the more charily named 'BRCA4' which are the topic of much research and discussion (Burns *et al*, 2003; Swisher, 2004; Da Silva & Lakhani, 2006; Spellman & Gray, 2011).

1.5 Breast Cancer Profiling

Due to the complex biologic heterogeneity of breast cancer, it has been widely accepted not as being a singular disease, but a cacophony of different diseases of the breast, each with their own distinct clinical, pathological and histopathological features, genetic and genomic variability and each pertaining to their own unique treatment responses and survival outcomes *yet all* originate from and affect the terminal duct lobular unit (TDLU) of the breast (Perou *et al*, 2000; Sørli *et al*, 2001; Robinson *et al*, 2004; Vargo-Gogola & Rosen, 2007; Weigelt *et al*, 2010).

It was through the seminal enquiry of Perou and colleagues in 2000 and their high-throughput microarray-based gene expression profiling assays which gave rise to the 'intrinsic' gene list (pertaining to genes which vary the most between tumours from different patients compared to samples of the same tumour and is now known as Stanford taxonomy) through which the molecular classification of breast cancers (represented in **table 1.2**); including luminal A, luminal B, Basal-like, HER-2 positive and normal subgroups, discussed below, was initially conceptualised, each of which pertaining to their own distinct prognoses and treatment responses (Sørli *et al*, 2001; Sørli *et al*, 2003; Hu *et al*, 2006).

The so-called luminal A and B (named thusly due to their molecular signature which bears a strong resemblance to the luminal cells of the breast duct (Robison, Perreard and Bernard, 2004) breast cancer subtypes; characterised by the presence of ER (and ER activation related genes such as estrogen-regulated LIV-1) and PR expression are the most commonly

diagnosed and account for 60% of all breast cancers (40% and 60% respectively)(Cyr & Margenthaler, 2014). These two subtypes are distinguished by a higher expression of proliferation genes a much lower expression of ER-related, luminal and basal-like genes and overall worse prognosis in luminal B cells to luminal A (Alizart *et al.*, 2012; Cyr & Margenthaler, 2014). Ki67 is a proliferative marker associated with ribosomal RNA transcription and production and is highly expressed in all cancer subtypes save for luminal A which may be an attributing factor to prognosis (McCubrey *et al.*, 2014).

The HER2-enriched subtype constitutes for around 10-15% of all breast cancers and are naturally characterised by a high expression of the oncogene HER2 (Human Epidermal Growth Factor 2) and other proliferation-related genes with a low expression of luminal and basal-like genes. It is significant to note however, that not all HER2-enriched subtypes pertain to clinically defined HER2-positive breast cancer; that is to say, not all HER2 mutations lead to protein overexpression and cancerous statue of the tissues and vice versa (Robison, Perreard and Bernard, 2004; Alizart *et al.*, 2012; Cyr & Margenthaler, 2014).

The Basal subtype (15-20% of all breast cancers) is characterised by the high expression of genes of the proliferation cluster such as PCNA, BUB1, and CDC2 and expression of transcription factors such as c-fos, c-jun, and fos B with negligible PR/ER/HER2 (triple negative) expression. Again, although most basal-like cancers are triple negative; not all triple negative cancers are basal-like. Of all the subtypes within the intrinsic list, cancers categorised as triple negative (HER2, Basal) are linked with the worst overall survival prognoses (Robison, Perreard and Bernard, 2004; Cyr & Margenthaler, 2014).

Finally, the normal-like subtype is characterised by gene expression typical of normal breast adipose tissue. Previously suggested to be an artefact of tumour sampling, it is now widely accepted as being a genuine cancer subtype (Alizart *et al.*, 2012).

Although never intended as having any prognostic value during its inception (Cyr & Margenthaler, 2014), it has been observed that within the intrinsic list, cancers of luminal A subtype have the best prognosis, followed by luminal B, with the others following suite. It has however, not enough during

clinical assessment to prognosticate a patient's survival using molecular profile alone as decided in a consensus conference in 2012 (Schwartz *et al.*, 2012).

As technology continues to advance, newer, more precise array technologies arise, and knowledge expands and disseminates, new multigene classifiers have emerged to reduce heterogeneity within the existing cancer subtypes of the intrinsic list as well as to define new subgroups, namely claudin-low, molecular apocrine and interferon subgroups (Alizart *et al.*, 2012). The claudin-low subtype is defined by low HER2 and low activity of the proliferative gene clusters associated with basal and luminal B identification. The molecular apocrine group (mApo), characterised by the presence of androgen receptors (AR) and associated genes serves to further categorise non-basal triple negative cancers that fall under luminal B and HER2 taxonomy and accounts for about 15% of all invasive cancers (Alizart *et al.*, 2012). The following table serves to consolidate the subtypes of Stanford taxonomy as well as claudin-low, mApo and interferon subgroups, their common histological types and additional features.

ER Division	Molecular Subtype	HER2	Ki-67	Histological Grade	Additional Features
ER+	Luminal A	(-)	low	1 or 2	Luminal cytokeratin +; E-cadherin +/-
	Luminal B	(-/+)	high	2 or 3	Luminal cytokeratin +; <i>TP53</i> mutations
ER-	HER2	(+)	high	2 or 3	<i>TP53</i> mutations
	Basal-like	(-)	high	3	Basal cytokeratin +; <i>TP53</i> mutations
	Normal-like	n	high	n	normal adiposic features
	Claudin-low	(-)	high	3	Cancer stem cell-like; EMT-like;
	mApo	(-)	high	3	Androgen receptor +

	Interferon-related	(-)	high	3	STAT1
--	--------------------	-----	------	---	-------

Table 1.3: Characteristics of Molecular Subtypes (Stanford and new subtypes); illustrating 5 known subtypes of breast cancer, (Adapted from Alizart et al., 2012).

1.6 Diagnosis of Breast Cancer

Women are urged by organisations such as breastcancercare.org to be vigilantly aware of the changes that may occur in their breasts in order to address pathogenesis as soon as possible. For many women, the prospect of breast cancer diagnosis can be emotionally and psychologically distressing; as such it is imperative that the diagnostic methods and techniques offered are fast and reliable (Azu *et al*, 2007). The evaluation of possible breast abnormalities is typically executed with a triple assessment process which should include a thorough clinical examination, imaging techniques such as mammography, ultrasound and tissue sampling by fine needle aspiration or a core needle biopsy (Oldenburg *et al*, 2006). As the risk of breast cancer is understood to be directly correlated with age and subsequent survival rates positively correlated with timely diagnoses, it is imperative that the disease be screened for at earlier ages for better treatment and prognostic prospects (Trichopoulos *et al*, 2008; Jalalian *et al*, 2013)

X-ray mammography and ultrasonography are the two chief imaging techniques used in the screening of non-palpable lesions and the detection of breast cancer (Flobbe *et al*, 2001) and are ubiquitous worldwide due to their relatively inexpensive cost of operation. Ultrasonography may often be used as an adjunct imaging technique following mammography, serving to differentiate cysts from solid breast tumours in the clinic. These techniques often fall short however, as their sensitivity greatly depends on largely variable factors such as breast density, which can occasionally lead to falsely negative images resulting in patients with even so much as palpable breast cancers being treated as normal or benign on investigation (Chen & Hsiao, 2008). Ultrasonography is also very operator dependent and requires a keen eye and a knowledgeable practitioner for good diagnosis. Technical advances such as Doppler ultrasonography, and computer aided diagnostic (CAD) systems are becoming increasingly implemented and widely used to great effect to the benefit of the

radiologist, allowing for greater scope and detection of mammographic abnormalities (Fujita *et al*, 2008; Oliver *et al*, 2010; Jalalian *et al*, 2013)

More precise imagery techniques that are readily preceding these classic techniques include magnetic resonance imaging (MRI) demonstrated below in Figure 1.4 which has been proven in clinic to yield results with greater acuity to that of older techniques (Morrow *et al*, 2011; Davies, 2012). Other techniques include chest radiography, computed tomography (CT) and positron emission tomography (PET). Prospects for future diagnostic techniques include one which recently made its rounds on the medical scene which stems off widely studied circulating tumour DNA analyses which utilise biomarkers such as cancer antigen 15-3 used to determine patient's response to treatment; the assessment of circulating, cell-free DNA with tumour-specific somatic alterations in the bloodstream may be (given the inherent specificity of the somatic mutations) an important biomarker for both metastatic breast cancer (Dawson *et al* 2013).

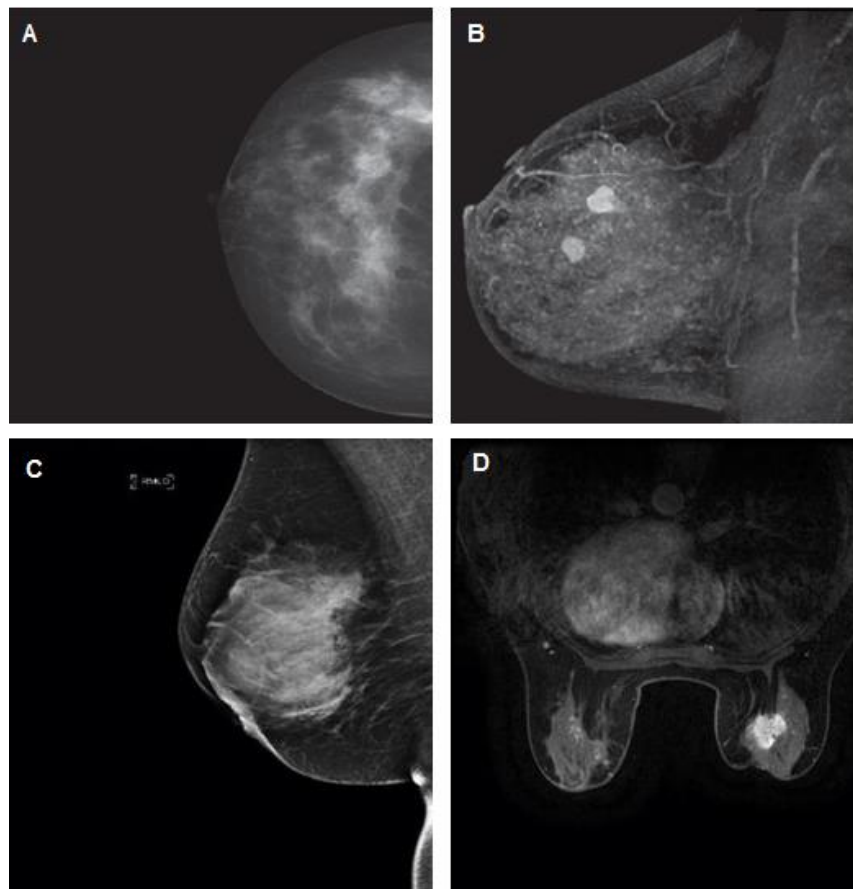


Figure 1.4: Comparison of X-ray Mammography vs. MRI (A) Negative X-ray mammogram of 43-year old woman. (B) contrast enhanced MRI of the same breast identifying multifocal carcinoma (C) sagittal X-ray mammogram revealing abnormal tissue density. (D) contrast enhanced MRI of same patient identifying (Morrow *et al*, 2011; Davies, 2012)

The TNM staging system, in which (T) denotes tumour size; (N), the extent of local spread of the disease to the lymph nodes and (M), the occurrence and extent of distant metastasis, is a widely employed stratagem by healthcare professionals to evaluate the extent or severity of cancers from the evidence given to them from the techniques previously discussed in order to ascertain treatment regimens and prognostic estimation (Compton, 2003). Cancers, such as adenocarcinomas that arise from the TLDU of the breast are characterised by tissue invasion and metastasis to distant soil and as such the application of the TNM system is ideal (Oldenburg, 2007). T, N and M are all evaluated in stages, cancer size (T) is gauged in 7 possible stages from TX/0 in which no primary tumour can be evaluated or seen to T1-4 which is a qualitative assessment of tumour size. (N), Designates the number of lymph nodes to which the tumour has spread and can range from NX/0 to N3 whilst (M), which signifies the distant travel only ranges from MX/0 to M1. The end result is a TNM which could read T4N0M0 meaning a very large tumour with no lymph or metastatic involvement that would then confer a specific stage, 0, carcinoma in situ, to IV which can vary depending on the type of cancer being evaluated due to inherent discrepancies in aggression (Cancer.gov (2012)). The routine staging of patients in the absence of signs or symptoms of metastatic onset is considered superfluous in some circles due to the relatively low incidence of disease of 2% (James *et al*, 2012), however, CT staging may be necessary in certain groups of patients with higher risk of metastases at time of presentation and must be put into consideration (James *et al*, 2012)

By far the most reliable survival indicator in patients with breast cancer is the presence of axillary node metastases (Robertson *et al*, 2011). Among the techniques thus far mentioned, relatively more invasive biopsy procedures of the axillary and sentinel lymph nodes (by either core or fine needle aspiration) may also be performed in order for the pathologist to visualise and assess the nature of the cells in question and is a crucial member of the diagnostic triad that helps to direct decisions in treatment. Whilst several types or subsets of grading systems are in place in different laboratories, there is ultimately little difference (Dalton *et al*, 2000; Saha *et al.*, 2013). During investigation, biopsy

sections are assigned a grade based on cell and tissue differentiation, such as tubule and gland formation, nuclear polymorphism and mitotic counts (Oldenburg *et al*, 2007). In the Nottingham Criteria; a grading system most commonly used in the UK, uses these three measures in order to produce a final grading score ranging from 1 (well differentiated) to 3 (poorly differentiated)(NHS, 2005).

1.7 Treatment

Up until the turn of the 20th century, surgical intervention had been the only known curative treatment option available for tumescent growths, and only up until the advent of anaesthesia and antibiotics had it been significantly useful due to apparent factors of pain and infection. Radiation therapy followed shortly after the discovery of x-rays by Wilhelm Roentgen in 1895 (which won him the Nobel Prize in 1901) which inspired hope to the population of a non-invasive cure for malignancy (Weber, 2000), the first documented success of which was recorded in 1879 where it was employed to cure severe cases of head and neck cancer (Sansare, Khanna and Karjodkar, 2011)

Today, in the modern school of cancer treatment the surgical excision of malignancy is still considered to be one of the main treatment options wherever possible (Wood, 2007). Adjuvant therapies such as radiotherapy and chemotherapy may be given in conjunction to surgery as a prophylactic (also known as salvage) measure to reduce the risk of relapse. This treatment may be given preoperatively (Neoadjuvant therapy) where applicable in order to make attempts to down grade and down stage cancerous masses prior to surgery (Chuthapisith *et al*, 2006; Yamaguchi *et al*, 2012). The direction of treatment is governed by information gained during the diagnosis of the individual patient, taking into consideration factors such as the grade and stage of the cancer and also factors such as the cancer location (as not all cancers are feasibly operable) (Mitra & Khoo, 2009).

1.7.1 Chemotherapy

Chemotherapy (in relation to cancer), first coined by Paul Ehrlich in the early 1900's (DeVita, 2008), can be defined as the clinical use of systemic chemical compounds to arrest the proliferation of cancerous growth through the mediation of cell apoptosis (programmed cell death) (Becker *et al*, 2009). At first, the idea of treating cancer with chemotherapy from the early days of its conceptualisation, even up to the discovery of its utility post WWII was met with much vitriol in its initial debut on the medical scene (DeVita & Chu, 2008) and was not until the 1970's that adjuvant chemotherapeutic methods were widely applied in cancer treatment.

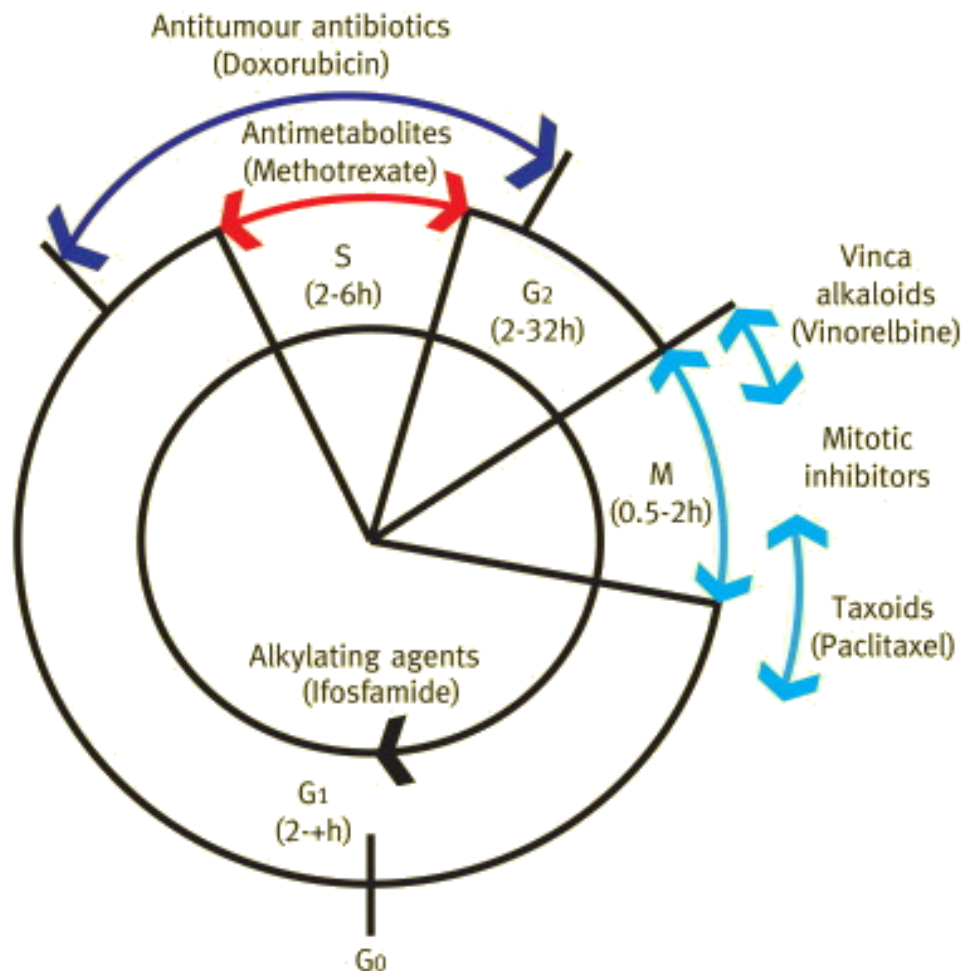


Figure 1.5: The effect of antitumor antibiotics on different phases of the cell cycle, adapted from Brown *et al* (2011)

Chemotherapeutic treatment can be subdivided into four separate schools; Curative chemotherapy, for which the disease state can be effectively cured (in a very small number of cancers) by a combination of chemotherapeutic agents; the previously discussed adjuvant and neoadjuvant approaches and finally palliative care, which while not curative may help to extend prognosis of the patient (Parnell & Woll, 2003; Sridhar & Symonds, 2009; English, 2010).

The cytotoxic drugs that make up the known list of chemotherapeutic drugs are divided into several classes based on their method of action, they consist of;

- i.) Vinca alkaloids- administered intravenously, these drugs inhibit cell division by binding to tubulin within cells preventing the synthesis of mitotic spindles. Vincristine and vinblastine are both members of this family (English, 2009).
- ii.) Antimetabolites- such as methotrexate are used intrathecally in the chemotherapeutic treatment of CNS derived malignancy such as non-Hodgkin's lymphoma or acute lymphoblastic leukaemia. They act by inhibiting DNA and RNA synthesis through the inhibition of metabolic processes (Sridhar & Symonds, 2009; English, 2009).
- iii.) Alkylating agents- are used in a wide range of malignancies, they act by covalently bonding with DNA bases causing single or double stranded DNA breaks (Sridhar & Symonds, 2009)
- iv.) Taxanes- which include paclitaxel and docetaxel; they act against microtubules to inhibit mitotic activity of cells (English, 2009)

To much the disdain of the pharmacologist, chemotherapeutic drugs act upon healthy cells as well as malignant tissues which may cause side effects such as bone marrow suppression, nausea and vomiting, hair loss, kidney and heart failure and even neurotoxicity (Sridhar & Symonds, 2009)

1.8 Tamoxifen

Tamoxifen has been used as the first port of call in the treatment of advanced breast cancer for the last 40 years. Since its discovery in the 1970's its uses have expanded to include early breast cancer, ductal carcinoma *in situ* (DCIS) and more recently in the chemoprophylaxis of breast cancer. Due to tamoxifen's good tolerability profile and efficacy in both pre and post-menopausal women, it has managed to retain its position as number one hormonal treatment of choice in patients with ER+ (oestrogen receptor positive) breast cancers thus making it the benchmark for which newer endocrine therapies are tested against (Clemons *et al*, 2002)

1.8.1 History of Tamoxifen

The use of tamoxifen as an endocrine based chemotherapeutic agent emerged in the wake of an era of cytotoxic chemotherapy heralded by Cooper (1963) with the American Association for Cancer Research. Venturing further back towards the dawn of the 20th Century, Beatson (1897) discovered that advanced breast tumours in premenopausal women were sometimes responsive to bilateral oophorectomy, thus the hypothesis could be formed that the progress of oestrogen dependent tumours could be truncated through subsequent deprivation of oestrogen (Clemons *et al*, 2002).

Subsequent to this discovery, ablative surgical treatments such as hypophysectomies and adrenalectomies were commonly employed in the treatment of advanced breast cancer, however, in light of these developments, a non-surgical endocrine approach was still sorely needed; the forerunners of which, although efficacious, were limited by their toxicity. Initially developed as a post-coital contraceptive, tamoxifen, (formerly ICI 46,474), emerged in the 1960's during a series of anti-hormone efficacy tests spearheaded by Arthur L. Walpole on triphenylethylene derivatives following the development of the two anti-oestrogens MER-25 and clomiphene (**Fig 1.5**) through the substitution of the chlorine in clomiphene with alkyl groups. At the time, clomiphene, although showing promise as an effective anti-oestrogen agent, was being linked with an increased incidence in cataracts in animal models (Newberne *et al*, 1966) necessitating the development of an analogue with similar dose-response efficacy but with decreased morbidity. Tamoxifen proved to be just that drug, although the discovery of its truly anti-oestrogenic conformation came later after the prior discovery of its cis-isomer which acted as a pure oestrogen much like

its predecessors before it, making it potent fertility agent. It was only after a study on the pharmaceutical effects of cis vs trans isomer conformation that the trans-isomer was shown to play a primarily anti-oestrogenic role, the first of such discovery of its kind which heralded the dawn of targeted therapy as we know it today (Clemons *et al*, 2002).

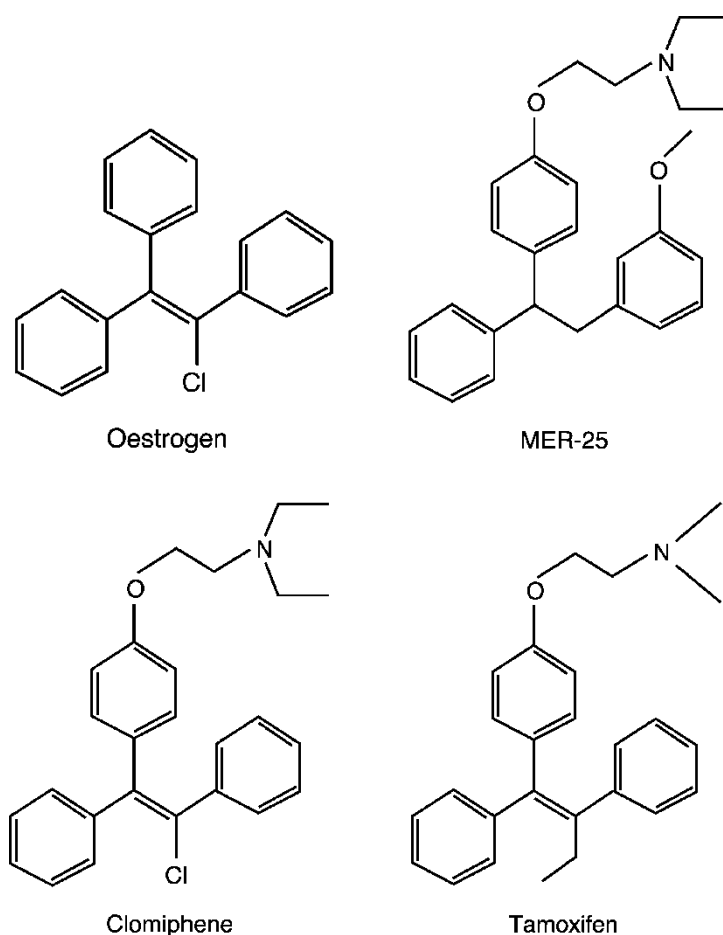


Figure 1.6: Oestrogen with antioestrogen competitors, Clemons *et al*, 2002

It is the work of the eminent pharmacologist Craig Jordan, who's vital exploits and commitment to the field helped transform ICI 46,474 from failed contraceptive to the gold standard for targeted therapy in breast cancer that it is today, whose work includes but is not limited to the discovery of 4-hydroxytamoxifen with its 100x greater binding affinity over the non-hydroxylated drug, the determination of tamoxifen's prophylactic benefit in a rat model and the specialisation of tamoxifen from palliative drug to the long-term adjuvant it is currently used as today (Jordan, 2008).

1.8.2 Properties of Tamoxifen

The anti-oestrogen tamoxifen (a triphenylethylene derivative) is a selective oestrogen receptor modulator (SERM) which competes with oestrogens for the binding to the two homologous oestrogen receptors ER α & ER β thus negating the cytotropic effects of oestrogens. 4-Hydroxytamoxifen (4-OHT), formed by the hydroxylation of tamoxifen that exhibits a higher affinity to oestrogen receptor (50 to 100 \times) to that of its parent metabolite and exists as both Z (trans) and E (cis) isomers, with the latter (cis) exhibiting a weaker affinity akin to that of tamoxifen (Singh *et al*, 2007; Brauch & Jordan, 2009). Endoxifen (4-hydroxydesmethyltamoxifen), which exhibits a similar ER affinity to that of 4-OHT, is the latter product of tamoxifen metabolism and is thought to be the principal antioestrogenic metabolite for antitumour activity in breast cancer patients due to higher serum levels of endoxifen compared to 4-OHT after treatment with tamoxifen of up to six fold (Lim *et al*, 2006); Brauch & Jordan, 2009)

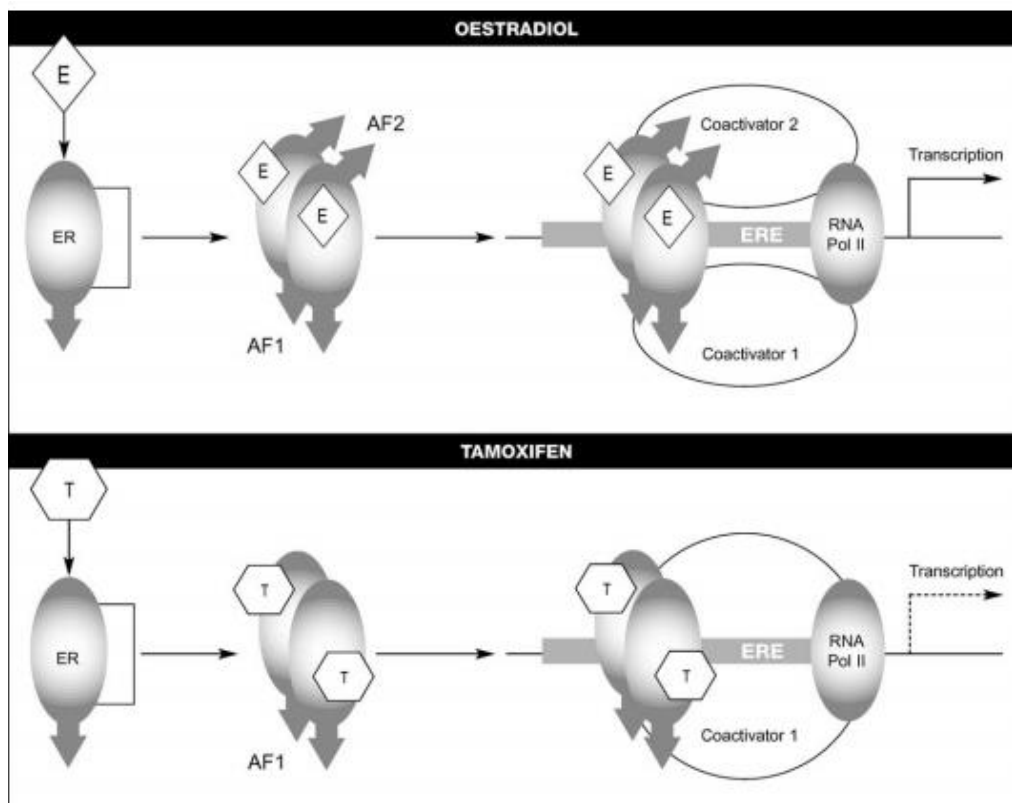


Figure 1.7: Mode of action of oestradiol and tamoxifen. Clemons et al, 2002

Additionally, it has been reported in recent years that tamoxifen exhibits ancillary oestrogen receptor independent processes such as the inhibition of PKC pathways which contribute to the overall chemotherapeutic outcome of the drug as postulated from the effect of tamoxifen on oestrogen negative and oestrogen independent cancer cell lines in which cell migration, invasion and metastasis was markedly inhibited (Matsuoka *et al*, 2009).

1.8.3 Tamoxifen in Cancer Therapy

To this day, SERMs such as tamoxifen remain the most prescribed anti-neoplastic for ER-positive breast cancers worldwide for both men and women. Studies by the NCI report the reduction of invasive breast cancer by 50% in postmenopausal women when used in prophylaxis to the disease (Vogel *et al*, 2006). It is generally well tolerated with acute side-effects similar to the symptoms of menopause, such as hot flushes, irregular menses *etc.* (Loprinzi *et al*, 2000) however one of the more serious adverse effects it may cause is that of an increased incidence of endometrial cancer; a likely result of its oestrogenic activity (Clemons *et al*, 2002). Tamoxifen has also emerged as a potential management option for symptoms of non-steroidal anti-androgenic treatment for males with prostate cancer where it may be considered in lieu of surgical or radiotherapy options to prevent or reduce neoplastic breast events (Kunath *et al*, 2012).

Although new ways and strategies are constantly being devised to target oestrogen and ERs, approximately, 30% of ER α -positive breast cancers do not respond to tamoxifen therapy, with the majority of initially responsive tumours soon developing resistance and following suit over the course of treatment despite the continued presence of ER α (Riggins *et al*, 2007). Additionally, small numbers of ER α -negative but PR-positive tumours have been found to respond to antioestrogen treatment made feasible by the assumption that PR-positive tumours may retain a functional ER α signalling pathways due to the fact that PR expression is oestrogen regulated (Riggins *et al*, 2007).

1.9 Chloroquine

There is an ever increasing need to develop and refine the current repertoire of effective cancer treatments with newer, more effective modalities. A study of 68 then approved drugs in 2003 by DiMasi and colleagues estimated that the cost of developing a single effective cancer antibiotic to be put at an average of 15 years and \$800 million. With such a substantial toll to pay, it has become fashionable for researchers to comb the pre-existing annals of drugs which have long had their pharmacokinetics and safety profiles clarified, and approved by regulatory bodies for human use which would allow any novel uses to be hastily appraised in phase II trials in the hopes of repurposing them for chemotherapeutic use (Solomon & Lee, 2009).

With the current limitation of drug concentrations used in therapy (mainly due to side effects), it is speculated that combinational modalities consisting of a

suite of drugs with synergistic effect may provide a better response to that of conventional practice.

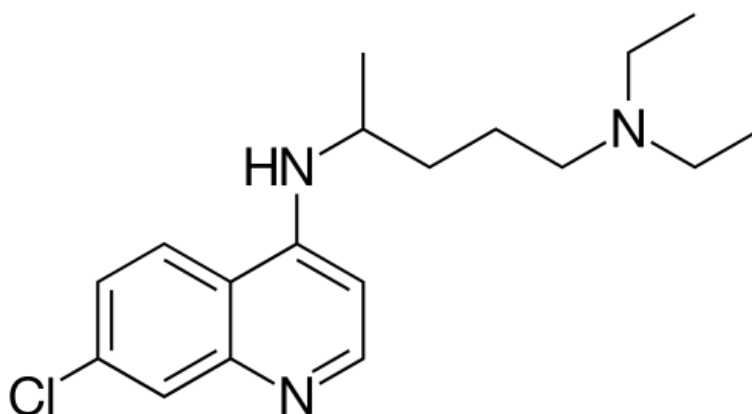


Figure 1.7: Molecular Structure of Chloroquine

Chloroquine (CQ) is a 4-aminoquinoline (possessing a 4-aminoquinoline scaffold) renowned world-wide for its use in the prophylaxis and treatment of malaria for which, since its discovery has enjoyed six decades of unrivalled usage in the treatment of the disease due to its economical nature, both fiscally and in its efficacy. Amongst its primary application, CQ's anti-inflammatory properties have seen to it being used in the treatment rheumatoid arthritis, systemic lupus erythematosus and amoebic hepatitis (Jiang *et al*, 2010) with further clinical trials exploring its use in realms of antiretroviral treatment,

radiation therapy as well as in combinational modalities in chemotherapy (Hu *et al*, 2008). Several recent studies have shown that the drug has an extensive range of biological effects on human cells and tissues such as cell growth inhibition and/or lysis seen in human leukaemia K562 cells, human breast cancer Bcap-37 cells, human lung cancer A549 cells and also in the mediation of radiosensitivity in the MDA-MB-231 breast cancer cell line (Jiang *et al*, 2010)

1.9.1 Properties of Chloroquine

CQ is conventionally prepared as a diphosphate salt, a diprotic weak base that can exist in both a protonated (i.e. charged) and unprotonated (i.e. uncharged) (Solomon & Lee, 2009). Uncharged at neutral pH, CQ enters the cell by passive diffusion and can freely diffuse across cell and into the endosome pathway or through the cytosol to other organelle membranes. Once inside an acidic vesicle such as a lysosome, CQ becomes protonated, preventing it from diffusing out of the vesicle. The trapped chloroquine molecules accumulate within the lysosomes which purportedly results in an increase in lysosomal volume; a change that often heralds the apoptotic or necrotic cell death response. It is thought that the increase in lysosomal volume by any means either intrinsic or otherwise can change the mode of cell death from apoptosis to necrosis and that disparity in lysosomal pH may influence endocytosis, exocytosis and phagocytosis (Hu *et al*, 2008).

As a lysosomotropic agent, CQ causes dynamic changes in intracellular protein processing and extensive trafficking of autophagic vacuoles within the cell (Zaidi *et al*, 2001). This property has seen chloroquine and its derivatives and analogues in the quinine family be redefined as late-stage inhibitors of autophagy.

Macroautophagy (hereafter referred to as autophagy) is the catabolic process commonly associated in the recycling of damaged and general turnover of cytoplasmic components (Levine and Klionsky, 2004). Referred to as a 'housekeeping mechanism' (Donohue *et al*., 2011), the process entails the formation of phagophores; sequestering membranes which expand and engulf

cytoplasmic material to then fuse into double membrane autophagosomes. Autophagosomes then fuse with lysosomes which result in the degradation of the autophagosomes and their contents by the acidic hydrolases of the lysosomes, the products of which are then released into the cytosol where they are then recycled by the cell through macromolecular synthesis (Cufí *et al.*, 2013).

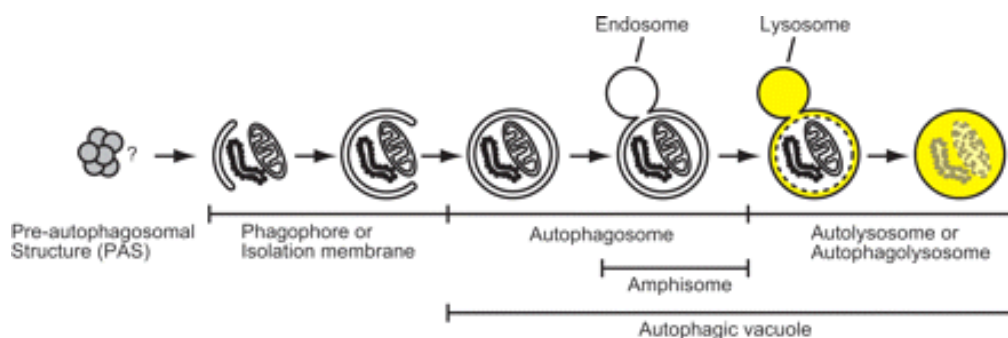


Figure 1.8: The progress of macroautophagy in mammalian cells (Mizushima, 2007)

Autophagy may also function adaptively in the maintenance of cellular homeostasis and may be stimulated in response to cellular stress and insult such as in the case of oxidative stress, amino acid depletion and chemotherapeutic agents and is thought to be thoroughly exploited in cancer cells, attributing to the resilience of several cell lines (Mizushima, 2007; Donohue *et al.*, 2011; Esteve and Knecht, 2011).

Persistent, excessive autophagy such as that in response to causes stated above may result in caspase-independent (type II) programmed cell death through the extensive catalysis of organelles (Bursch *et al.*, 2000; Amaravadi and Thompson, 2007). To further delineate the role of autophagy, it may be subdivided into “basal autophagy” and “induced autophagy”; basal being the typical ‘housekeeping’ role in the general turnover of organelles whereas induced autophagy refers to autophagy following starvation in the requisition of amino acids (Mizushima, 2007).

1.9.2 Quinines in Cancer Therapy

As stated before, it has been the effort of various teams to work on elucidating the worth of CQ as a modality in chemotherapeutic medicine; of note are Fan and colleagues’ (2006) extensive examination on the effects of

CQ on the A549 lung cancer cell line. Their findings described not only morphological impact on the cell line in presence of CQ, with cell shrinkage, detachment and blebbing apparent at concentrations surpassing 64 μM , but also pronounced findings in regards of cell cytotoxicity and inhibition of cell proliferation, with MTT and LDH assays exhibiting antiproliferative and cytotoxic effects upon the cells in a time dependent manner, with concentrations exceeding 32 μM exhibiting significant cytotoxicity. Of note in their investigations, the volume of acidic compartments (endosomes, lysosomes and the like) were seen to be increased in concentrations less than 32 μM but decreased when investigated in higher concentrations by which point apoptosis had already occurred. Lee & Tannok (2006) advocated that through raising the pH of acidic compartments with CQ, the sequestration of other anti-cancer drugs within the endosomes would be limited due to an increased permeability of the vesicles, potentially increasing the bioavailability of co-mediated drugs which would otherwise have been stored and metabolised within the lysosomes, potentially increasing the efficacy of such drugs through solid tumour masses where the effect of such drugs may otherwise have a lesser effect.

1.10 Drug Resistance

In cancer treatment, we are always faced with the harsh reality that, over time and in the absence of resolution of the disease, resistance to chemotherapy will occur. As a result, much research has been done in the effort to understand the evolutionary dynamics of resistance (Bozic *et al*, 2013), with one central conclusion being that within any large solid tumour exists a small number of cells resistant to any targeted agent and are selected for and thus clonally expand once therapy has been administered, resulting in tumour recurrences particularly following treatment with a single agent (Diaz *et al.*, 2012; Bozic *et al*, 2013).

Multidrug resistance is the term given to the mechanisms by which cancers develop resistance to chemotherapeutic drugs and is a contributing factor to their failure. It has been observed that tumours may consist of a mixed population of drug resistant and drug sensitive cells; in an uncanny similarity to

the resurgence of drug resistant microbes such as MRSA (Gould, 2007), chemotherapy kills drug-sensitive cells, however a large proportion of drug-resistant cells will be left behind and form more resistant tumours in relapse which may cause future therapies to fail (Persidis, 1999). Paclitaxel has been reported to manifest multidrug resistance in many incidences of relapse after initial favourable response, likely due to inefficient bioavailability allowing for resurgence of resistant cells (Yao *et al*, 2011). Two molecular pumps which are believed to commonly confer drug resistance to these cells, namely P-glycoprotein (P-gp) and the aptly named multidrug resistance-associated protein (MRP) (Gottesman *et al*, 2009).

P-gp (encoded by the MDR1 gene) is reportedly responsible for multidrug resistance in about 50% of all human cancers (Gottesman *et al*, 2009). Besides from being expressed by chemoresistant cancer cells, P-gp is also expressed in other tissues of the body, especially in the gastrointestinal tract where it highly expressed and involved in the low peroral bioavailability of drugs such as paclitaxel (Panchanglula, 1998; Yao *et al*, 2011). It is still a mystery as to how the P-gp pump recognises and expels hundreds of different drugs (Gottesman *et al*, 2009), the bright side is that we know it cannot expel them all (Persidis, 1999)

MRP is another proteinaceous pump that confers drug resistance to cells. Initially isolated in a small cell lung cancer cell line (Stewart *et al*, 1996; Persidis, 1999) studies have shown that it is synthesised in the same tissues as P-gp however it is not expressed in the liver (Sugawara *et al*, 1997). There is a dilemma in multidrug resistance and the treatment thereof in that whilst these proteins confer resistance to tumours, they also protect the chemosensitive tissues of the body such as the bone marrow, there making targets for tissues a difficult process (Persidis, 1999)

The possible mechanisms which may confer resistance to tamoxifen span much more than the over-expression of drug efflux pathways and are well documented. Such pathways for resistance include but are not limited to the altered expression and/or modification of any number of growth factor receptors and downstream signalling molecules (Riggins *et al*, 2007).

Research by Bozic and colleagues (2013) on a mathematical model of chemotherapy resistance presented the conclusion that no matter the nature of

resistance, the presence of a mutation that may confer cross-resistance to two or even three targeted agents will not result in sustained benefit, thus it is imperative for the future development and application of combination therapies in which the various drugs act through distinct pathways to offer the largest chance of survival.

1.10.1 Drug Combination and Resistance

Due to the swift and inevitable phenomenon of chemotherapeutic selection that occurs from the moment of treatment, subsequent resistance to any one particular drug during long-term therapy is expected to occur within a matter of months (Bozic *et al*, 2013; Munck *et al.*, 2014). Through treatment with drugs which target different pathways it is inferred that the onset of resistance to such treatments would be much slower than any individual modality; conversely, studies show that if there is any possibility for cross-resistance between combination modalities, such treatments would have the resistivity as if just a singular drug were to be used (Bozic *et al*, 2013)

1.2 Aims & Objectives

The aim of this investigation was to investigate the chemotherapeutic effects of both tamoxifen and chloroquine and the possible collaborative effects between them, studies were performed on the cell lines MCF-7 WT, MCF-7 TMX and MDA-MB-231 first independently (single drug) in order to attain benchmark readings for latter investigation. These readings; chiefly the ED₅₀ values, that is, the half maximal effective concentration for are key to determining the necessary concentrations for use in conjunctional study of the two drugs in combination to effectively witness the differences in response between ER⁺ and ER⁻ breast cancer cell lines.

Chapter Two

2.0 Methods & Materials

2.0 Materials and Methods

2.1 Materials

2.1.1 Safety Measures

- Howie-style lab coat with cuffed sleeves for cell culture
- Safety glasses
- Nitrile powder-free gloves
- Sleeve protectors

2.1.2 General Equipment Required

- Water bath OLS200 (Grant, UK)
- Centrifuge Allegra X-15R (Beckman Coulter, UK)
- Inverted microscope Eclipse TE2000-S (Nikon UK)
- Fluorescence microscope (Nikon, UK)
- Incubator Galaxy R CO₂
- Class II Microbiological Safety Cabinet TriMAT² (Medical Air technology, UK)
- Vortex Mixer (Clifton)
- Falcon tubes, 14ml & 50ml (Corning, US)
- Eppendorf tubes (Sarstedt, Germany)
- 0.45µm filter (Sterilin, Bargoet)
- Cell scrapers (Sarstedt, Germany)
- Automatic pipettes: P1000, P200 & P20 (Gilson, USA)
- Pipette tips: P1000, P200 & P20 (Neptune CLP, USA)
- Pasteur pipettes (Iasa, Spain)
- Pipette holder (IBS Integra Biosciences, Switzerland)
- Tissue culture flasks T25cm²
- Timer (Quantum)
- Beakers; 100ml. 200ml & 800ml (Pyrex)
- Kimcare medical wipes (Kimberly-Clark Professional, UK)
- Test tube rack 20mm (Nalgene, UK)
- Measuring cylinder 500ml (SIMAX Technologies, UK)
- Deionised Water

- 70% Alcohol (3:7 distilled water to absolute alcohol) (Fisher Scientific, UK)
- Phosphate Buffered Saline (PBS)1X Concentration PH7.4-7.6 (Sigma, UK)
- Virkon 500g (Antec International, UK)
- Forceps
- Ice
- Kitchen foil paper
- Cling film

2.1.3 Reagents used for cell culturing

- MCF-7 WT Cell line
- MCF-7 TMX Cell line (Johns Hopkins University)
- MDA-MB-231
- Iscov's modified Dulbecco's medium, IMDM (Sigma, UK)
- Foetal calf serum (Sigma, UK)
- Penicillin-Streptomycin (Sigma, UK)
- Amphoterecin-B (Sigma, UK)
- Glutamine (Sigma, UK)

Preparation of complete culture medium: foetal calf serum (100ml/L), antibiotics (10ml/L) and glutamine (2mM) were added to the IMDM basal medium and mixed thoroughly to produce what is to be referred to as complete cell culture medium. Once made, the complete medium should be used within one week.

- Filtered phosphate buffered saline (Fisher BioReagents, UK)
- Trypsin solution (0.25%), containing 0.02% EDTA (Sigma-Aldrich) stored in 10ml aliquots at -20°C to be thawed at 37°C when needed.

2.1.4 Reagents and equipment used for cell counting

- Filtered 0.4% Trypan blue (Sigma Alrdich, UK)
- Filtered PBS (Fisher Bioreagents, UK)
- Pipettes (Gilson, UK)
- Chosen cell suspension
- Inverted Microscope (Nikon, JP)

For Manual Cell Counting

- Haemocytometer (Hawksley, England)
- Microscopy cover slips; 22mm x 22mm
- Tally counter

For Automatic Cell Counting

- TC-20 Automatic Cell Counter (Bio-Rad, UK)
- Disposable cell counting slides (Bio-Rad, UK)

2.1.5 Reagents and equipment used for cryostorage

- Dimethyl sulfoxide (DMSO) (Sigma, UK)
- Isopropanol (70%) freezing container (Sigma, UK)
- Complete cell culture medium
- 1.8ml cryopure tube
- Foetal calf serum (Sigma)
- Ultra low temperature freezer KR10 (New Brunswick scientific, UK)
- Liquid nitrogen cryogenic storage dewar

2.2 Methods

2.2.1 Safety note- *All investigations took place within a level 2 microbiology laboratory under strict hygienic protocol for the protection of both scientists and research alike; lab coats, nitrile gloves, forearm protectors and protective eyewear were worn at all times whilst in the laboratory. The majority of work took place within a sterilised level 2 microbiology cabinet wherever possible to ensure an axenic environment when working with the cells.*

2.2.1 Aseptic technique

In addition to all cell culture work being carried out in the cell culture cabinet, all instruments, including glassware and pipette tips were sterilised by autoclaving at 120°C for 15 minutes at 10lbs/in². All instruments were to be wiped down with 70% ethanol prior to introduction to the cabinet to reduce the possibility of introducing exogenous pathogens. Apparatus marked as sterile disposable were used once before being discarded for incineration. Unless otherwise stated, most non-sterile reagents for use in tissue culture were filtered before use through 0.45µm pore size filter (Sterilin, Bargoet).

2.2.2 a Culture media preparation

The necessary reagents for the culture medium are all taken from storage and brought to room temperature in a waterbath. The complete cell culture medium consists of Iscove's modified Dulbecco's medium (IMDM) which is prepared with 10% foetal calf serum (FCS), 1% penicillin/streptomycin and 2mM of L-glutamine. To prevent phenotypic drift of tamoxifen resistant MCF-7 TMX, these cells are cultured with a modified complete medium containing an addition 1µM of 4-hydroxytamoxifen.

2.2.2 b Cell Culture Procedure

All culturing of MCF-7 WT and JH MCF-7 TAM cell lines was carried out in vented 25 cm² tissue culture flasks (Sarstedt, Germany). The cells were maintained in complete cell culture medium at pH 7.3 in a humidified incubator which was kept at 37 °C with 5% CO₂ and 95% air (Wolf Laboratories, UK). Media and all reagents for cell culture were heated in a water bath at 37 °C before being used. Every day, the flasks were observed for changes in to colour of the culture medium and overall cell confluency through the use of an inverted microscope (Nikon, UK). The medium was changed every 3-4 days by adding

4ml of complete cell culture medium. Once 90-100% cell confluency has been obtained, the cells were subsequently subcultured in a 25cm² culture flask.

2.2.2 c Subculture

The cell lines were to be sub-cultured once reaching +90% cell confluency. As MCF-7 is an adherent cell line, cell detachment was necessary through the use of 0.25% trypsin containing 0.02% EDTA (Sigma-Aldrich). The trypsin, which was stored at -20°C in 10ml aliquots was thawed in the water bath at 37 °C and vortexed to ensure homogeneity before use.

Once ready for subculture, flasks were to be taken from the incubator using aforementioned aseptic techniques (2.2.2) and placed into the cell culture cabinet. The cell culture medium was extracted from the flasks with a 10ml serological pipette and cells were washed with PBS to remove any trace of the old medium. Washing was performed through the addition of 5ml filtered PBS to the empty flasks which were then gently rocked manually for 10 seconds and then removed with another pipette (this process was generally repeated at least 3 times). 5ml of 0.25% trypsin was then to be added to the flasks which were then incubated for around 5 minutes (a stopwatch timer is always used to keep the time as trypsin is known to have cytotoxic effect after prolonged exposure).

Once 5 minutes had elapsed, the cells were then gently rocked manually before examination under the inverted microscope to ensure detachment. Once returned to the cabinet, the trypsinised cells were then introduced to a 14ml falcon tube (using a 10ml serological pipette) containing an equal (5ml) amount of basal medium which is used to neutralise the effect of the trypsin. Residual cells were a rare occurrence in the flask and thus a cell scraping was never necessary. The cells were then centrifuged at 1200rpm for 12 minutes at ambient room temperature. After discarding the supernatant, the cell pellet was then dislodged in 1ml of complete cell culture medium. Cell counting may be performed through haemocytometry. After this procedure, the cells were then placed in T25cm² cell culture flask (labelled with the appropriate cell line, date and passage) containing 5ml of complete cell culture medium using an automatic pipette. In general, subcultures were established using 1/10 of the reconstituted pellet (100µl).

2.2.3 Cell Counting

Following cell detachment with trypsin and centrifugation, it is necessary to count the cells in order to establish the necessary volume of cells required for any individual assay. To this end, the cells were counted using a haemocytometer and the vital stain trypan blue (Sigma Aldrich) which may be used to establish cell viability. Trypan blue achieves this effect through the selective colourization of dead cells.

Use of an automated cell counter such as the TC-20 (Bio-Rad) in the image provides a quick high throughput way to assess cell number and viability as well as overall growth. The peaks shown on the display show the population of cells within specific diameters; the three closely grouped peaks represent the MCF-7 cells, the middle and largest peak illustrates the majority population of cells, the two outlying peaks the cells which are slightly smaller or larger being those on either on the cusp of mitosis or new daughter cells, thus it is possible to determine at what point in the cell division cycle the majority of the cells are. 25µl of the reconstituted cell suspension was transferred to a 500µl Eppendorf tube and then mixed well with an equal number of trypan blue through aspiration and ejection with a pipette. 10µl of this trypan blue/cell suspension would then be ejected onto a haemocytometer mounted with a 22x22mm coverslip for counting underneath a light microscope. The cells within the 16 squares of an individual quadrant of the haemocytometer would then be counted and the final sum multiplied by the dilution factor (2) and then by 1×10^4 to give the total number of cells within 1ml of the original reconstituted cell suspension. From this point it is then possible to determine the volume of the reconstituted cell suspension necessary for any subsequent assay

2.2.4.5 Using the Haemocytometer

This procedure uses the reagents and apparatus described in 2.1.4. Prior to usage, the haemocytometer is cleaned with 70% ethanol to minimize false positives from previous counts. To affix the coverslip to the haemocytometer,

the corners are gently moistened before careful application to the haemocytometer field. Newton's rings may be observed when the coverslip is correctly affixed. An alternative method of affixing the coverslip is by exhaling on to the back of the coverslip as to cause condensation before carefully applying it to the haemocytometer. Prior to counting, the supernatant trypsin/culture medium supernatant must be discarded and the remaining pellet resuspended to make up a 1ml cell suspension solution. In order to achieve the most reliable results from counting, the harvested cell suspension must be thoroughly mixed through gentle aspiration and ejection with a serological pipette (Gilson). Shortly after mixing to prevent sedimentation, 50 μ l of cell suspension should be extracted from the cell suspension and transported to an Eppendorf tube. 50 μ l trypan blue is then added to the Eppendorf tube making 100 μ l trypan blue/cell suspension. From the 100 μ l trypan blue stained cell suspension, 10 μ l is drawn up using a Gilson pipette. The haemocytometer is then gently filled as the tip of the pipette rests at the edge of the chamber to ensure stability. It is important to make sure that the haemocytometer chamber is not overfilled and, to that extent, not all 10 μ l of trypan blue may be necessary; allow the cell suspension to be drawn out by capillary action until the chamber is completely filled. Once filled, the haemocytometer may then be observed by either upright or inverted light microscopy at 10X objective magnification.

Figure 2.2 illustrates grid layout.

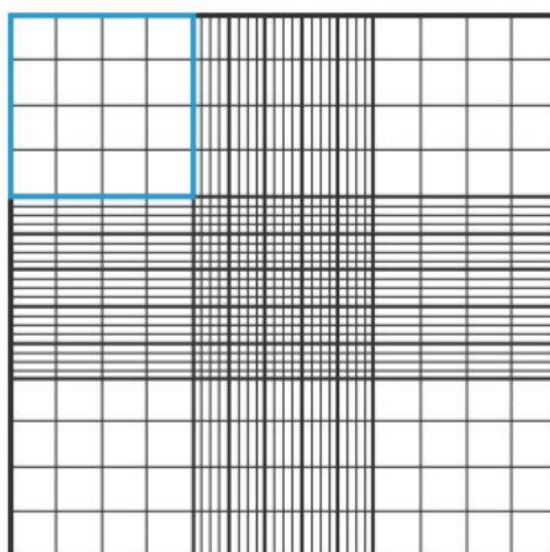


Figure 2.1: The gridlines of a haemocytometer chamber. 16 squares make up each corner quadrant (blue) in a chamber. (Abcam 2015)

of the haemocytometer chamber. The focus should be set to the set of 16 squares that made up one of the four corner quadrants of the chamber on that half of the haemocytometer. The cells within the 16 squares are then counted

using a hand tally; dead and dying cells show up stained blue whereas the healthy ones remain unstained by the trypan blue dye. It is important to only count cells that are within the square and any positioned on the right hand or bottom of the boundary line. By counting the dead cells, it is possible to also calculate the viability of the cell population. This process is repeated for the other 3 remaining quadrants of the chamber until all 4 sets of 16 squares are counted. The haemocytometer is designed so that the number of cells in one corner quadrant is equivalent to the number of cells $\times 10^4 \text{ml}$, thusly, to calculate the number of cells from a harvest the following equation must be made:

$$\frac{\text{Sum of 4 Quadrants}}{4} * 2 * 10000$$

The sum of the four quadrants are divided by 4 to give an average, this figure is then multiplied by 2 to account for the 1:1 dilution of cells to trypan blue dye. Finally, the figure is multiplied by 10^4 to give the total amount of cells within the original 1ml cell suspension. In order to calculate total cell viability, the following calculation is made.

$$\frac{\text{Live Cell Count}}{\text{Total Cell Count}} = \text{percentage viability}$$

2.2.4 Cryostorage and Recovery

The cryogenic solution consisted of 900 μl of foetal calf serum (Sigma, UK), 100 μl of DMSO (Sigma, UK) which was used as a cryoprotectant, and 950 μl of the cell suspension. The solution was then mixed gently with a Pasteur pipette in a cryogenic capsule and then placed within a freezing container with propan-2-ol and placed in the -80 freezer overnight to gradually step down the temperature of the constituents. After 24 hours the cryogenic tube was then placed within the cryogenic compartment containing liquid nitrogen with an appropriate entry filled within the laboratory catalogue.

In order to recover the cells from storage, they are first taken from the liquid nitrogen compartment and left to acclimatise for 1 minute in atmosphere (preferably in the Class II cabinet) and a further 5 minutes stood in a water bath at 37°C before being transferred to 5ml of complete medium in a T25 (or T75, if the known cell number is over half a million cells) and left overnight to attach to the flask. After 24 hours, the flask should be washed with PBS and replaced with 5ml of new complete medium in order to eliminate toxic DMSO from the flask.

2.2.5 Waste Disposal

All biological waste is to be disposed of as mandated by the facility. Biological waste includes pipettes, Eppendorf tubes, tissue culture flasks, syringes and cell culture media and any other disposable equipment that interfaces with these instruments. All biological waste is treated with a Vircon solution before being deactivated by autoclaving before disposal in marked receptacles for this class of refuse.

2.2.6 MTT (3-(4,5-dimethylthiazol-2-yl)-2,5-diphenyltetrazolium bromide) Cytotoxicity Assay

2.2.6.1 MTT Cell Preparation

For this assay, cultures of MCF-7, MCF-7 TAM and MDA-MB-231 are harvested from their respective cell culture flasks. For all colorimetric assays, cells were seeded into 96 well plates in complete medium. An optimal seeding density of 10,000 had been previously standardised by the cell culture laboratory for these cell lines.

2.2.6.2 MTT Assay Specific Reagents and Setup

MTT Stock Solution 5mg/ml- Desiccated MTT powder is dissolved 5mg:ml in autoclaved dH₂O. It may be stored at -20°C.

MTT Assay Solution 1mg/ml- Complete medium is added to MTT stock solution. This assay solution must be used on the day.

2.2.6.3 Preliminary Investigation

As stated previously, each quantitative assay was to be performed in two parts; the preliminary assessment, in which the cell lines were given singular treatment in order to attain IC values necessary to calibrate functional combination therapy assays. As such, the methods detailed below will be discussed accordingly.

For all the preliminary MTT assays each drug dose was recorded in duplicate, that is, two wells per concentration of drug per cell line. Additionally, all MTT assays were performed in duplicate, that is, each plate assaying concentrations in triplicate were run with an identical sister plate to allow for a fairer test and more reliable results. Typically, when plating out the cells into the microtitre plates, the outer ring of wells was filled with distilled water or basal medium in order to protect the central wells from desiccation during incubation periods.

Figure 2.1 illustrates the basic template used for conducting the preliminary MTT assay. The blanks are left empty until reading.

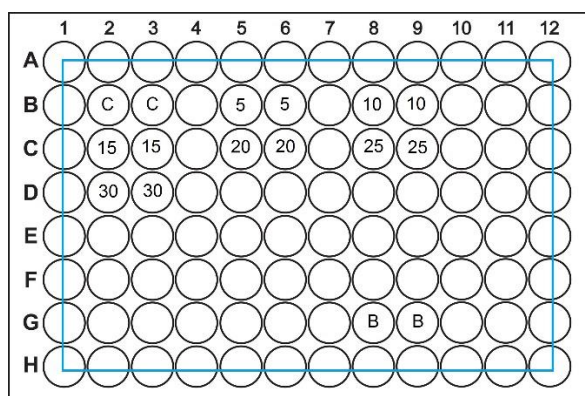


Figure 2.2: Preliminary MTT schematic for tamoxifen schematic. Blue line – dH₂O; C – control with complete medium blank, figures – drug concentration (μ M), B- Empty blank

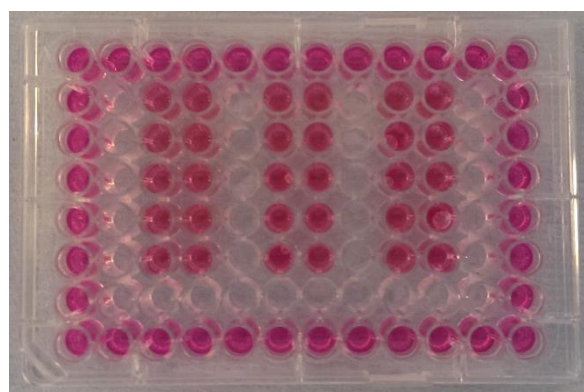


Figure 2.3: Plate freshly set up for preliminary MTT testing. Peripheral wells filled with basal medium to protect the central wells from desiccation.

Early preliminary work served to establish the effective range for the drugs under investigation with reference to data collected from other laboratories (Fan *et al.*, 2006; Zheng, Kallio and Härkönen, 2007) to cast that 'net'. Through the course of this early investigation and in the tests that follow, the incremental difference of drug concentrations was narrowed (*i.e.* from every 10µM to every 5µM and so on) to increase the resolution of results and highlight critical junctures. The MTT procedure will be discussed in the plural with the assumption of two plates being used for reasons discussed above.

2.2.6.4 MTT Procedure

After a 24-hour incubation period (@37°C, 5%CO₂) in which the cells become adhered and acclimatise to the 96 well plates reaching near confluency of about 90%, the plates are checked under inverted light microscope to ensure uniformity between the wells. They are subsequently aspirated, save from the peripheral 'guard' wells and filled with drugged medium at increments discussed in the previous section before being returned to incubation (@37°C, 5%CO₂). Although no drug is added to the control wells, their complete medium is still refreshed. During the earliest preliminary work for this assay, the post-inoculation incubation times for each drug and cell line was assessed with both 24, 48 and 72 hours being considered. It was determined that a 48-hour incubation period was ideal for comparative studies between the two drugs. *The remainder of this assay is to be performed in a darkened environment as the formazan product is light sensitive.* Following this 48-hour incubation period, all wells, again save for the barrier wells were gently aspirated of drugged medium and replaced with 50µl of 1µg/ml of MTT in complete medium. 100µl of DMSO was used for each of the blank wells. The plates are then incubated for 3.5 hours, a time previously standardised by the laboratory for MTT assays. Foil paper is used to cover the plates at this juncture to further protect the process from any discrepancies from reacting with light in a shared laboratory. Following incubation, the wells are then aspirated with great care as to not disturb any living cells which remain adherent to the microtiter plate and 150µl of DMSO is added to each well including the blanks. The plates, still covered in foil are then placed on a rocker at moderate speed for 10-20 minutes to ensure the complete

dissolution of the formazan product. Once the formazan-DMSO solution is adequately homogenised, the plates are then read at 540nm in a colorimetric plate reader. From the data attained from the assay, dose-response curves may be then drawn out using a spreadsheet application (In this case, Microsoft Excel). Using the information gathered from latter preliminary tests, it should then be possible to extrapolate the ED_{50} of the drugs which may then be used for determining the values to be used in drug combination assays.

2.2.6.5 MTT Combination Assay

Once the ED_{50} values of tamoxifen and chloroquine were determined for all three cell lines, investigation in to combination treatment could then be performed. The initial stage of this assay began with high resolution (increments of $2\mu M$) tamoxifen MTT assays similar to previous tests however with chloroquine being used as a constant variable. This has been illustrated by **Figure 2.3** where the concentration of tamoxifen (black) increases as chloroquine (red) remains constant. Initially tests were performed to standardise the concentration to be used for the chloroquine constant and to that extent, a plate assembled (in duplicate) which kept the typical ascending order of tamoxifen while in addition using the ED_{50} of chloroquine ($40\mu M$), employing the hypothesis that without either pharmacodynamics inhibition or potentiation between the two drugs, one can assume that the combined ED_{50} of one metabolically separate drug and another would lead to IC_{100} ; complete cell death.

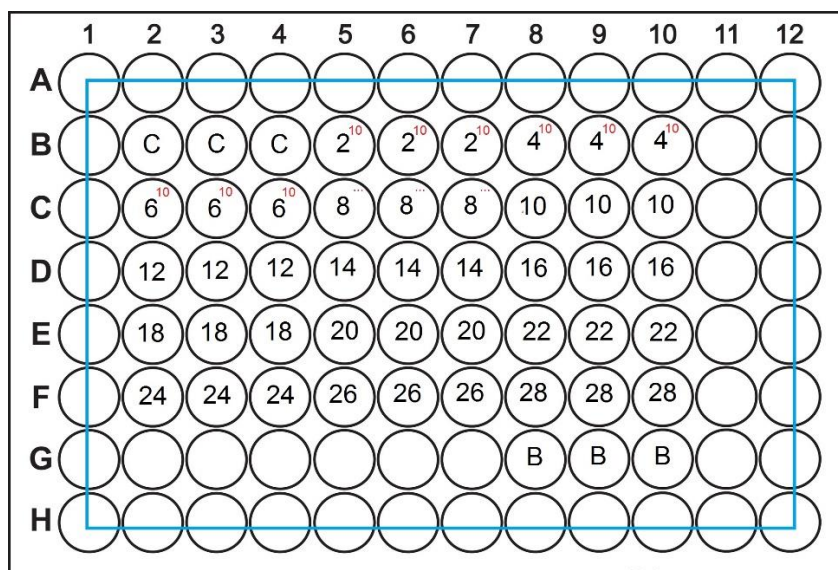


Figure 2.4: Typical template for drug combination assay. Blue = dH₂O, Black Figures = tamoxifen (μM) Red Figures = chloroquine (μM). Note all doses are done in triplicate.

Once it became apparent through a massive discrepancy in the sum of ED₅₀ between tamoxifen and chloroquine that there was some form of drug interaction taking place, MTT assays utilising smaller titres (10μM, 20μM & 30μM) of chloroquine were used to further investigate this relationship. The information gathered from this detailed MTT analysis paved the way for a streamlined approach to the remainder of the investigation. Table 2.1 highlights the nine individual experiments completed as well as minimum work required; each experiment was performed in duplicate with additional efforts to ensure a high sample number and repeatability of results.

Modality			
Cell Line	Tamoxifen	Chloroquine	TAM+CQ
MCF-7 WT	2n	2n	2n
MCF-7 TMX	2n	2n	2n
MDA-MB-231	2n	2n	2n

Table 2.1: Illustrating the minimum work required for both MTT and Neutral Red evaluation of the breast cancer cell lines.

2.2.7 Neutral Red Assay

Second to the MTS (3-(4,5-dimethylthiazol-2-yl)-5-(3-carboxymethoxyphenyl)-2-(4-sulfophenyl)-2H-tetrazolium) and MTT protocols, the Neutral Red assay is one

of the main cytotoxicity tests used in environmental and biomedical sciences (Repetto, del Peso and Zurita, 2008). This technique is able to provide both a quantitative and qualitative estimation of cell viability through both absorbance spectrometry and light microscopy respectively. The assay depends on the ability of viable cells to integrate and bind this weakly cationic exogenous stain within acidic compartments such as lysosomes where they become positively charged, preventing egression. As perished cells may not take up the stain, overall cell viability may be assessed through the extraction of the dye from the population.

Because cell viability and proliferation (and thus cytotoxicity) may be demonstrated through pathways very dissimilar to that of the MTT, the Neutral Red assay allows us to support any developments on the relationship between chloroquine and tamoxifen with the aforesaid breast cancer cell lines.

2.2.7.1 NR Specific Reagent Setup

Neutral Red Stock Solution 4mgml⁻¹ - Neutral Red dye (Sigma Aldrich N4638) is dissolved in PBS 4mg: 1ml. This solution may be stored for up to 2 months at room temperature (20-30°C) protected by light with foil paper.

Neutral Red medium 40µg ml⁻¹ – The stock solution is diluted 1:100 with complete culture medium, for example, 12 ml of complete medium with 0.12 ml of stock solution (An ideal volume for one microtitre plate worth of work). This must be incubated at the culture temperature of the cells to be assayed to be used strictly the day before use.

Neutral Red Destain Solution- for extraction of dye from viable cells consisting of 50% 96%-ABV ethanol (Fisher Scientific), 49% deionized water and 1% glacial acetic acid (Fisher Scientific).

2.2.7.2 NR Cell Preparation

The MCF-7 WT, MCF-7 TMX and MDA-MB-231 cell lines were cultured and prepared in 96 well plates for fluorescence colourimetry as described in the previous chapter for MTT.

2.2.7.3 NR Preliminary Investigation

Due to the Neutral Red staining technique being similar in the fashion to the MTT assay as a measure of cell viability, much of the initial groundwork such as to narrow down effective dosage and attain the IC/ED values has already been done. However, it is still necessary to standardise this test to attain the variables for which to attain quantitative results supportive of the initial MTT. Two major variables were seeding density and incubation time

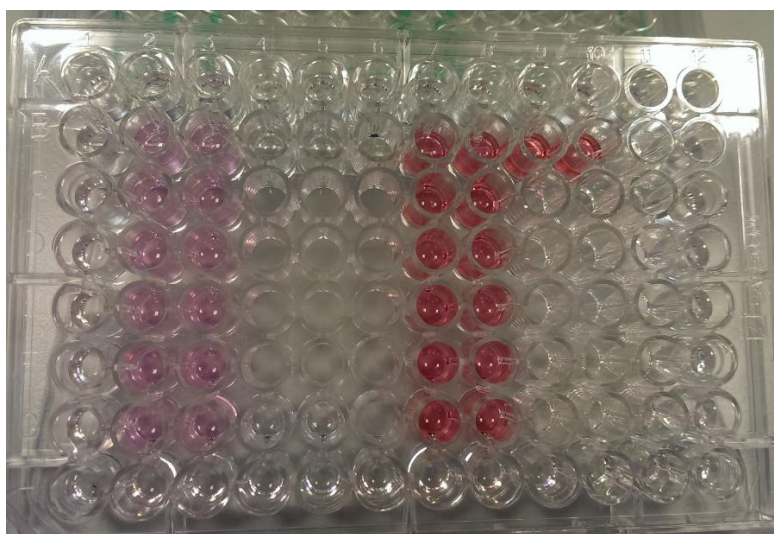


Figure 2.5: Visual colorimetric difference between seeding densities for chloroquine with MCF-7 WT after 4 hours

Figure 2.4 highlights visually the colorimetric difference in seeding density when MCF-7 cells were exposed steady to increments of chloroquine. This equivocal test, was performed by setting up a 96 well plate into two halves and seeding each half in duplicate to the dosing scheme used in the preliminary chloroquine MTT tests (0-140 μ M) with one half at a seeding density of 10,000 cells and the other at 15,000 cells after which they were subject to the Neutral Red assay (described below). This particular plate was intentionally incubated longer than recommended (Repetto, del Peso and Zurita, 2008) with the neutral red dye to visualise if and when either of the two sample sets reach saturation. As the sample set on the left had statistically significant gaps between each drug dose and the right sample set less so, it was decided that 10,000 cells per well was to be used as standard. Additionally, having many more than 10,000 of these cells per well may be damaging to the test as confluency is reached at a much faster rate leading to cell stress which may impact results accordingly.

2.2.7.4 NR Procedure

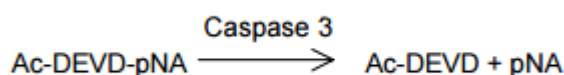
Once the preliminary assessment of the Neutral Red stain for compatibility with the cells at hand and the determination of necessary variables such as incubation time and seeding densities (with the help of the IC and ED figures attained from the previous MTTs) are complete, it is then possible to move on to the primary Neutral Red procedure.

Note: As with the MTT protocol, the following method is described with the assumption of working with a pair of sister plates.

Following the cell culture and seeding (see Figure 2.3 for typical plate layout) procedures laid out in the previous sections, the plates were then left to set and incubate for 24 hours (@37°C, 5%CO₂). The following day, the culturing medium is extracted from the wells by gentle aspiration and replaced by 150µl of medium drugged according to the template laid out in fashion identical to that in 2.2.6. Going ahead 48 hours, the previously made Neutral Red/Complete Medium was centrifuged for ten minutes at 600g to eliminate any precipitated dye crystals. The centrifugate is then decanted into a reservoir ready for use. All wells are drained of the drugged medium through gentle aspiration, after which 100µl of the 40µg/ml⁻¹ Neutral Red staining solution was added and left to incubate at 37°C for 2.5 hours after which point, the staining solution was then removed and 150µl of PBS (1x) was added to each well. At this juncture, each microtitre well may then be examined microscopically and images could be captured for qualitative assay of cellular morphology. All wells were photographed from each plate for each of the nine drug/cell modalities. Shortly after microscopic investigation, the PBS is then decanted from each of the treated wells including the blank and controls and 150µl of acidified ethanol destaining solution was then added to the wells to liberate the dye from the cells. After this stage, the plates would then be placed on a plate shaker at moderate speed for 10-20 minutes wrapped in foil as to avoid direct contact with light whilst separating the dye into the wells. After this point, the plate may then be inspected in a spectrophotometer at 540nm, the data from which can then be stored for subsequent quantitative analyses.

2.2.8 Caspase 3 Colorimetry Assay

The quantitative colorimetric analysis of the apoptosis biomarker caspase 3 is achievable in this assay through the observation of the hydrolysis of the peptide substrate acetyl-Asp-Glu-Val-Asp p-nitroanilide (Ac-DEVD-pNA) by caspase 3 and the subsequent release of p-nitroaniline (pNA) functional group as shown in this equation.



As pNA has a high absorbance (405nm), it may be easily assayed through the use of a spectrophotometer, thus caspase 3 activity may be easily observed through the cleavage of pNA from Ac-DEVD-pNA.

Caspase 3 belongs to a family of proteases important for the mediation of programmed cell death (apoptosis) for which it is a critical member. Caspase 3 is classed as an effector caspase and is one of the most widely investigated of the caspase family with its mechanism of action firmly characterised thus making it a key metabolite in the investigation of cell death.

2.2.8.1 Caspase 3 Assay Kit Components

5x Lysis Buffer

10x Assay Buffer

Caspase 3 powder

Ac-DEVD-pNA substrate

Ac-DEVD-CHO Inhibitor

p-Nitroaniline Standard

Water (17 megohm)

2.2.8.2 Caspase 3 Assay Cell Preparation

The kit insert for this procedure suggested using a volume of cells equal to 10^7 Jurkat cells thus, for this assay, a population of around 5 million MCF-7 WT, MCF-7 TMX and MDA-MB-231 cells were needed for each drug modality used

thus a total of four 6 well microplate wells are necessary per cell line as illustrated in **Figure 2.8**. Due to the sheer number of cells required, plates are seeded with around 2 million cells per well and incubated at 5% CO₂ at 37°C. After seeding to the 6 well plates, cells are incubated until 90+ confluency is reached in each of the plates, generally between 24 to 48 hours.

2.2.8.3 Caspase 3 Assay Procedure

Once the cells have reached 90+% confluency, the complete media in all the wells is discarded and replaced with drugged media respective to the ED₅₀ values of each drug for the cell line to be assayed and left to incubate at 5%

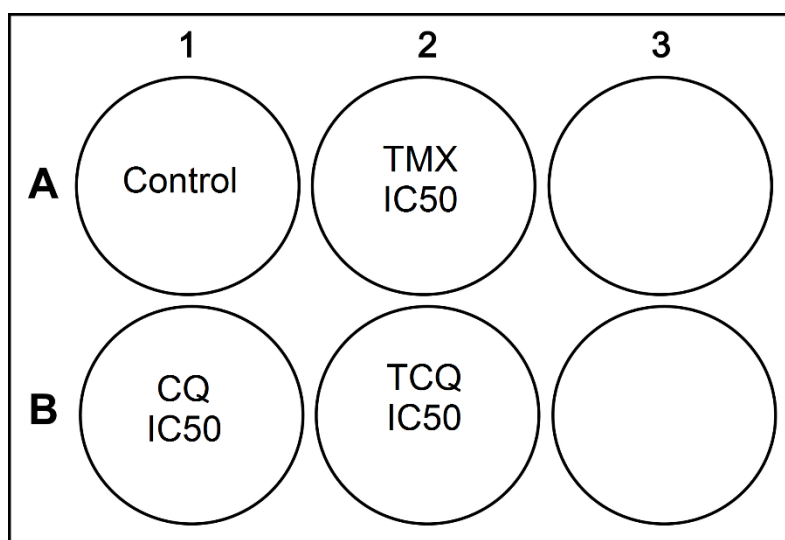
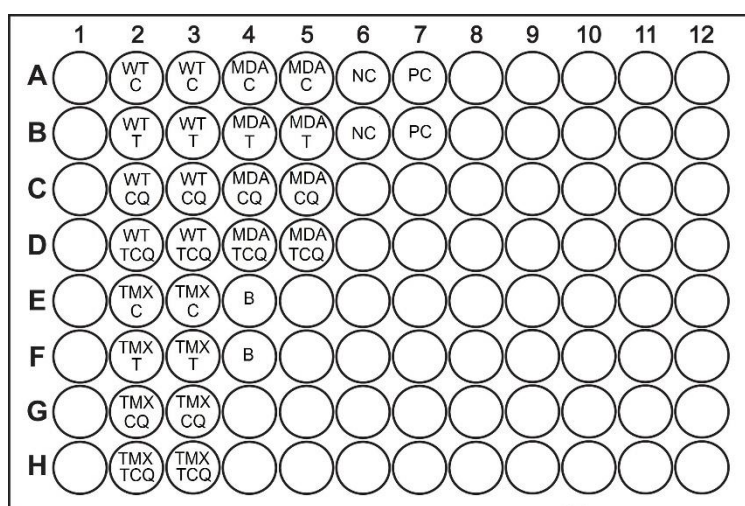


Figure 2.6: General seeding layout for cells in 6 well plate for c3pNA colorimetry assay

CO₂ at 37°C for 48 hours. After this incubation period, all the cells are pelleted by centrifugation at 600 x g for 5 minutes at 4°C. With the supernatant gently removed by aspiration, the cell pellets are then washed with 1ml of PBS by centrifugation. With the supernatant removed once more, the cells are then re-suspended in 100µl lysis buffer and incubated on ice for 20 minutes before centrifuging the lysed cells once more at 20,000 x g for 15 at 4°C. The supernatants (containing the now exposed intracellular components of cells) is then transferred to new Eppendorf tubes. These samples may then either be frozen at -80°C or used immediately for analysis. A 96 well plate is prepared as described in **Table 2.2** which is adapted from the kit insert illustrates the reaction scheme for the assay. As illustrated in **Figure 2.9**, the plate should consist of 4 wells per cell line, in duplicate, as to include the sample lysates from the control and three drug modalities. Wells should also be prepared for the positive and negative controls, also in duplicate. 5µl of cell lysate or

Caspase 3 Positive Control are added to their respective wells as indicated in **Table 2.2** and **Figure 2.9** and Caspase 3 Inhibitor to the negative control wells. The reaction is started by adding 10µl of caspase 3 substrate to each well and mixed by gentle shaking whilst avoiding foaming of the reagents. The plate was then covered and incubated at 37°C for 90 minutes to allow for cleavage and liberation pNA from its parent molecule. Incubation may be left overnight if signal is too low. The plate was then read at 405nm absorbance.



2.2.9 Annexin V ELISA

	Cell lysate	Caspase 3 5 µg/ml	1x Assay buffer	Caspase 3 inhibitor Ac-DEVD-CHO 200 µM	Caspase 3 substrate Ac-DEVD-pNA 2 mM
Reagent blank	----	----	90 µl	----	10 µl
Non-induced cells	5 µl	----	85 µl	----	10 µl
Non-induced cells + inhibitor	5 µl	----	75 µl	10 µl	10 µl
Induced cells	5 µl	----	85 µl	----	10 µl
Induced cells + inhibitor	5 µl	----	75 µl	10 µl	10 µl
Caspase 3 positive control	----	5 µl	85 µl	----	10 µl
Caspase 3 positive control + inhibitor	----	5 µl	75 µl	10 µl	10 µl

a family of calcium dependent phospholipid binding proteins. Although the Annexins as a whole have been well investigated in structure, their exact nature as a whole has yet to be determined however, Annexin V specifically has been found to play a major role in matrix vesicle-initiated cartilage calcification as a collagen-regulated calcium channel (Abcam). It has been determined that Annexin V has a high affinity to procoagulant phospholipids, specifically phosphatidylserine. It is the nature of phosphatidylserine (PS) and its relationship with Annexin V which makes Annexin V a metabolite of interest in this investigation. PS is housed intracellularly and is exposed during apoptotic events where it binds to Annexin V thus endogenous levels of Annexin V may be used as a marker for the initiation of apoptotic events.

2.2.9.1 Annexin V ELISA Assay Kit Components

20X Assay Buffer Concentrate

20X Wash Buffer Concentrate

Adhesive Films

Biotin-Conjugate anti-human Annexin V monoclonal antibody

Human Annexin V Standard

Microplate coated with monoclonal antibody to Human Annexin V (12x8)

Sample Diluent

Stop Solution (1M Phosphoric Acid)

Streptavidin-HRP

TMB Substrate Solution

2.2.9.2 Annexin V ELISA Cell Preparation

For this procedure, only the culture medium from MCF-7 WT, MCF-7 TMX and MDA-MB-231 cells was needed in order to investigate extracellular Annexin V expression as the usage of cell lysate would be unspecific to apoptotic role of PS/Annexin V. To this extent, the cell lines were cultured in a 12 well microplate as illustrated in **Figure 2.6**

Figure 2.9: The ELISA strip layout for Annexin V assay. This is repeated in duplicate.

WT = MCF-7 WT
TMX = MCF-7 TMX
MDA = MDA MB 231

a seeding density of 250,000 cells per well. These wells are then incubated for

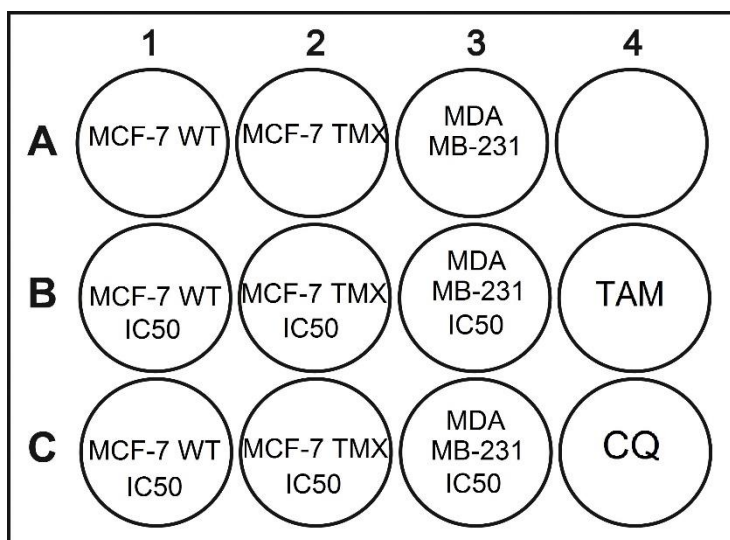


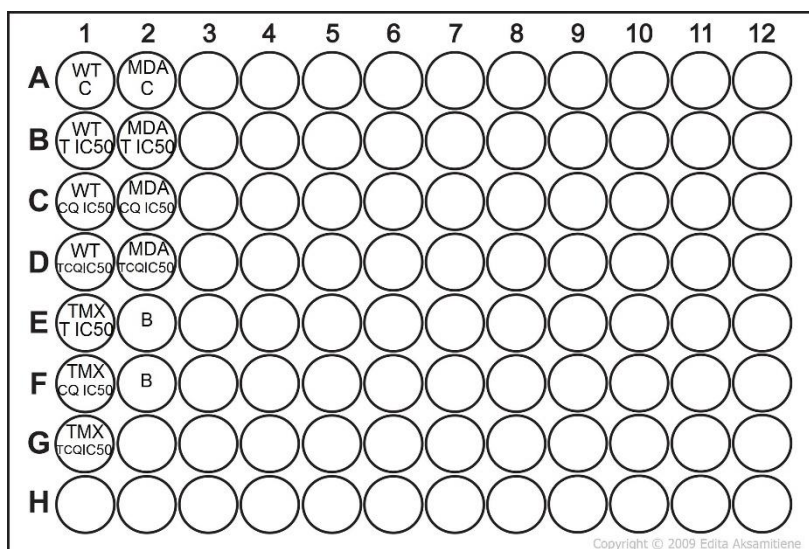
Figure 2.8: The 12 well microplate cell culture template used in cell culture for the Annexin V ELISA assay.

24 hours in 5% CO₂ at 37°C (or until around 95% confluency is attained).

2.2.9.3 Annexin V ELISA Procedure

24 hours after the initial incubation period, the cell culture medium of all the cells is discarded and refreshed. Wells in row B and C were then treated with their ED₅₀ concentration values for each cell line respectively attained from the prior 48 hour MTT assays (Row A was the control row and thus cells in this well were not treated). After administration of treated medium to the wells, the plate was then returned to the incubator for a further 48 hours.

On the day of assay all materials and reagents were equilibrated to room temperature before being prepared and diluted to their appropriate 1x concentrations. In total, 6 microplate strips were to be used; four for the sample assay and two for the standard, both in duplicate. Figure 2.7 overleaf illustrates the general layout of the assay. The necessary micro well strips for all the samples, standards and controls were twice washed by thorough pipette aspiration with 400µl of 1X Wash Buffer for 10-15 seconds each per wash taking care not to scratch the surface of the microplate. After washing, the wash



buffer was removed by gentle percussion onto an absorbent paper towel and left facing face down. 100µl of prepared standards and negative control were applied to the microplate strip marked for it. 50µl of cell culture medium taken from the cultured cells in the 12 well plate was added to the appropriately marked wells with 50µl of sample diluent. 50µl of 1X Biotin Conjugated Antibody was applied to all wells. The assay strips (on the ELISA plate provided) were then allowed to incubate in room temperature (18°C to 25°C) for 2 hours on a plate shaker set to 100rpm. After this incubation period, the adhesive film was removed and the wells carefully emptied and washed four times with 1X Wash Buffer solution before 100µl of 1X Streptavidin-HRP was added to the wells, including the blanks. The wells were then further covered with adhesive film and left to incubate again at room temperature for 1 hour on a shaker set to 400rpm. After incubation, the strip was removed and the plates washed a further four times before they are refilled with 100µl of Tetramethylbenzidine (TMB) Substrate Solution for ten minutes in the dark. To monitor the colour progression of the TMB Substrate Solution, the plate was left to incubate within the plate reader until the primary standard reaches an optical density (OD) of 0.9-0.95 (which should be around the region of 10 minutes after the addition of TMB). Once this critical point is reached, 100µl of stop solution is added to each well in a quick, uniform manner through the use of a multi-channel pipette (Gilson) and read at 450nm with a spectrophotometer.

2.2.10 Acridine Orange Assay

Acridine Orange (AO) is a nucleic acid binding dye permeable in both living and dead cells and stains nucleated cells to create a green fluorescence. It may be used in the qualitative assessment of cell viability where nuclear fragmentation and lysosomotrophy may be visualised thus making it a valuable adjuvant to the continuing investigation. Like Neutral Red, AO is slightly cationic allowing it to exploit the pH gradients of cells however once protonated causes the dye to become trapped within the acidic compartments of cells such as the lysosomes and nucleoli. Through proton pump driven lysosomal acidity in living cells, AO becomes efficiently concentrated within these organelles; this aggregation may result in the precipitation of AO within the lysosomes into aggregated oligomeric granules which exhibit a red shift (640nm) compared to the monomeric AO which emits elsewhere at 525nm allowing for effective differentiation of the lysosomotrophy from the surrounding cellular structures (Immunochemistry, 2013). Through fluorescence microscopy it is possible to create composite images from both 640 and 525nm wavelengths to differentiate acidic compartments (orange) from the rest of the cellular bodies (green) such as in **Figure 2.5**.

2.2.10.1 AO Specific Reagent Setup

Acridine Orange Stock Solution 1mM (266 µgml⁻¹)- *Acridine Orange (Sigma Aldrich) stain dissolved in filtered PBS to make 1mM AO stock solution*

Acridine Orange Staining Solution 2.7µM (1 µgml⁻¹)- *The AO Staining solution is diluted with complete medium to a final concentration of 1µg/ml*

2.2.10.2 AO Cell Preparation

The MCF-7 WT, MCF-7 TMX and MDA-MB-231 cells are harvested from their respective cell culture flasks. Prior to subculture, Circular 13mm diameter coverslips (Fisher Scientific) are sterilised in absolute ethanol for ten minutes in a petri dish and then washed twice with autoclaved PBS. The discs are then placed individually in a 24 well plate as shown in the template of **Figure 2.6**. It may be advisable to coat the coverslips in poly-L-lysine (Sigma Aldrich) for several minutes and rinse with PBS to ensure cellular attachment to the coverslip. Each well is then seeded with 100,000 cells to ensure an even +/-80%

confluency in 1ml of complete medium and left to incubate overnight (@37°C, 5%CO₂).

2.2.10.3 AO Procedure

The following day after seeding, the 24 well plate is inspected by light microscopy to assess and record cell adhesion and overall morphological state. Depending on confluency and how well the cells take to the coverslip, it is permissible to allow the cells one more day. On the day of testing, the wells are drained of culture medium and 500ul of medicated media is added to the wells as illustrated by **Figure 2.6** and left to incubate for 48 hours (@37°C, 5%CO₂). The drug concentrations chosen for this assay include the IC/ED 50 values ascertained from the prior MTT assay.

The wells were treated with 1ml of drugged medium (as detailed in **Figure**) and left to incubate for 48 hours at 37°C.

Following incubation with drugs, wells may be decanted of medium and coverslips removed (in succession) and transplanted on to a microscopy slide. The slide is then carefully bathed in 1µg/ml Acridine Orange/complete medium solution for 15 minutes before being gently aspirated off again. The coverslip is then washed very gently twice with distilled water before viewing under a fluorescent microscope.

2.2.11 Statistical Analysis

Two-way ANOVA followed by Tukey's multiple comparisons test was performed using GraphPad Prism version 6.00 for Windows, GraphPad Software, La Jolla California USA, www.graphpad.com". The data was presented as mean standard error (±SE) with values of P<0.05 being considered to be statistically significant and p<0.01 as highly significance.

Chapter Three

3.0 Results

3.0 Results

3.0.1 Subculture & Counting

Subculture of the three breast cancer cell lines; ER⁺ MCF-7 wildtype, MCF-7 TMX (tamoxifen resistant analogue) and ER⁻ MDA-MB-231 (oestrogen resistant line) was carried out as previously mentioned in chapter 2.2.3 b. The cell confluency was observed throughout culture period in order to both document and monitor the proliferation of the cells prior to subculture (**Figures 3.1-3.3**). MCF-7 WT and TMX cells would reach a confluence of around 80% in about 3 days of culture (@37°C, 5% CO₂) seeded at 2.5×10^5 while MDA-MD-231 cells took about 5-6 days to reach optimal subculture confluence. A typical low passage of either MCF-7 or MDA-MD-231 cells are strongly adherent and thus scraping may be necessitated in order to achieve maximum harvest during subculture.



Figure 3.1: MCF-7 WT with grape-cluster morphology typical of luminal breast cancer cells after four days of culture. Magnification x10
Figure 3.2: MCF-7 TMX cell line with four days after culture. Magnification x10

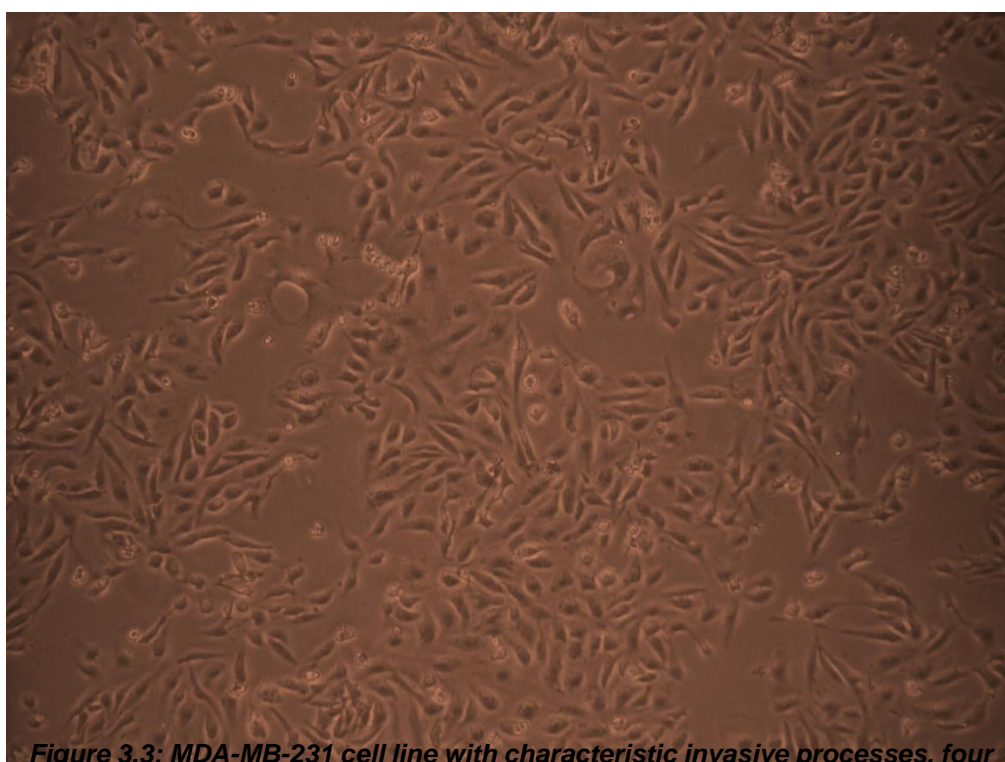


Figure 3.3: MDA-MB-231 cell line with characteristic invasive processes, four days after culture. Magnification x10

3.0.2 Doubling time assay

This basic proliferation assay is crucial when investigating any cell line in a laboratory; the understanding of doubling times for the cells permits a researcher more intimate knowledge of the cell lines and gives one the ability to estimate the time it will take to achieve a certain number of cells in preparation and execution of an assay. Independently, the number cell lines for each cell line was recorded over each day from an initial seeding density of 2×10^4 over the course of a week in 24 well plates. The results revealed MCF-7 TMX as the fastest rate of proliferation and MDA-MB-231 to be the slowest as evidenced from the images in section 3.1.1.

Cell type	MCF-7 WT	MCF-7 TMX	MDA-MB-231
Doubling Time (hours)	37	25	40

Table 3.1: Doubling times of the three cell lines MCF-7 WT, MCF-7 TMX and MDA-MB-231 as extrapolated from proliferation assay (\pm SE, n=3)

3.1 Quantitative Assay

3.1.1 MTT

Overleaf are the results achieved from the MTT assay (**Figures 3.1.1.1-3.1.1.1.9**) used to determine the cell viability and proliferation of the three breast cancer cell lines (MCF-7 WT. MCF-7 TMX and MDA-MB-231). Three drug modalities were investigated per cell line (with tamoxifen alone, with chloroquine alone and with a combination of chloroquine and tamoxifen) a total of three times per cell line (n=3). The data has been normalised to be represented in terms of cell survival as a percentage rather than absorbance in order to present the data in a way which all data sets may then be comparable with each other.

	TAM (μ l)	CQ (μ l)	TCQ (μ l of TAM + 10 μ l CQ)
MCF-7 WT	15.4	54	12
MCF-7 TMX	18	72	12
MDA-MB-231	18.5	44	12

Table 3.2: ED_{50} values for MTT assay of each cell line with drug modalities TAM, CQ & TCQ

3.1.1.1 MTT MCF-7 WT with Tamoxifen

MTT Cytotoxicity Assay of MCF-7WT against Tamoxifen

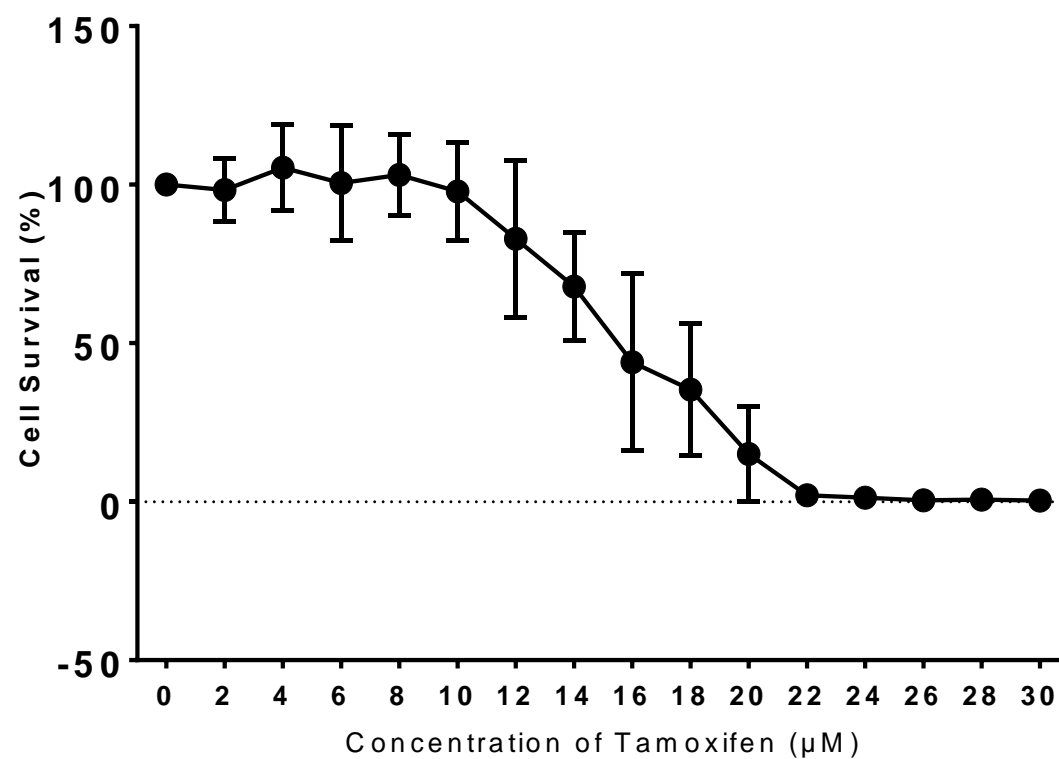


Figure 3.4: MTT cytotoxicity assay showing the effect of tamoxifen on MCF-7 WT (\pm SE, $n=3$). ED_{50} concentration reads at 15.4 μ M of tamoxifen. Signal fall significantly from 14 μ M onwards. There is near 100% cell death by 22 μ M

3.1.1.2 MTT MCF-7 WT with Chloroquine

MTT Cytotoxicity Assay of MCF-7 WT against Chloroquine

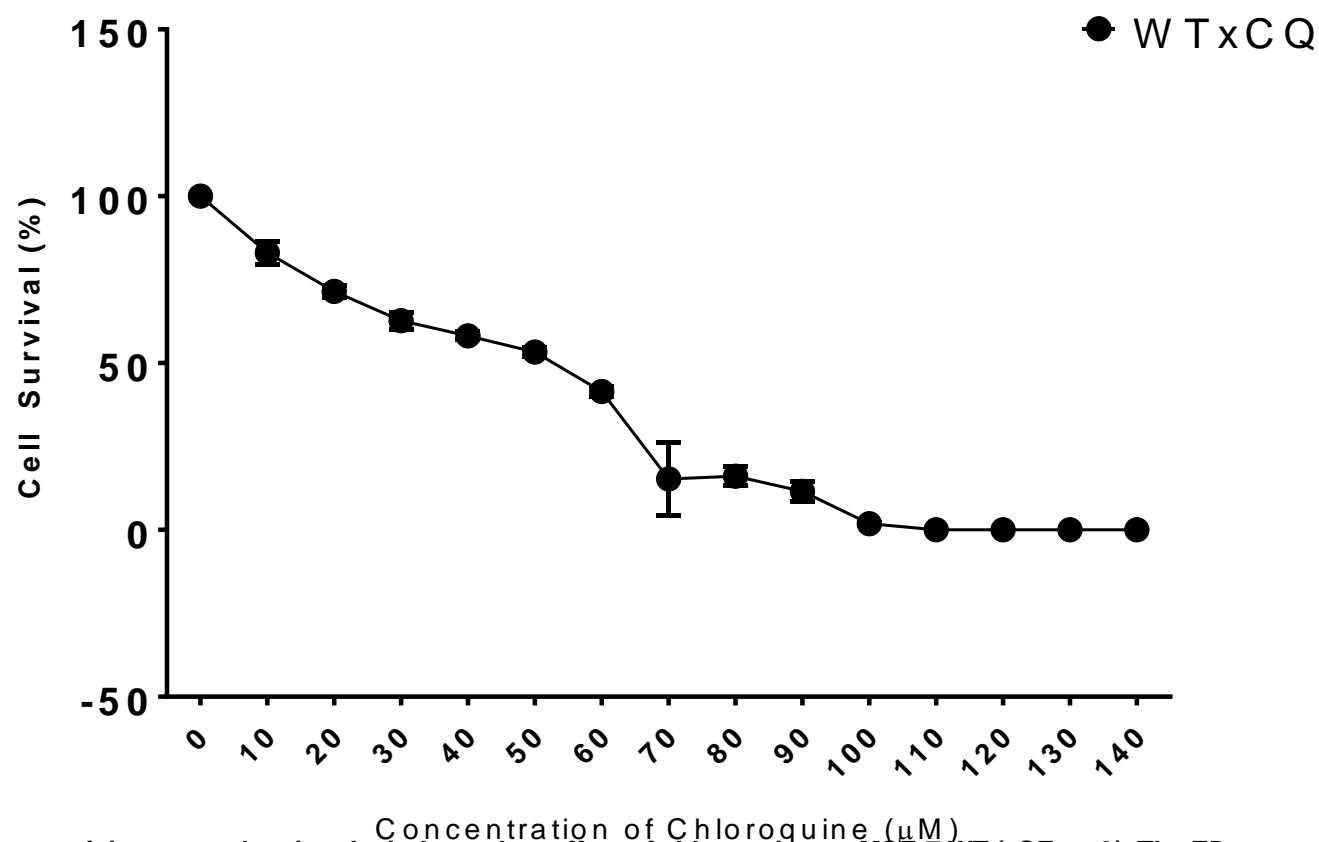


Figure 3.5: MTT cytotoxicity assay showing the independent effect of chloroquine on MCF-7 WT ($\pm\text{SE}$, $n=3$). The ED_{50} concentration reads at $52\mu\text{M}$ of chloroquine.

3.1.1.3 MTT MCF-7 WT with Tamoxifen and Chloroquine combined

MTT Cytotoxicity Assay of MCF-7 WT against Tamoxifen (10 μ M) and Chloroquine Combined

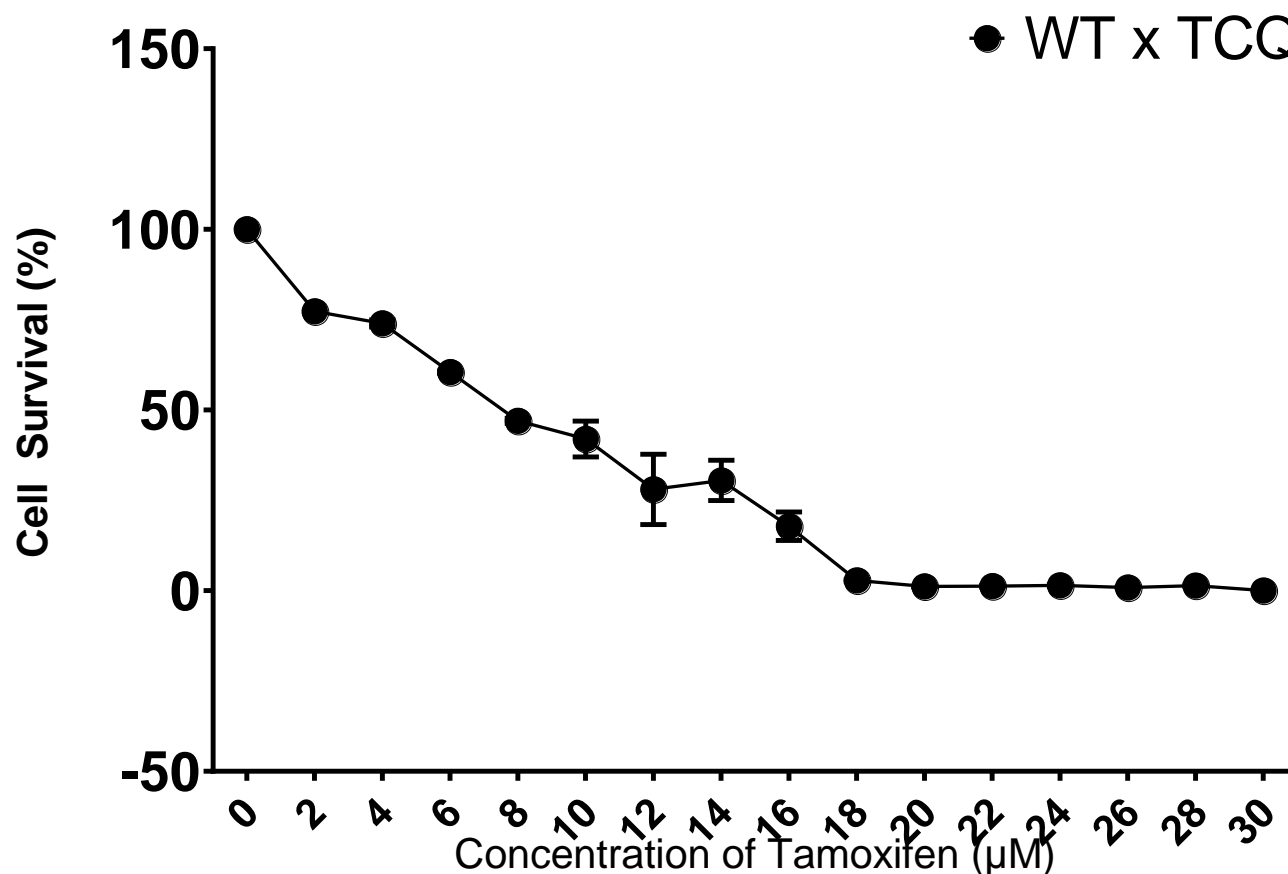


Figure 3.6: MTT cytotoxicity assay showing the combined effect of tamoxifen and chloroquine on MCF-7 WT (\pm SE, $n=3$). For this assay, the concentration of chloroquine is a static 10 μ M. The ED_{50} concentration reads at 12 μ M of tamoxifen.

3.1.1.4 MTT MCF-7 TMX with Tamoxifen

MTT Cytotoxicity Assay of MCF-7 TMX with Tamoxifen

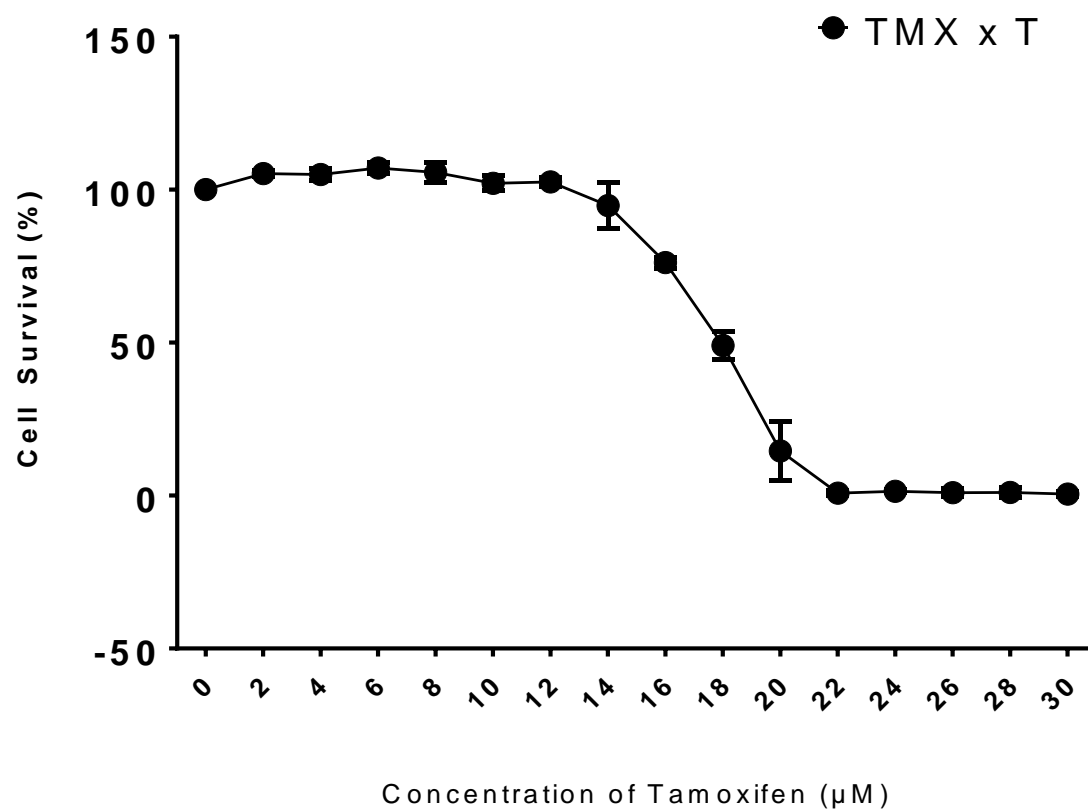


Figure 3.7: MTT cytotoxicity assay showing the independent effect of tamoxifen on MCF-7 TMX ($\pm\text{SE}$, $n=3$). ED_{50} concentration reads at $18\mu\text{M}$ of tamoxifen.

3.1.1.5 MTT MCF-7 TMX with Chloroquine

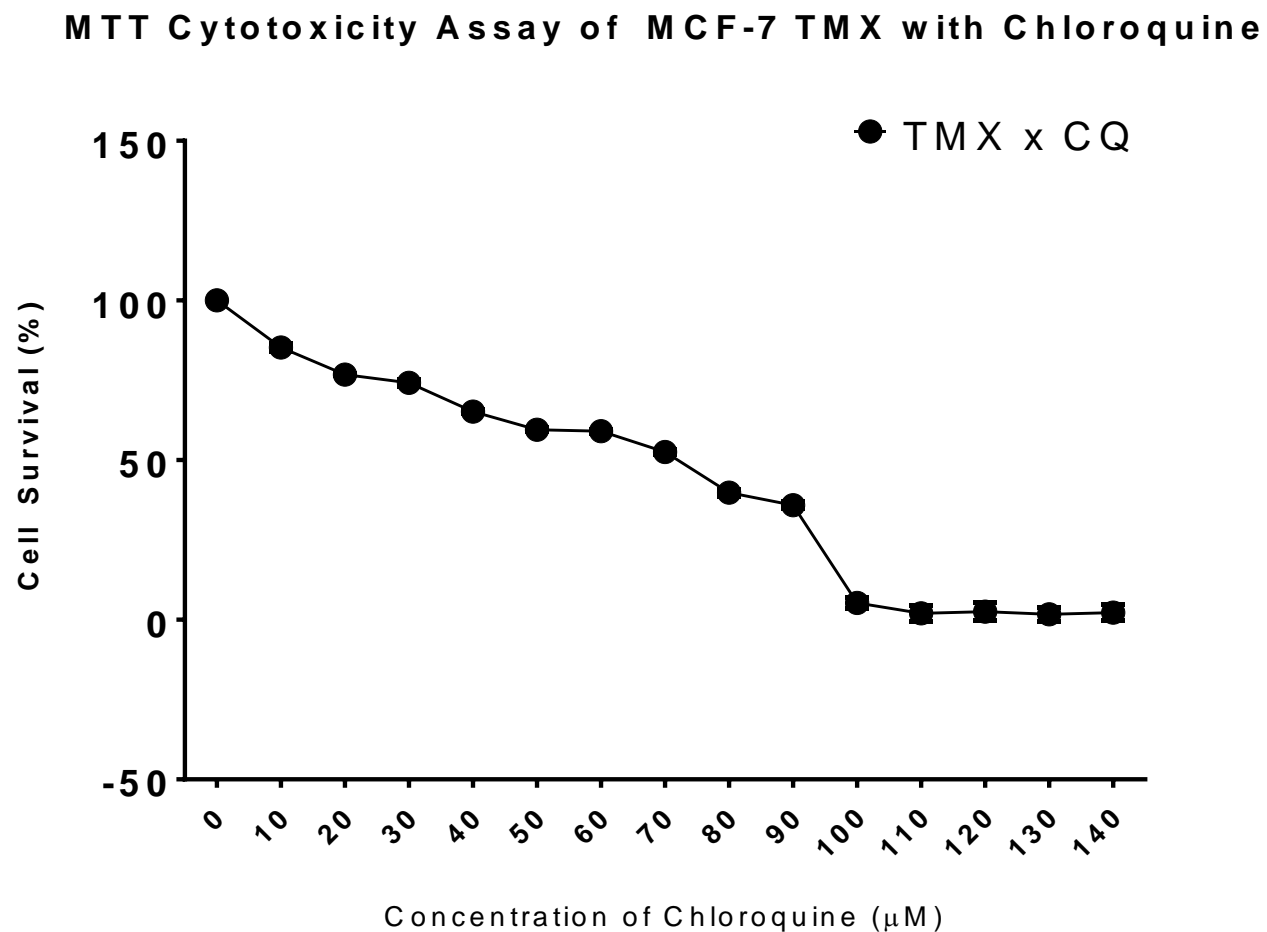


Figure 3.8: MTT cytotoxicity assay showing the effect of chloroquine on MCF-7 TMX ($\pm\text{SE}$, $n=3$). ED_{50} concentration reads at $72\mu\text{M}$ of chloroquine.

3.1.1.6 MTT MCF-7 TMX with Tamoxifen and Chloroquine combined

MTT Cytotoxicity Assay of MCF-7 TMX against Tamoxifen (10 μ M) and Chloroquine Combined

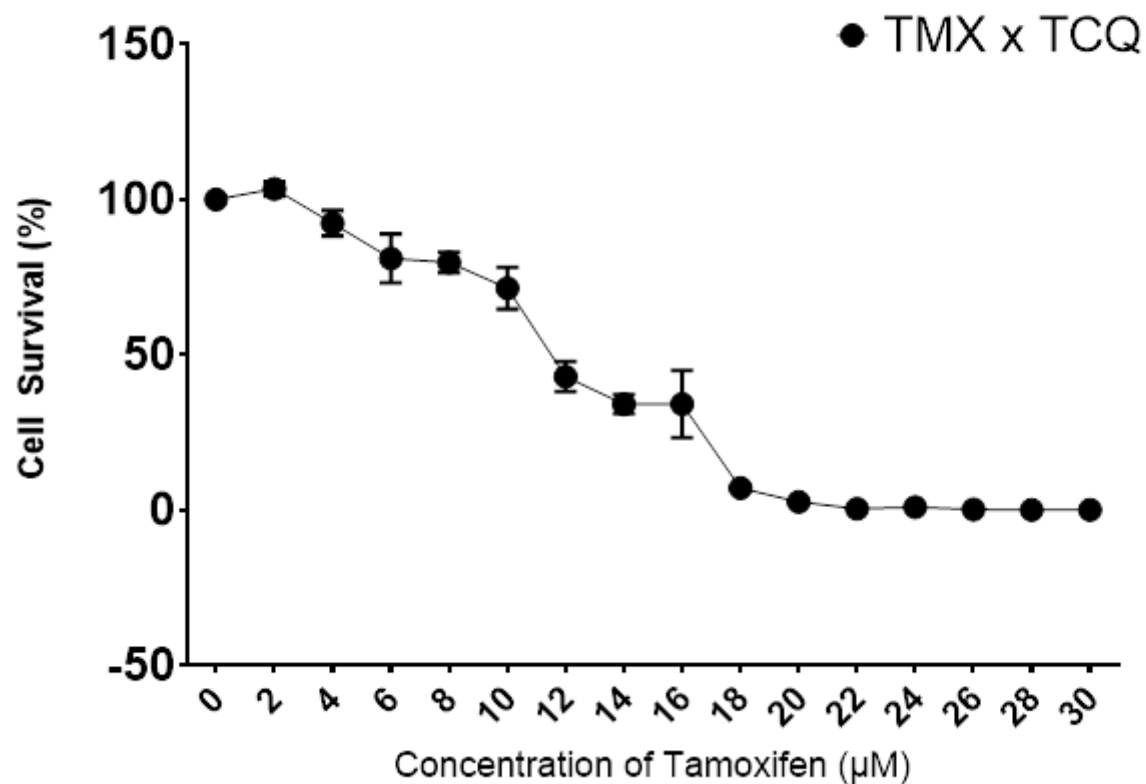


Figure 3.9: MTT cytotoxicity assay showing the combined effect of tamoxifen and chloroquine on MCF-7 TMX (\pm SE, $n=3$). ED_{50} concentration reads at 11.8 μ M of tamoxifen.

3.1.1.7 MTT MDA-MB-231 with Tamoxifen

MTT Cytotoxicity Assay of MDA-MD-231 with Tamoxifen

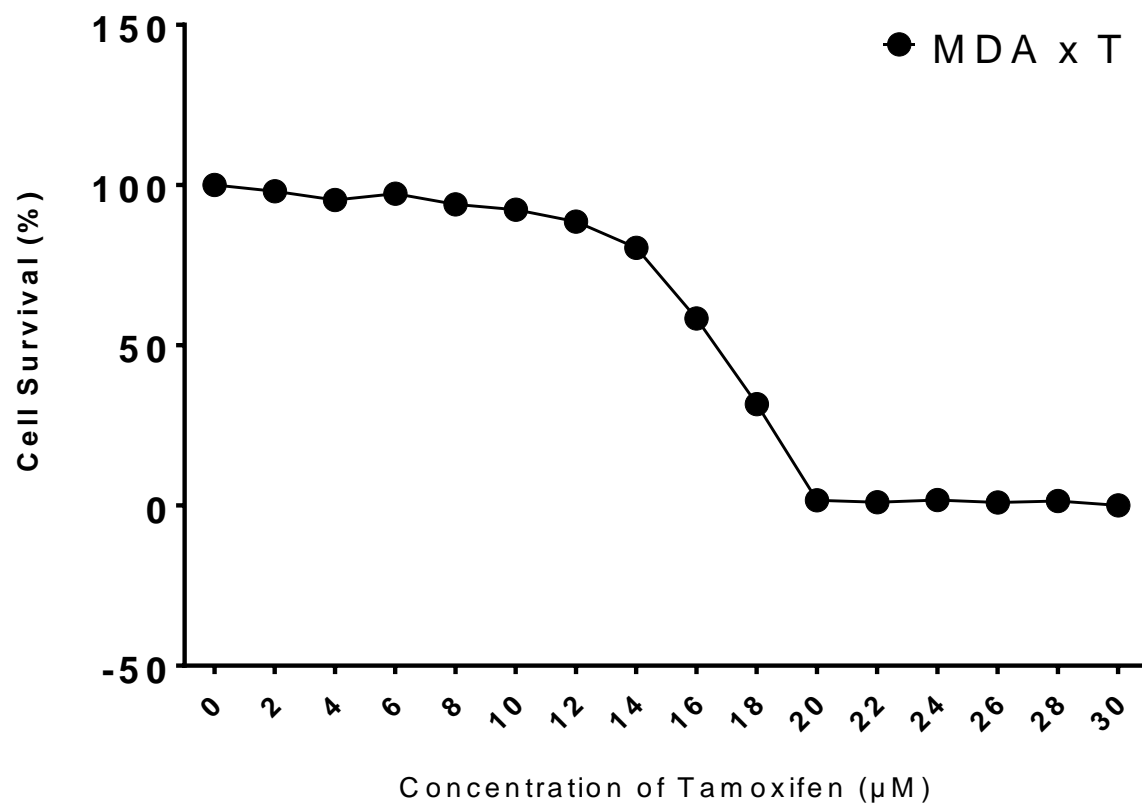


Figure 3.10: MTT cytotoxicity assay showing the independent effect of tamoxifen on MDA-MB-231 ($\pm\text{SE}$, $n=3$). ED_{50} concentration reads at $18.5\mu\text{M}$ of chloroquine.

3.1.1.8 MTT MDA-MB-231 with Chloroquine

MTT Cytotoxicity Assay of MDA-MD-231 with Chloroquine

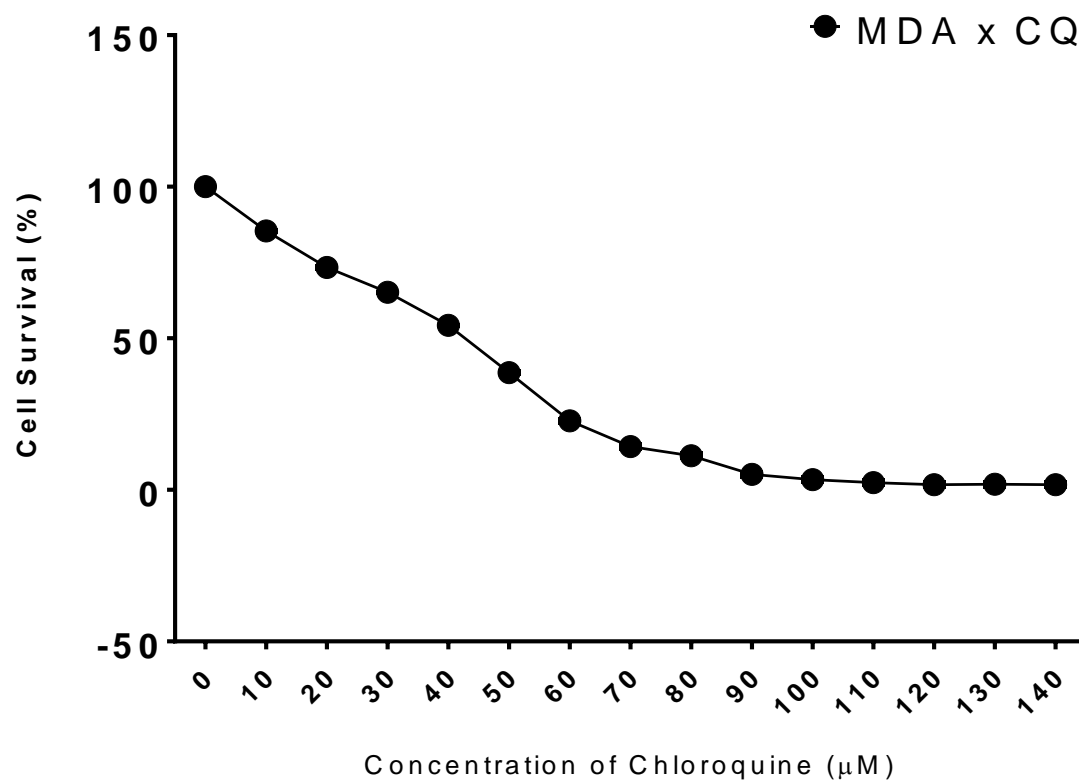


Figure 3.11: MTT cytotoxicity assay showing the independent effect chloroquine on MDA-MB-231 ($\pm\text{SE}$, $n=3$). ED_{50} concentration reads at $44\mu\text{M}$ of chloroquine.

3.1.1.9 MTT MDA-MB-231 with Tamoxifen and Chloroquine combined

MTT Cytotoxicity Assay of MDA-MB-231 against Tamoxifen (10 μ M) and Chloroquine Combined

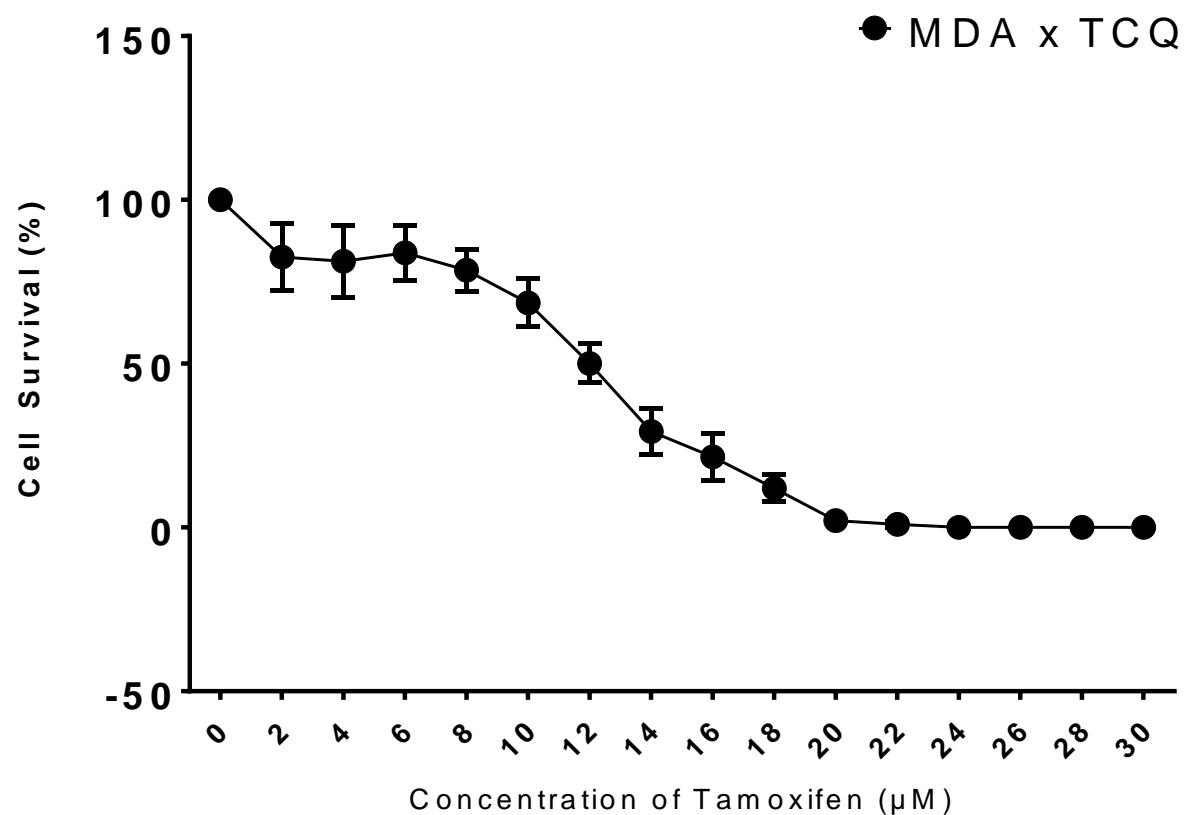


Figure 3.12: MTT cytotoxicity assay showing the combined effect of tamoxifen and chloroquine on MDA-MB-231 (\pm SE, $n=3$). Chloroquine kept as a static dose of 10 μ M. The ED_{50} concentration reads at 12 μ M of tamoxifen.

3.1.2 Neutral Red

The Neutral Red viability assay was performed on the three cell lines (MCF-7 WT, MCF-7 TMX and MDA-MB-231) as described in the Methods section. The data has been normalised to present the results as a percentage of total lysosomal/acidic compartment volume relative to that of the initial control values.

By serving as an alternative viability assay, NR staining was chosen as a means to verify the findings from the MTT assay. As seen in **Figures 3.1.2.1 to 3.1.2.9**, Neutral Red staining tends to exhibit initial absorbance peaks above that of the control when treated with the three drug modalities. In the MTT assay, the doses which present these NR peaks do not change significantly, implying a cytostatic drug effect; the NR assay allows one to witness the autophagic events that occur during this period which would have otherwise been mistaken as senescence. The exception, however is seen in MDA-MB-231 which presents more classical kill-curve when treated singularly with tamoxifen. All cell lines present the highest initial rise in signal when exposed to the tamoxifen-chloroquine drug combination with MCF-7 WT, MCF-7 TMX and MDA-MB-231 respectively reaching lysosomal volume levels of 170, 240 and 175% greater than that of their initial controls. These results suggest that all three drug modalities elicit autophagic events and that the combined effect of the two drugs is potentiative.

In a similar fashion to that of the MTT assay, each drug modality conducted to at least 3 individual times (n=3), doses within each individual plate were also applied in triplicate and the mean value attained.

3.1.2.1 Neutral Red MCF-7 WT with Tamoxifen

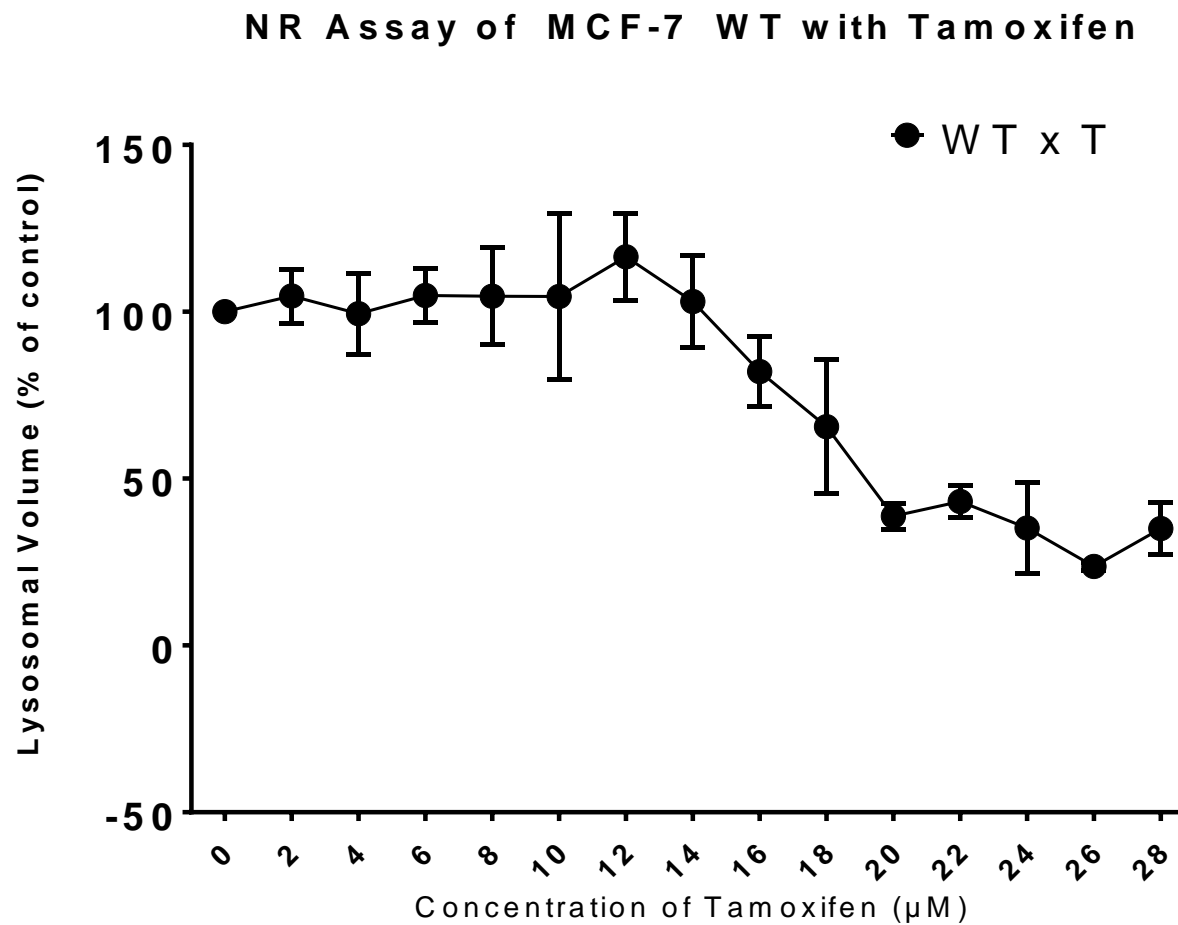


Figure 3.13: NR viability assay showing the effect of tamoxifen on MCF-7 WT ($\pm\text{SE}$, $n=3$). Peaking becomes evident at 12 μM tamoxifen

3.1.2.2 Neutral Red MCF-7 WT with Chloroquine

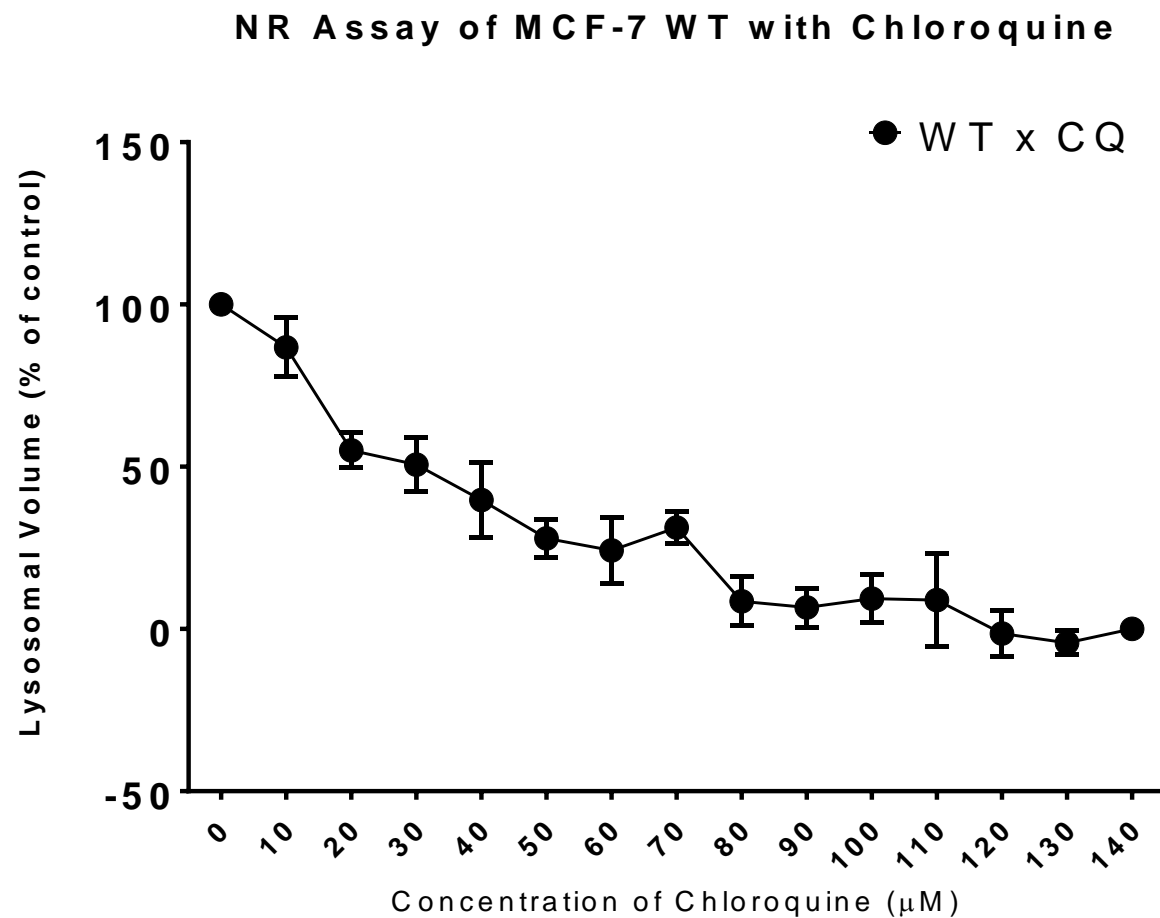


Figure 3.14: NR viability assay showing the effect of Chloroquine on MCF-7 WT ($\pm\text{SE}$, $n=3$). Peaking becomes evident after the first dose at $10\mu\text{M}$ of Chloroquine.

3.1.2.3 Neutral Red MCF-7 WT with Tamoxifen and Chloroquine Combined

NR Assay of MCF-7 WT with Tamoxifen (10 μ M) and Chloroquine Combined

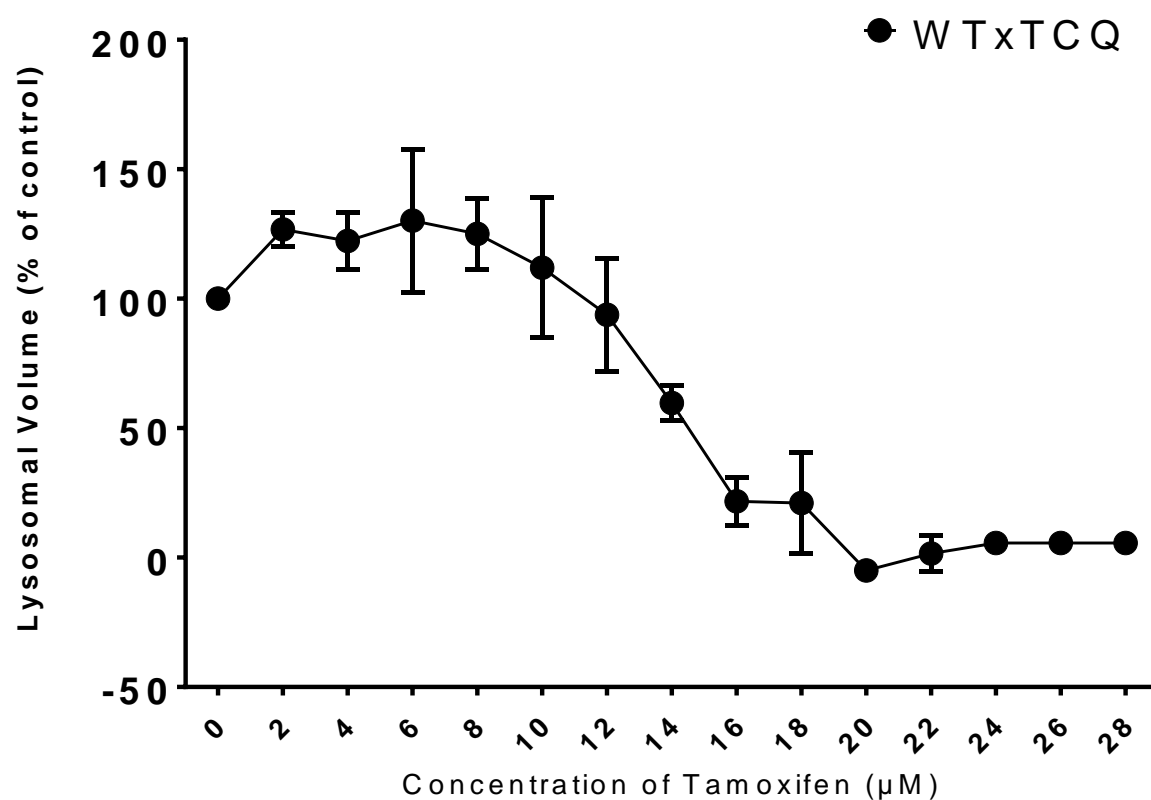


Figure 3.15: NR viability assay showing the effect of variable doses of tamoxifen (μ M) with a static concentration (10 μ M) of chloroquine on MCF-7 WT (\pm SE, $n=3$). Peaking becomes evident after the first dose at 10 μ M of Chloroquine.

3.1.2.4 Neutral Red MCF-7 TMX with Tamoxifen

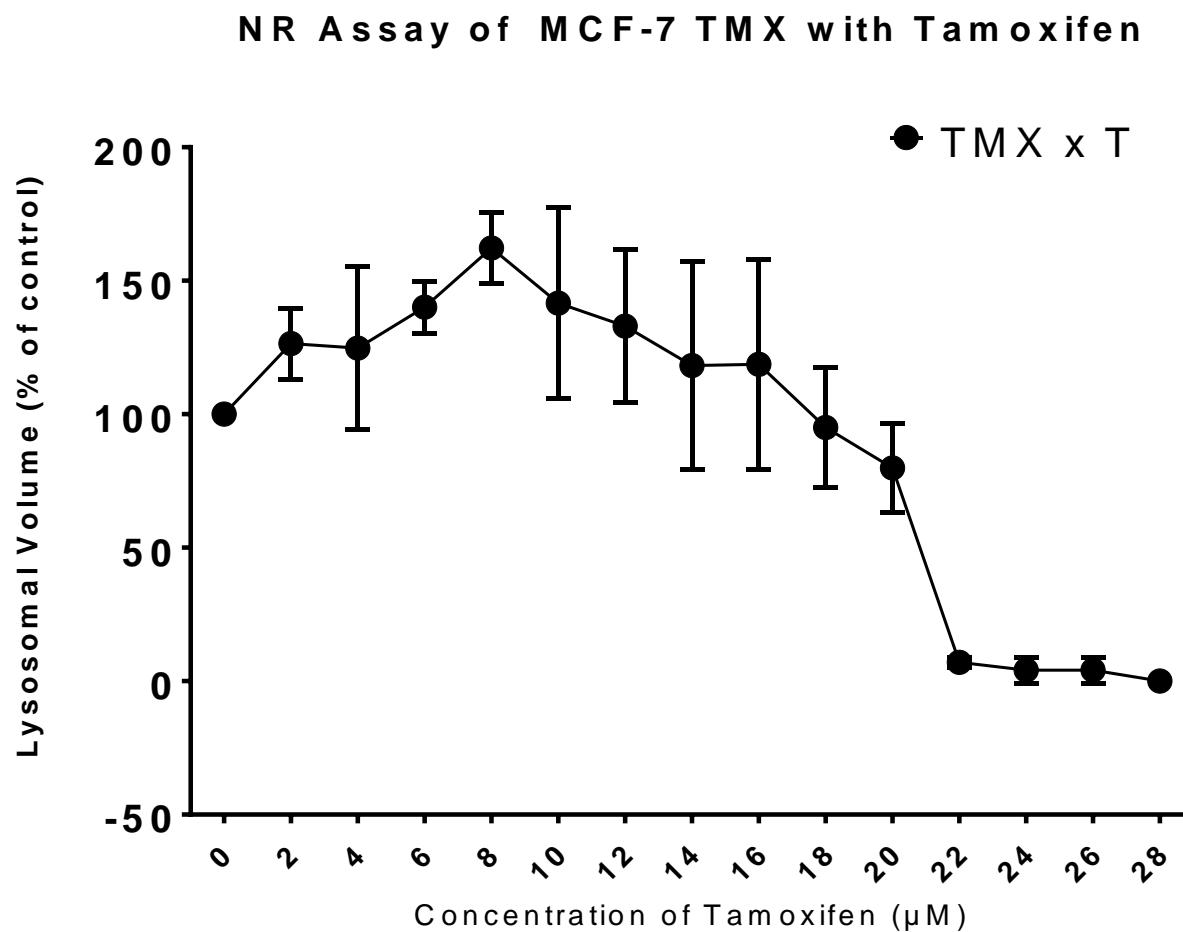


Figure 3.16: NR viability assay showing the effect of tamoxifen on MCF-7 TMX ($\pm\text{SE}$, $n=3$). Signal increases immediately after the first dose at $2\mu\text{M}$ of TAM and peaks at $8\mu\text{M}$ of TAM

3.1.2.5 Neutral Red MCF-7 TMX with Chloroquine

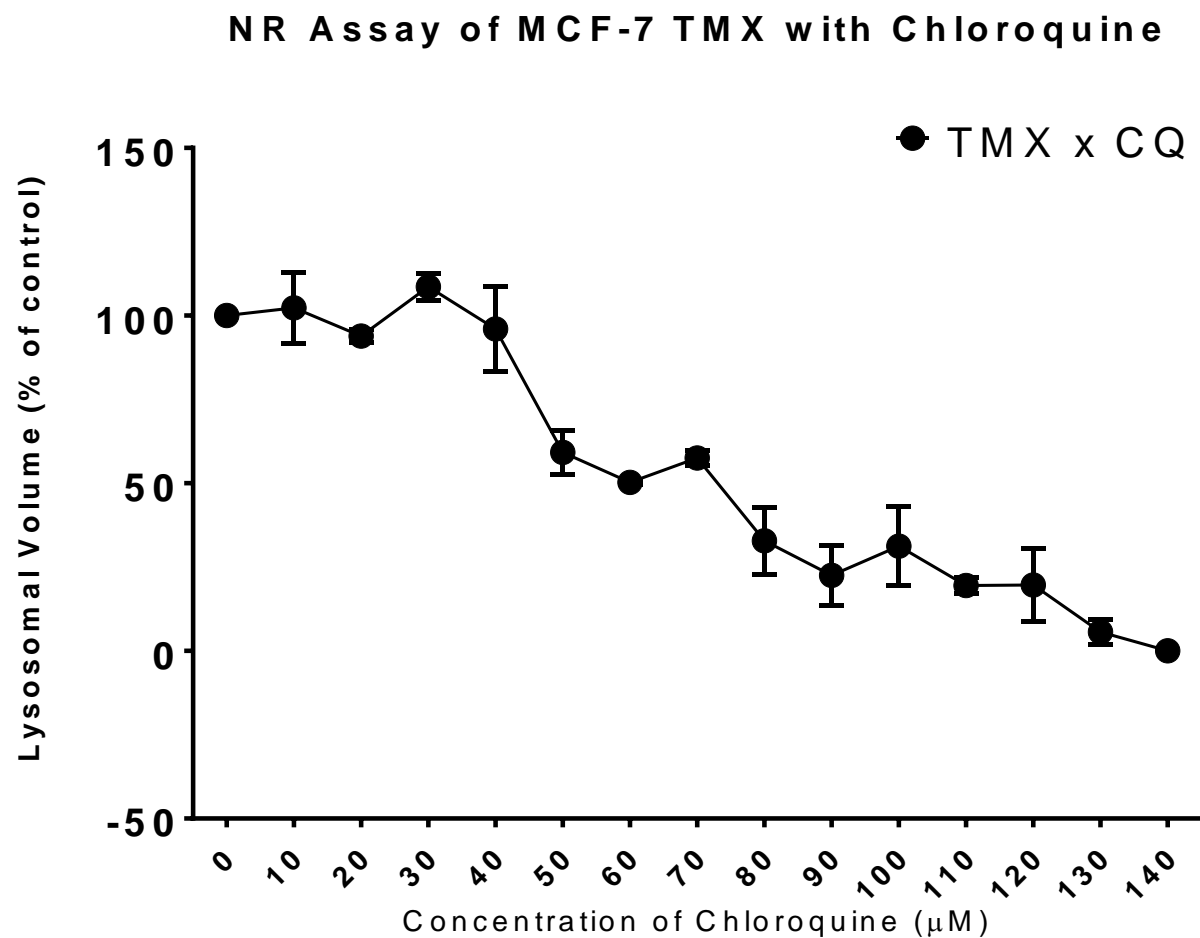


Figure 3.17: NR viability assay showing the effect of chloroquine on MCF-7 TMX ($\pm\text{SE}$, $n=3$). Signal increases immediately after the first dose at $10\mu\text{M}$ of TAM and peaks at $40\mu\text{M}$ of TAM

3.1.2.6 Neutral Red MCF-7 TMX with Tamoxifen and Chloroquine combined

NR Assay of MCF-7 TMX with Tamoxifen and Chloroquine (10 μ M) Combined

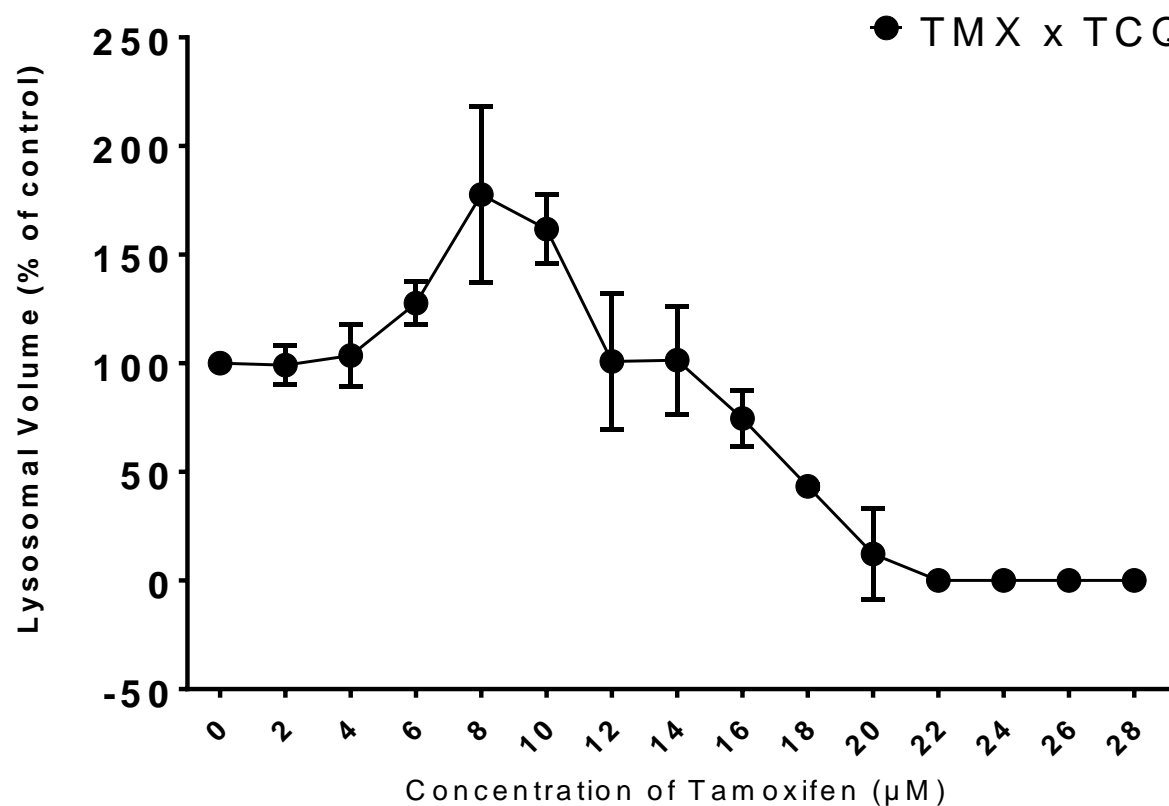


Figure 3.18: NR viability assay showing the effect of chloroquine on MCF-7 TMX (\pm SE, $n=3$). Signal increases immediately after the first dose at 10 μ M of TAM and peaks at 40 μ M of TAM

3.1.2.7 Neutral Red MDA-MB-231 with Tamoxifen

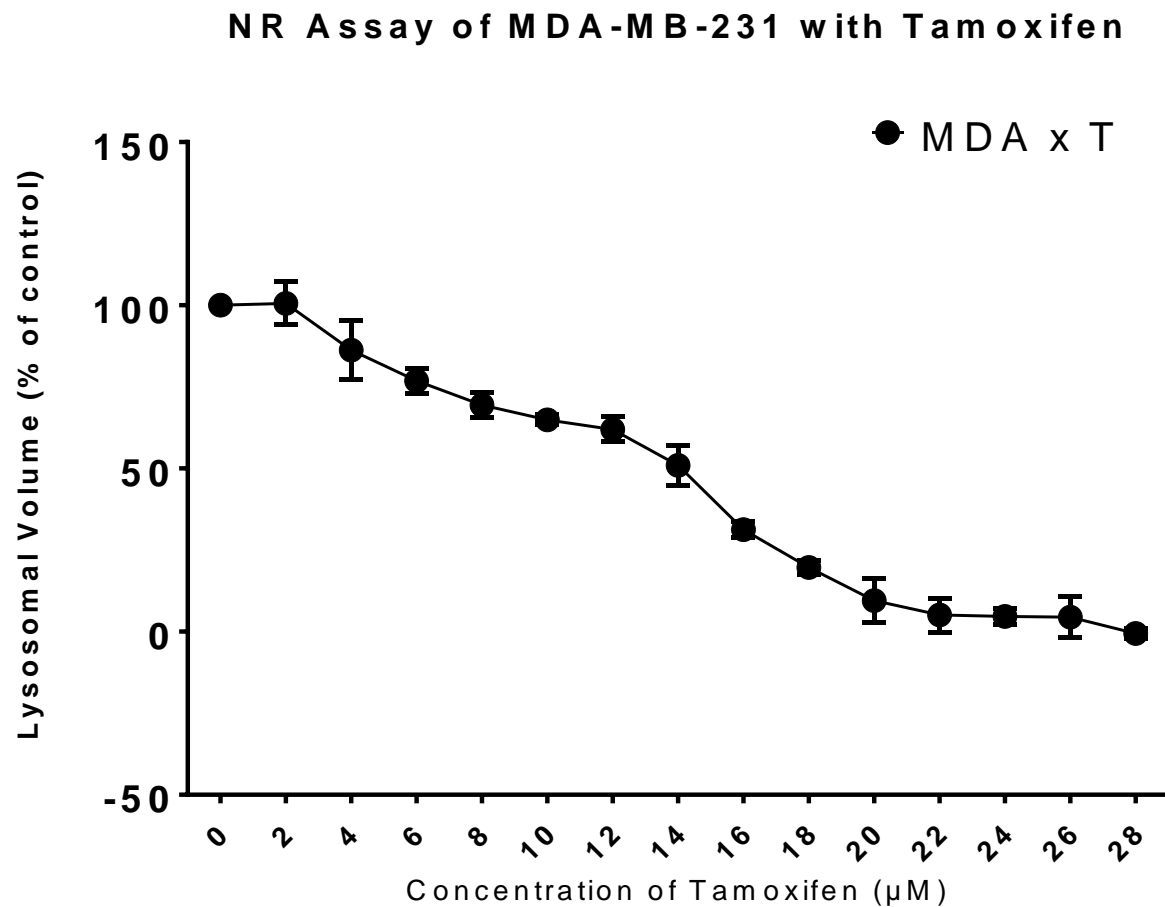


Figure 3.19: NR viability assay showing the effect of tamoxifen on MDA-MB-231 ($\pm\text{SE}$, $n=3$). Signal increases immediately after the first dose at $10\mu\text{M}$ of TAM and peaks at $40\mu\text{M}$ of TAM

3.1.2.8 Neutral Red MDA-MB-231with Chloroquine

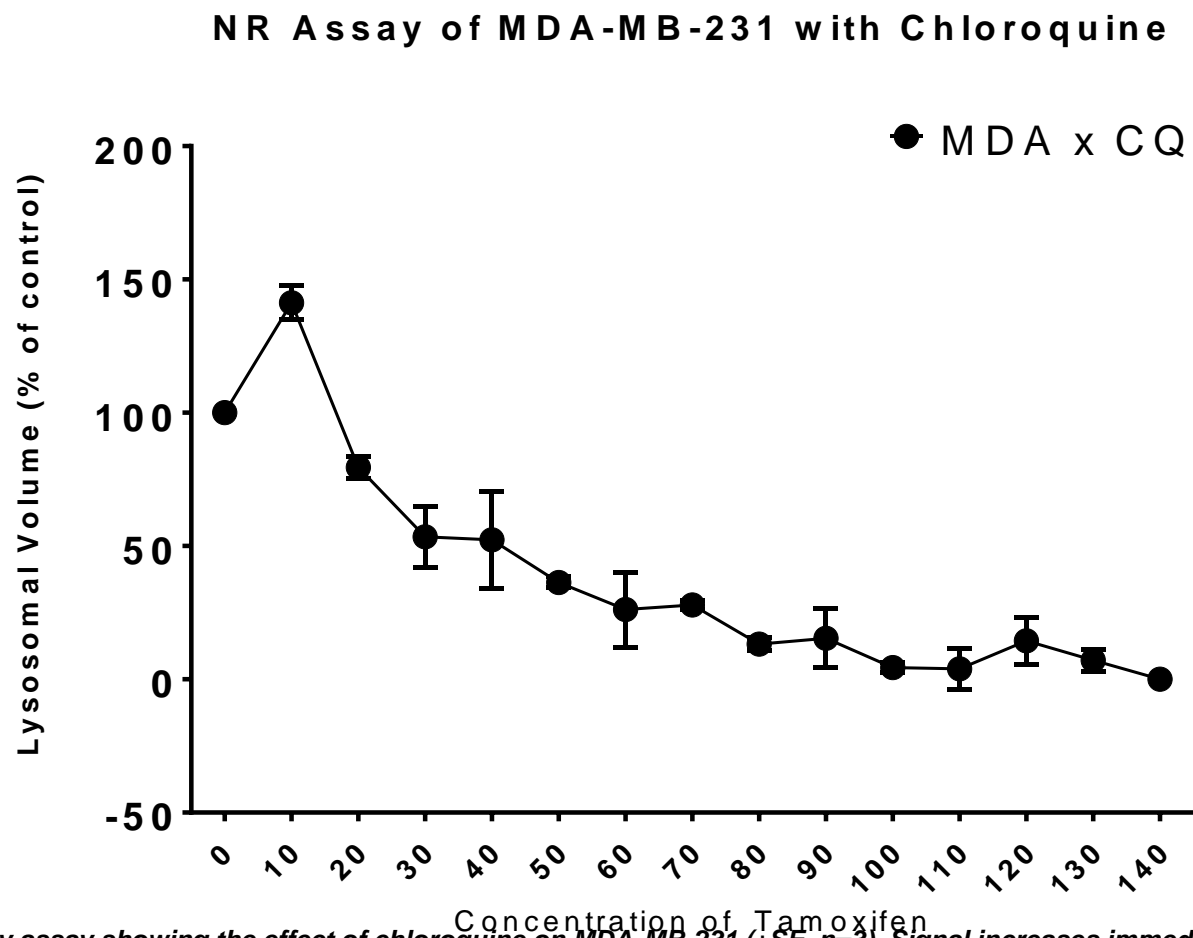


Figure 3.20: NR viability assay showing the effect of chloroquine on MDA-MB-231 (\pm SE, $n=3$). Signal increases immediately after the first dose at 10 μ M of TAM and peaks at 40 μ M of TAM

3.1.2.9 Neutral Red MDA-MB-231 with Tamoxifen and Chloroquine Combined

NR Assay of MDA-MB-231 with Tamoxifen and Chloroquine (10 μ M) Combined

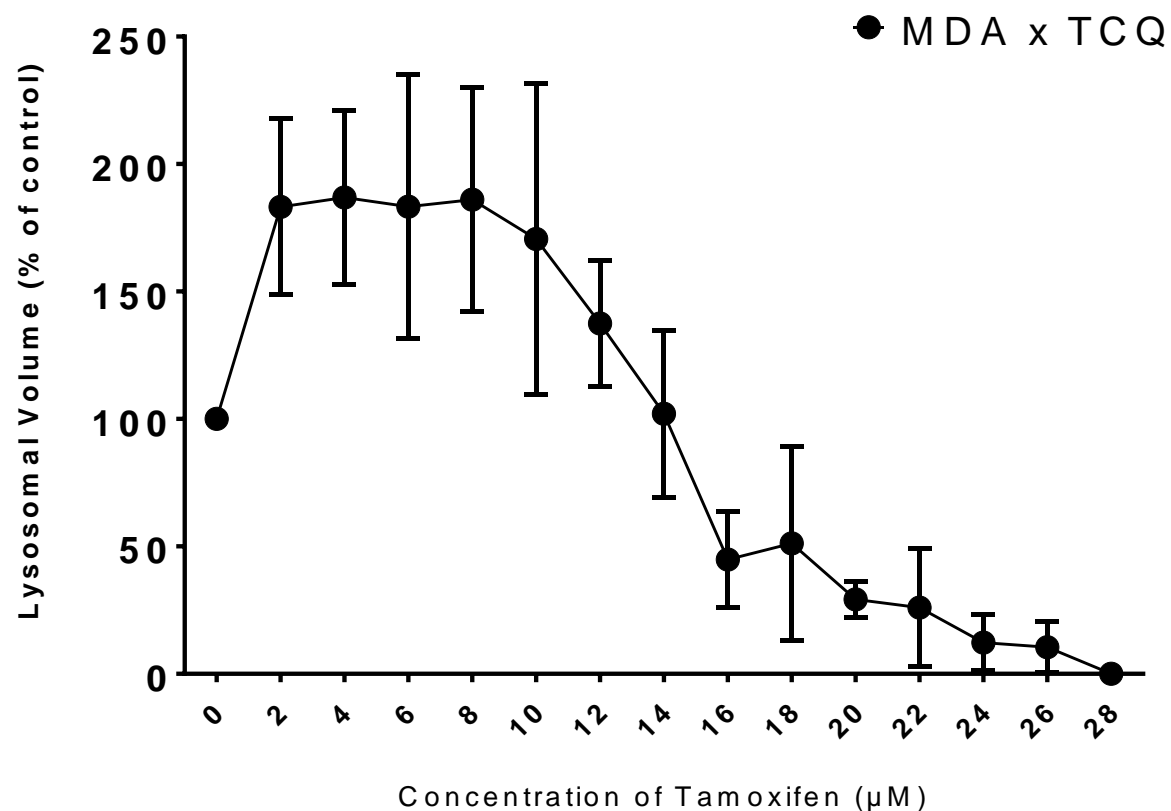


Figure 3.21: NR viability assay showing the effect of chloroquine (10 μ M) with a variable dosage of tamoxifen on MDA-MB-231 (\pm SE, n=3). Signal increases immediately to peak after the first dose at 2 μ M of TAM

3.1.3 Caspase 3 Colorimetry Assay

Caspase-3 colorimetry was employed in order to envisage the presence of caspase-dependent phenomena. The results from the colorimetric assay pictured below in figure 3.22 captures the findings from this assay. Caspase-like activity is detected in low levels throughout with the greatest expression being seen in cells treated with the combination (TCQ) modality. The most apparent caspase activity is visible from the MCF-7 WT cell line in response to combination treatment ($P \leq 0.001$). There is no real significant difference between the two controls and the treatment with tamoxifen yet chloroquine is seen to elicit a significant increase in caspase-like activity in both MCF-7 WT ($P \leq 0.001$) and MCF-7 TMX ($P \leq 0.05$) compared to untreated control. These results suggest that combined treatment has a high affinity for Caspase-3 activity relative to singular treatment.

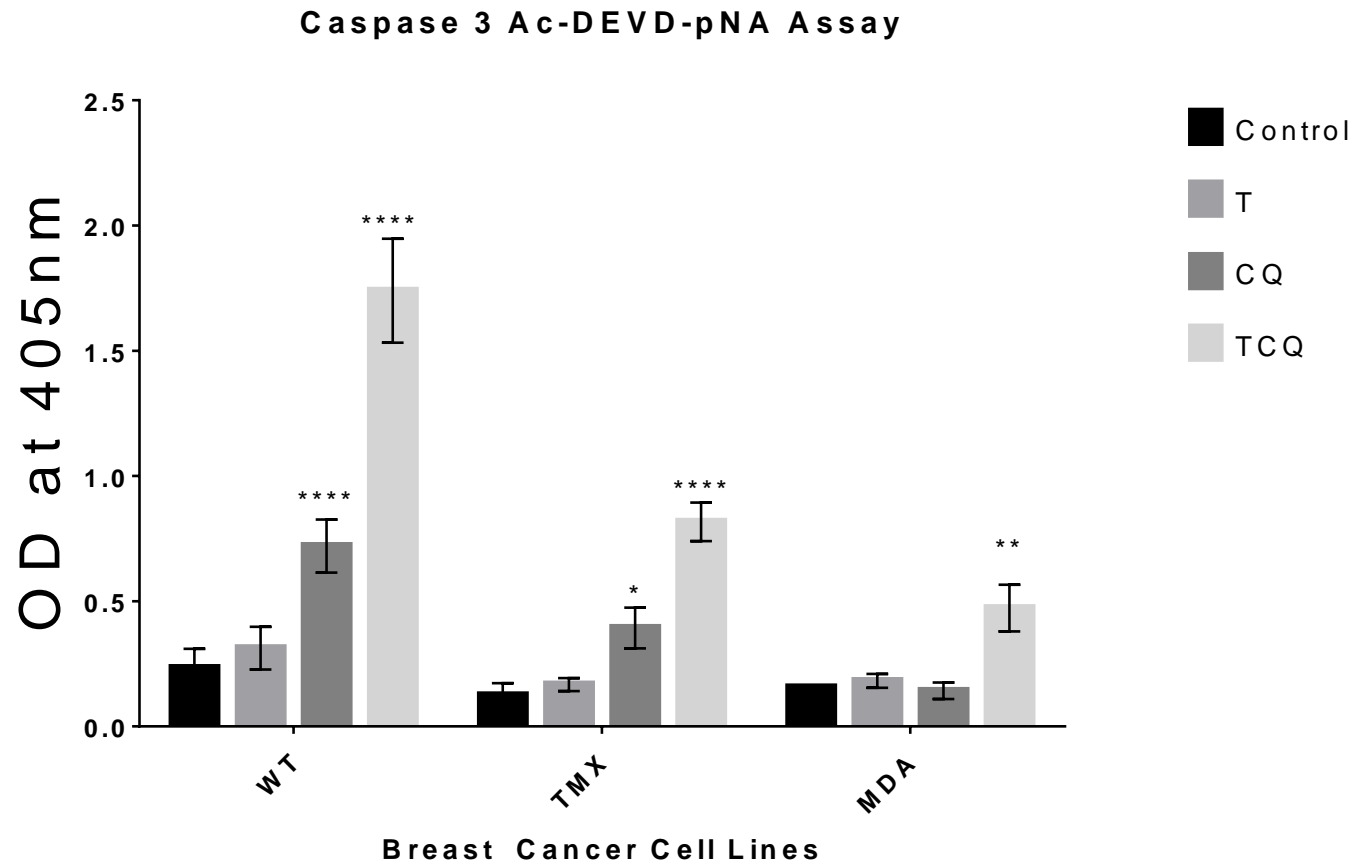


Figure 3.22: Relative caspase 3 activity after 48 hours' treatment with the 3 drug modalities on breast cancer cell lines MFC-7 WT, MCF-7 TMX and MDA-MB-231 with their respective ED_{50} dosage values. (C: control; T: tamoxifen; CQ: chloroquine; TCQ: tamoxifen/chloroquine combination)

3.1.4 Annexin V ELISA

The presence of Annexin V expression is thought to be associated with apoptosis, thus Annexin V ELISA (**Figure 3.23**) was performed 48 hours after treatment to give a snapshot of its activity at this time. The most significant Annexin V expression compared to its control sample is $P \leq 0.001$ was MCF-7 TMX's response to chloroquine. Conversely, there are visibly significant drops in Annexin V expression for the cell lines MCF-7 WT and MCF-7 TMX in response to tamoxifen ($P \leq 0.01$) and MDA-MB-231 in response to chloroquine ($P \leq 0.05$) compared to the readings of the untreated controls. These results are inconsistent with the high caspase-3 activity detected in combination treatment at this time and suggest low apoptotic activity present at this time point.

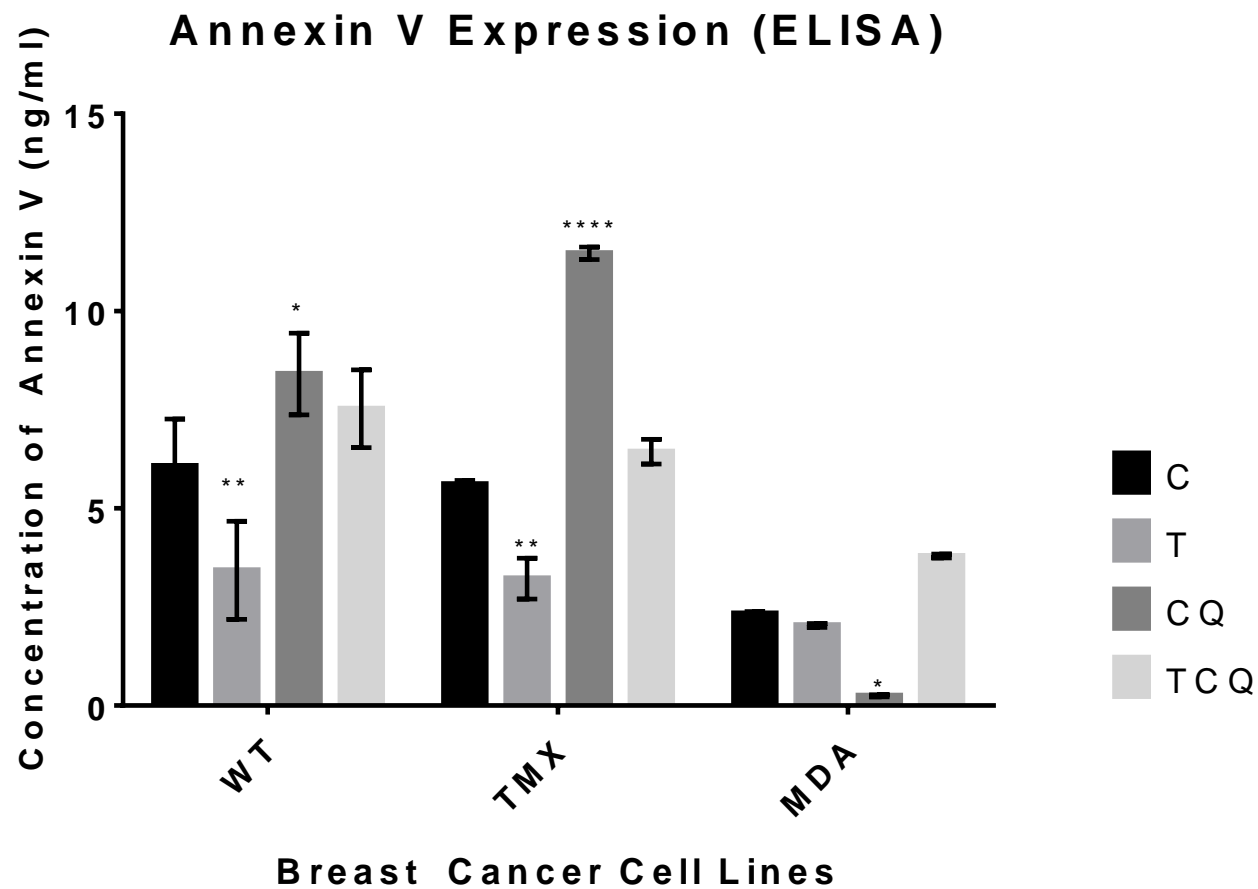


Figure 3.23: Relative Annexin V activity after 48 hours' treatment with the 3 drug modalities on breast cancer cell lines MFC-7 WT, MCF-7 TMX and MDA-MB-231 with their respective ED_{50} dosage values. (C: control; tamoxifen; CQ; chloroquine; TCQ: tamoxifen/chloroquine combination)

3.2 Qualitative Assay

The quantitative assays presented in the previous chapter were supplemented by a series of qualitative assays using light microscopy and fluorescence microscopy which would serve to better visualise the drug interaction with the three cell lines

3.2.1 Neutral Red Microscopy

Neutral red images (**Figures 3.2.2.1 - 3.2.2.4**) were attained simultaneously during the NR proliferation assay after the first wash step with PBS following incubation with the NR dye as stated in the chapter in the methods and materials (2.2.7), the wells were read under inverted microscope (Nikon) with phase contrast. Images were taken within ten minutes of immersion with PBS before the wells were subsequently aspirated and refilled with the NR destaining solution to continue the quantitative portion of the assay.

Qualitative analysis of Neutral Red serves to help visualise the uptake of the stain prior to spectroanalysis. For all cell lines, it was observed that of all the drug modalities, TAM conferred the least NR uptake, with CQ and TCQ both exhibiting a much greater uptake at comparable levels. The findings show that the treated cell lines convey a dose dependent response to the drugs, which peak in NR absorption at around their respective ED₅₀ values and to almost negligible levels at higher doses. This implies that autophagic events (And thus Type II Apoptosis) only occur up to a critical value before cells begin to take die through primarily caspase dependent or necrotic pathways.

3.2.2.1 Neutral Red Controls (All Cell Lines)

Control images were taken with an inverted light microscope from the sample plates on the same day which the Neutral Red assay was to be performed and thus were also subject to the NR Staining process. The red rods visible these images are neutral red crystals which get cleared after the second wash of PBS before detaining occurs. Faint neutral red uptake seen in all controls indicates the presence of lysosomes at rest.

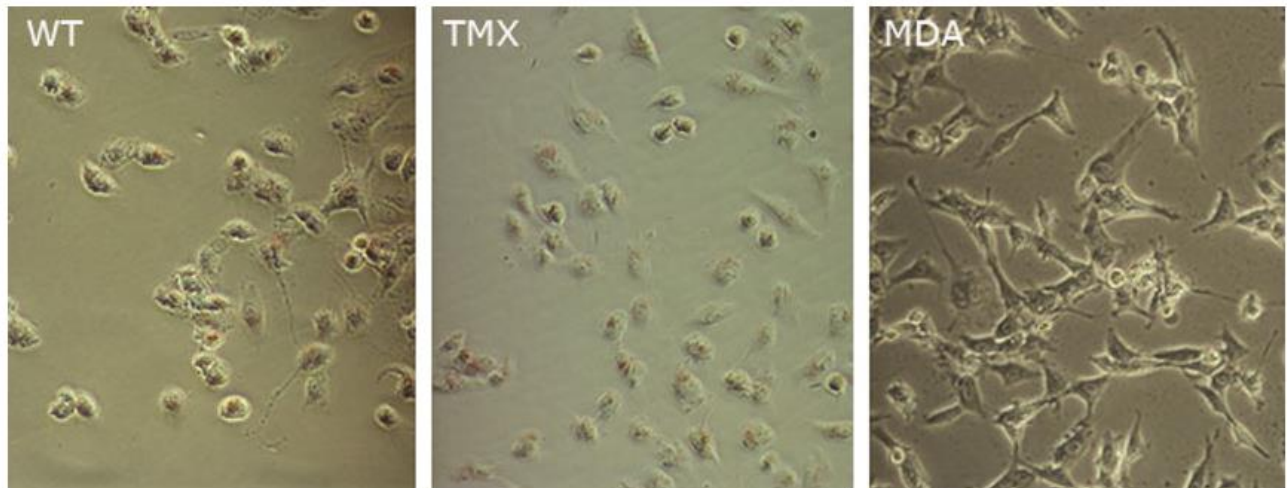


Figure 3.24: Neutral Red panel of control samples for MCF-7 WT, TMX and MDA, very low yet present neutral red uptake visible within cells indicating low lysosomal activity. Magnification x10

3.2.2.2 Neutral Red MCF-7 WT

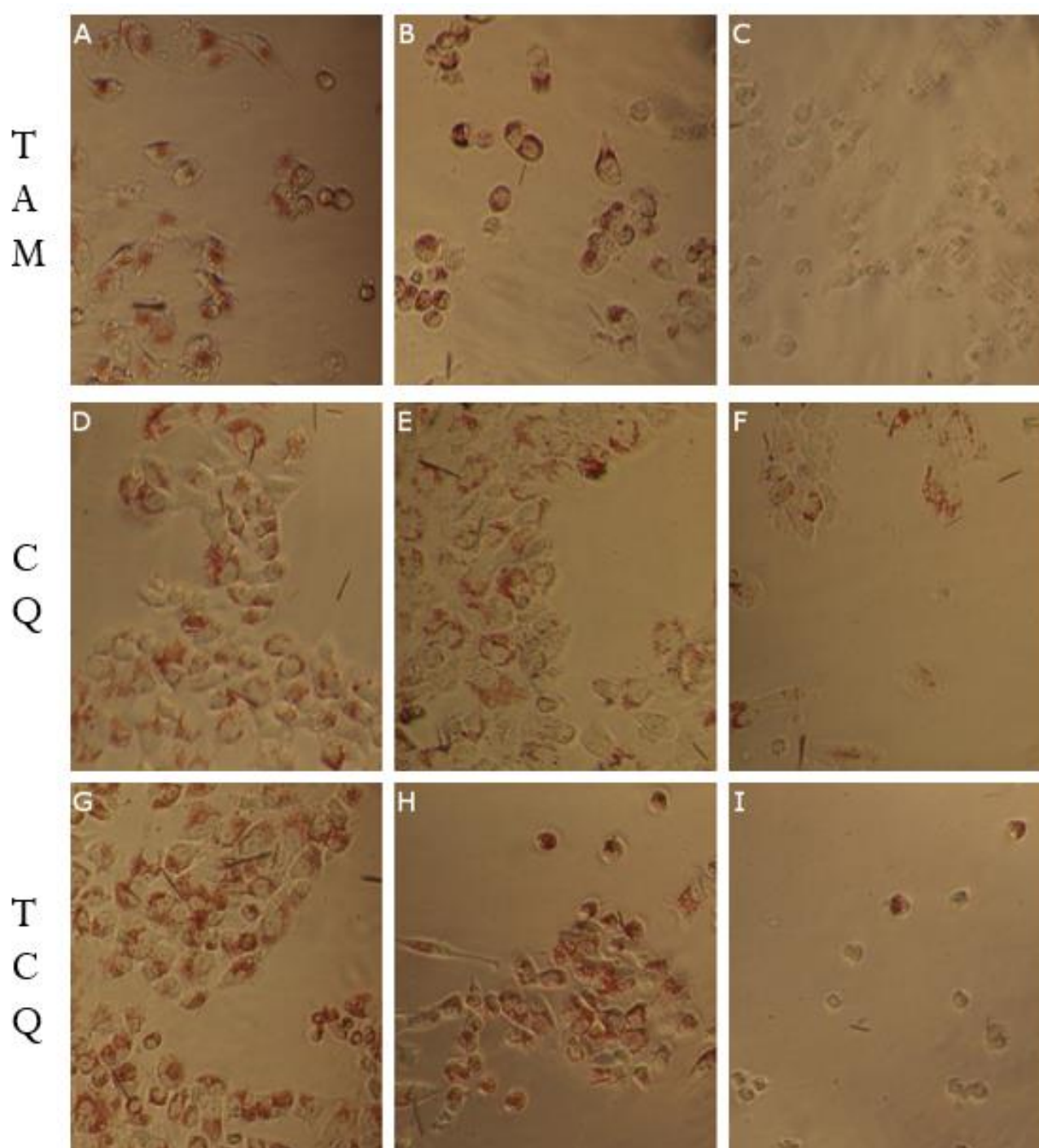


Figure 3.25: Panel illustrating the effect of TAM (A,B,C) CQ (D,E,F) and TCQ (G,H,I) on lysosomal profile of MCF-7 WT cells with Neutral Red. The cells were treated with TAM, 8, 16 and 24 μM ; 10, 40, 80 μM ; and TCQ 8, 16 and 24 μM TAM with a static dose of 10 μM Chloroquine. Cell death was most apparent in all rightmost slides with minimal NR retention. The richest lysosomal signal per-cell is visible in the ED50 (centremost slides) in dead cells are also present. (x10)

3.2.2.3 Neutral Red MCF-7 TMX

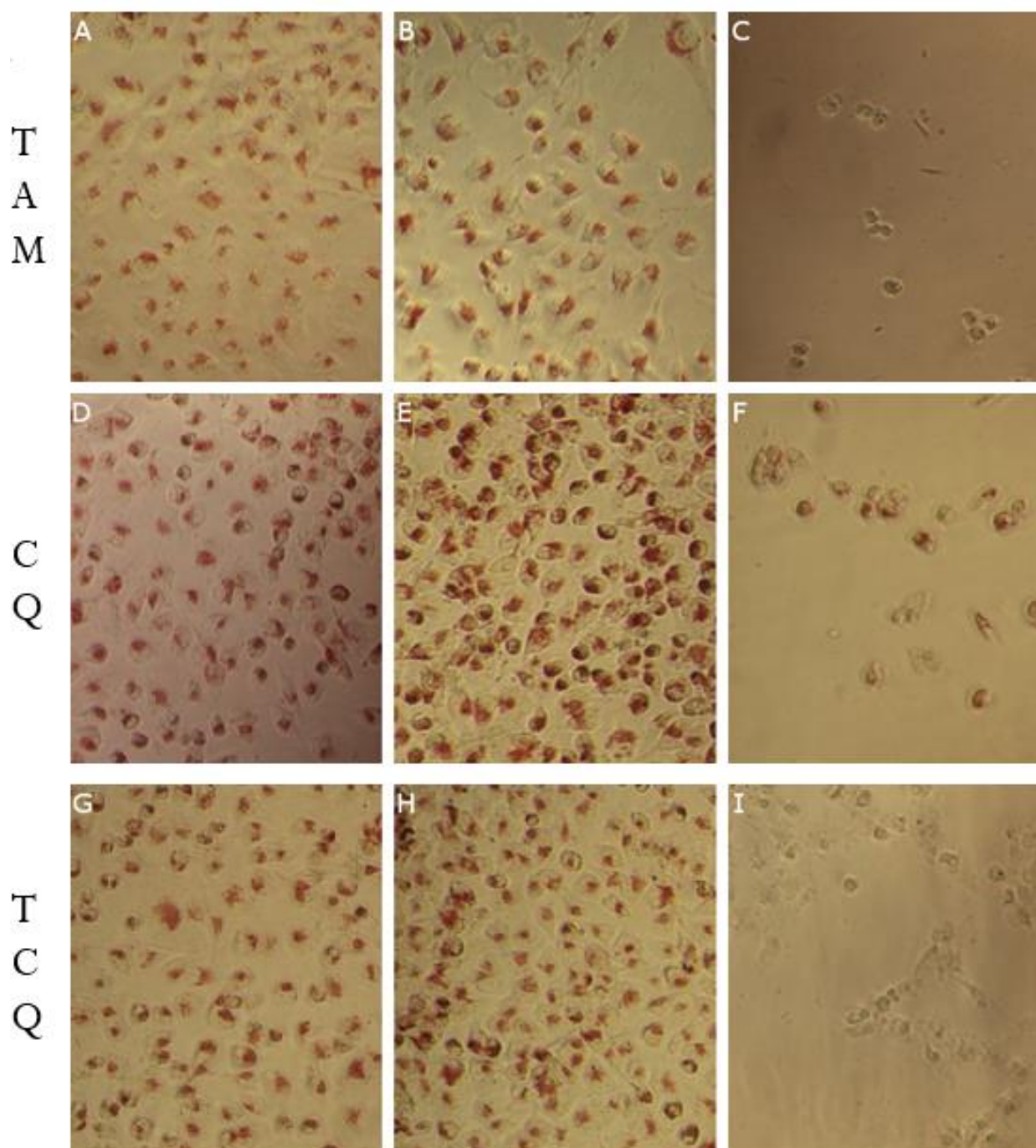


Figure 3.26: Panel illustrating the effect of TAM (A,B,C) CQ (D,E,F) and TCQ (G,H,I) on lysosomal profile of MCF-7 TMX cells with Neutral Red. The cells were treated with TAM, 8, 16 and 24 μM ; 10, 40, 80 μM ; and TCQ 8, 16 and 24 μM TAM with a static dose of 10 including controls (not pictured). Cell death and was most apparent in all rightmost slides with minimal NR retention. The richest lysosomal signal per-cell is visible in the ED50 (centremost slides) in dead cells are also present. (x10)

3.2.2.4 Neutral Red MDA-MD-231

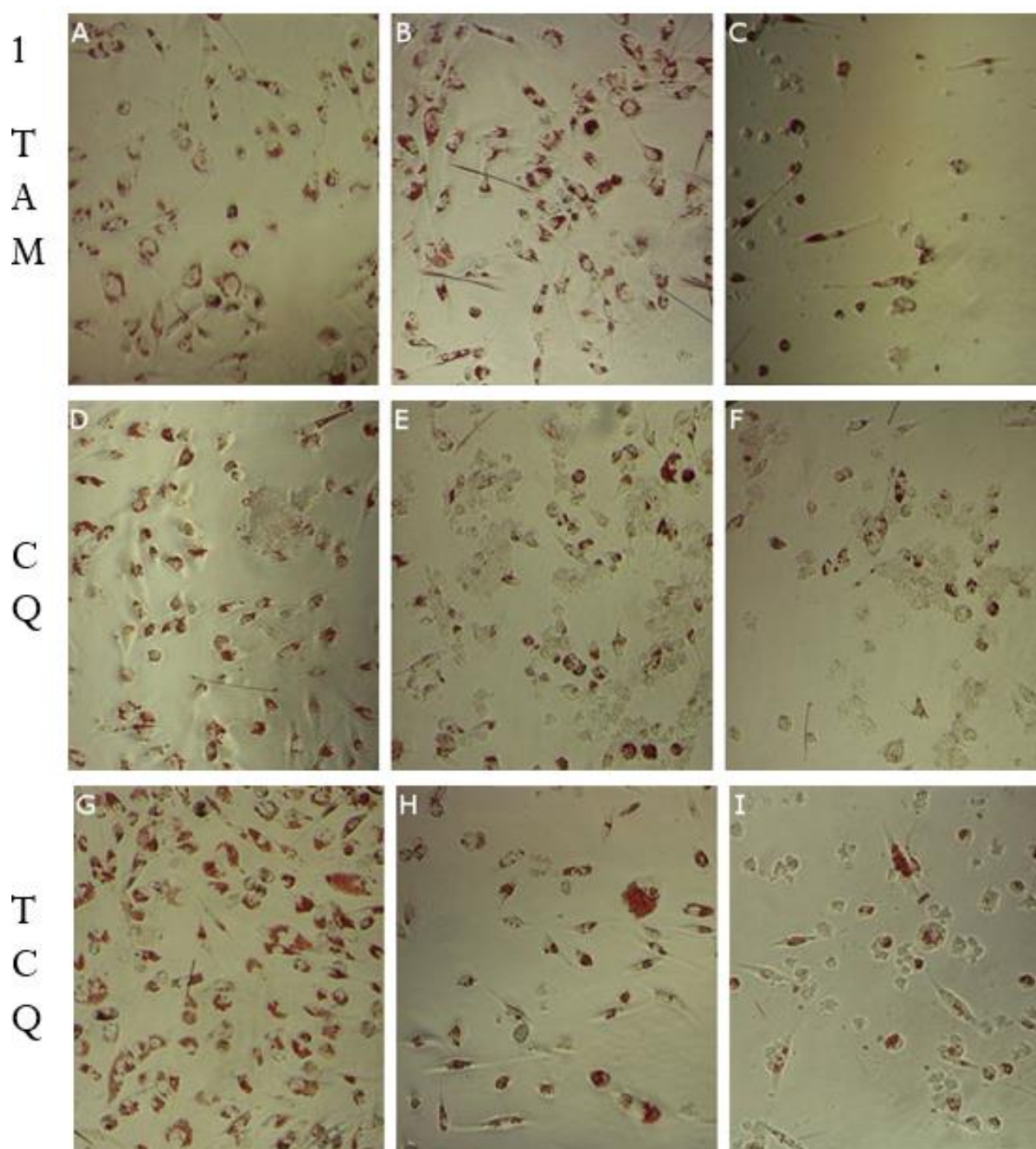


Figure 3.27: Panel illustrating the effect of TAM (A,B,C) CQ (D,E,F) and TCQ (G,H,I) on lysosomal profile of MDA-MB-231 cells with Neutral Red. The cells were treated with TAM, 8, 16 and 24 μM ; 10, 40, 80 μM ; and TCQ 8, 16 and 24 μM TAM with a static dose of 10 including controls (not pictured). Cell death and was most apparent in all rightmost slides with minimal NR retention. The richest lysosomal signal per-cell is visible in the ED50 (centremost slides) in dead cells are also present. (x10)

3.2.2 Acridine Orange Assay

The AO stain as described in Chapter 2 was the second qualitative assessment tool used in this investigation to visualise lysosomotropy; one of the primary mechanisms believed to facilitate cell death after exposure to CQ. Multiple images were taken of each slide; as AO is a dichromatic stain, each individual field was captured twice, once with the green (525nm) and red (640nm) filters and then compiled to produce composite images which allow differentiating acidic compartments within the cells from the rest of the cellular tissue.

The following images (**Figures 3.2.2.5- 3.2.2.8**) are a selection of composites of the green and red filtered micrographs taken from each cell line and drug combination assayed in the present study. The drug doses selected for the images taken were determined by the initial reactions observed from the Neutral Red spectroanalysis. Images were taken to include the control, the dosage of peak NR response, midway through the decay of signal and just before the final plateau. The control images for all the three cell lines presented with largely plain green fields with the faint presence sparse of orange spheres would represent the latent lysosomic population. There was a faint dose dependent response to tamoxifen relative to activity conveyed by NR quantitative study. All cell lines were very reactive to chloroquine with a vibrant orange signal apparent; however lysosomic signal was seen to drop at the higher dosages of the drug. The tamoxifen-chloroquine drug combination yielded images of very high orange signal for all cell lines at relatively lower levels of tamoxifen with lysosomotropic response at 4 μ M tamoxifen/10 μ M chloroquine being comparable of response seen at 40 μ M of independent tamoxifen exposure. These findings corroborate that of the NR stain and demonstrate a decreased affinity to lysosomic activity at higher doses and also serve to show that combined therapy appears to increase lysosomotropic response in all cell lines.

3.2.2.5 Acridine Orange Controls (All Cell Lines)

Control images are compiled from the 525 and 640nm filter pictures taken with the fluorescent microscope. The controls are subject to the same staining process as described in the Methods section of Chapter 2.

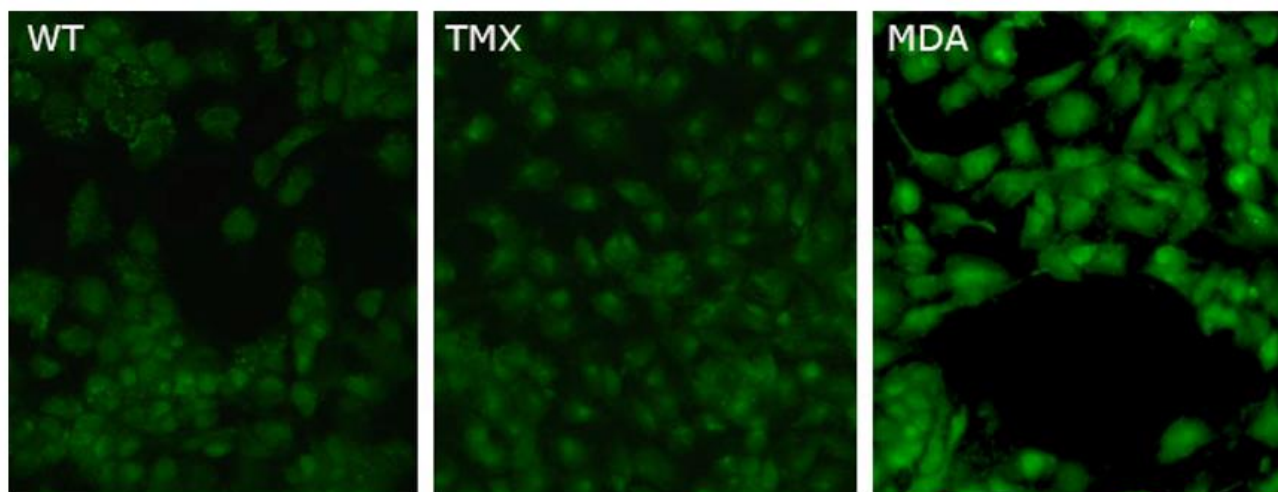


Figure 3.28: Acridine Orange panel of control samples for MCF-7 WT, TMX and MDA, monochromatic appearance of slides indicates low-volume of acidic compartments without drug treatment. Magnification x10

3.2.2.6 Acridine Orange MCF-7 WT

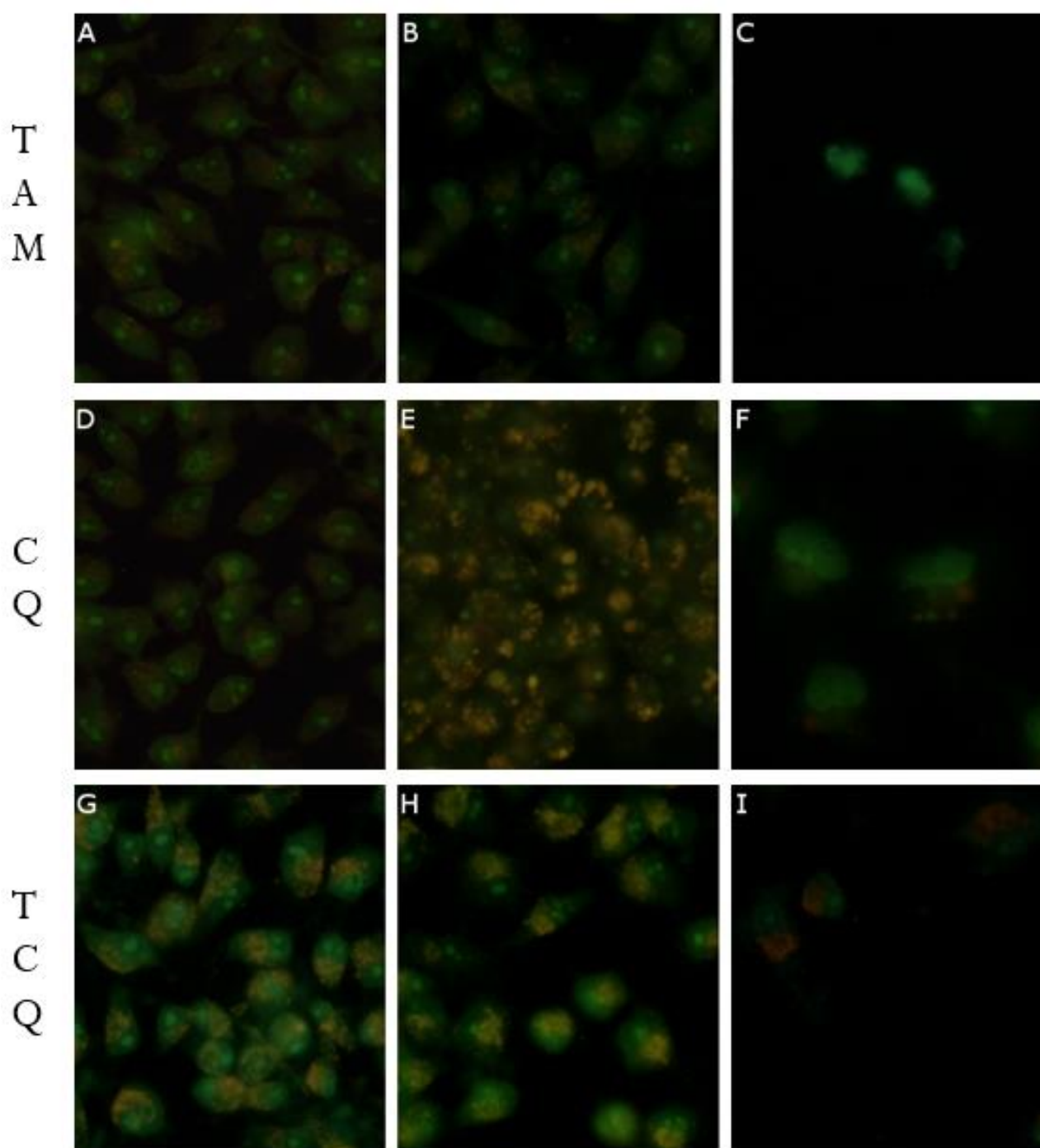


Figure 3.29: Panel illustrating the effect of TAM (A,B,C) CQ (D,E,F) and TCQ (G,H,I) on lysosomal profile and nuclear fragmentation of MCF-7 WT cells With Acridine Orange. The cells were treated with TAM, 8, 16 and 24 μ M; 10, 40, 80 μ M; and TCQ 8, 16 and 24 μ M TAM with a static dose of 10 including controls (not pictured). Cell death and nuclear fragmentation was apparent in all rightmost slides. The greatest lysosomal signal is visible in the ED₅₀ (centremost slides) and especially in the samples treated with CQ (D-I) in which nuclear fragmentation is also apparent. (x10)

3.2.2.7 AO MCF-7 TMX with Tamoxifen

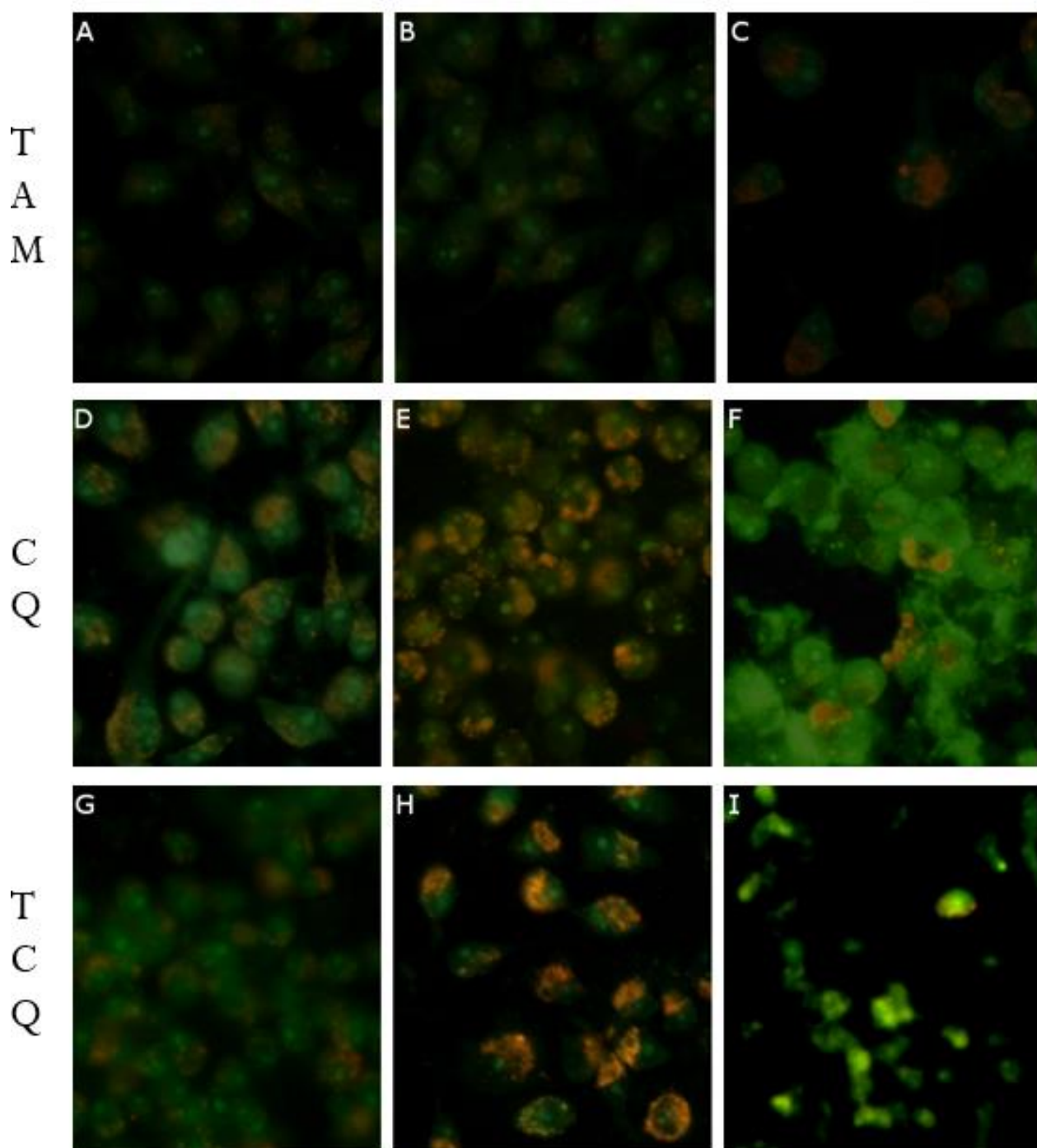


Figure 3.30: Panel illustrating the effect of TAM (A,B,C) CQ (D,E,F) and TCQ (G,H,I) on lysosomal profile and nuclear fragmentation of MCF-7 TMX cells with Acridine Orange. The cells were treated with TAM, 8, 16 and 24 μM ; 10, 40, 80 μM ; and TCQ 8, 16 and 24 μM TAM with a static dose of 10 including controls (not pictured). Cell death and nuclear fragmentation was apparent in all rightmost slides. The greatest lysosomal signal is visible in the ED_{50} (centremost slides) in which nuclear fragmentation is also apparent. (x10)

3.2.2.8 AO MDA-MB-231 with Tamoxifen

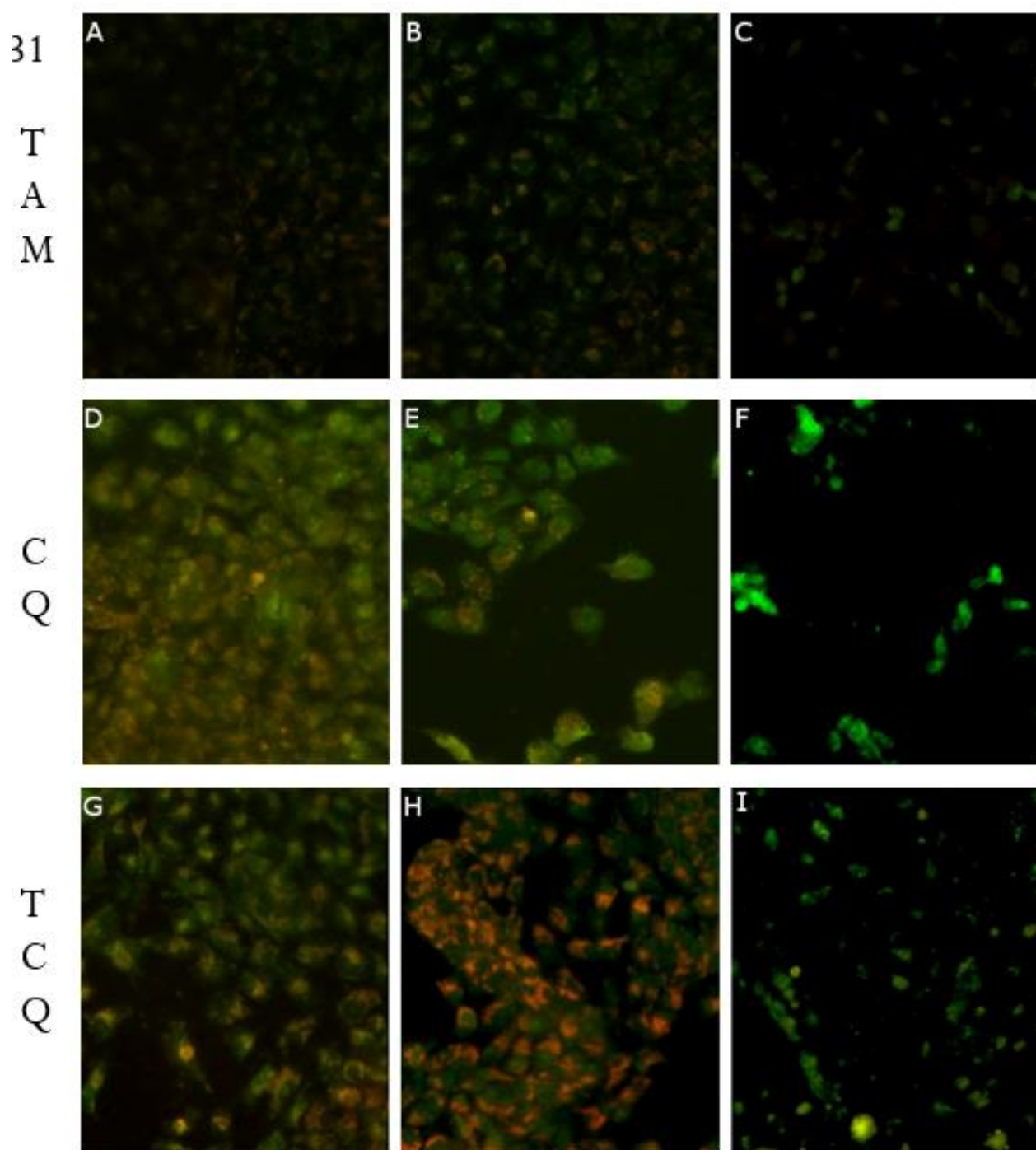


Figure 3.31: Panel illustrating the effect of TAM (A,B,C) CQ (D,E,F) and TCQ (G,H,I) on lysosomal profile and nuclear fragmentation of MDA-MB-231 cells with Acridine Orange. The cells were treated with TAM, 8, 16 and 24 μ M; 10, 40, 80 μ M; and TCQ 8, 16 and 24 μ M TAM with a static dose of 10 including controls (not pictured). Cell death and nuclear fragmentation was apparent in all rightmost slides. The greatest lysosomal signal is visible in the ED₅₀ (centremost slides) in which nuclear fragmentation is also apparent. (x10)

Chapter Four

4.0 Discussion

4.0 Discussion

As stipulated in Chapter 1.2, the aim of this investigation was to elucidate and explore the possible relationship between the anti-oestrogen tamoxifen and chloroquine through individual and combined study on their effect on the three cell lines MCF-7 WT, MCF-7 TMX and MDA-MB-231 in order to see any discrepancies or similarity in effect on cells lines with differing oestrogen receptor profiles. The convincing findings of Fan and colleagues (2006) of Shandong University on the effect of chloroquine on A549 lung cancer cell lines laid down the framework to the question as to the cytotoxic effect (and thus medical application) of chloroquine on models of breast cancer cells. As of writing, the singular effects of quinine products on breast specific cancer cells have been slowly surfacing, with studies presenting that the lysosomotropic events initiated through chloroquine activity may cause drug sensitisation (Maycotte *et al.*, 2012; Cufi *et al.*, 2013) while researchers at George Mason University, Virginia in their clinical trials hope to see, independent chemotherapeutic activity on breast cancer precursor cells (Paid Clinical Trials - Clinical Trial News and Opinion, 2015). Specific drug interaction/sensitisation of any breast cancer cell line with chloroquine is therefore new ground with no currently available literature on the synergistic effects of chloroquine on tamoxifen in particular which is why that called for the design of this three pronged (three drug modalities per cell line) investigative approach. The aim of this study was in fact two fold; both cellular and molecular; to elucidate the effect of the drug on a cellular population and then to observe the intracellular molecular phenomena which occur. To this extent, the first objective was to investigate the unique effects of tamoxifen and chloroquine on three breast cancer cell lines; MCF-7 WT, an oestrogen dependent breast cancer adenocarcinoma cell line isolated from 69 year old Caucasian woman Frances Mallon which is a popular candidate for hormone studies due to its ER⁺ profile; an analogue, MCF-7 TMX developed with apparent tamoxifen resistance at John Hopinks University, USA; and MDA-MB-231 an invasive (*in vitro*) adenocarcinoma line characterised as ER⁻ (Holliday & Spiers, 2011) for which to serve as a benchmark for further experiments. The mechanisms that lend to the cytotoxicity of tamoxifen and chloroquine are known to be molecularly disparate, with tamoxifen acting as an intracellular oestrogen receptor

modulator and cell growth inhibitor and chloroquine as an inducer of lysosomotropic apoptosis. The hypothesis is that the chloroquine mediated lysosomotrophy would increase the bioavailability of tamoxifen due to the disruption of autophagic mechanisms of the cell resulting in increased tamoxifen sensitivity and thus overall synergistic cytotoxicity, indeed chloroquine has been found in this way to restore Trastuzumab in HER-2 positive breast cancers (Cufí *et al.*, 2013). Through the use of the ED₅₀ values attained from the primary investigation, analysis of the effects of drug combination could be commenced using concentrations inference from the initial study. Subsequent tests would then be made to narrow down the effective range of drug interaction. Molecular investigation revolved around the study of lysosomes, specifically the presence of and stimulation of lysosomal activity through the use of light and fluorescence microscopic techniques.

4.1 Cell Culture Characteristics

The characteristic behaviour and morphologies of the cells lines detailed in this report (MCF-7 WT, MCF-7 TMX & MDA-MB-231) were recorded throughout the investigative process. Images as seen in the previous chapter as well as surplus imagery in the appendix were taken with an inverted microscope at various stages of cell development as well as after exposure to the various drug modalities at various time periods. All cell lines grew as an adherent monolayer with morphological traits following much the same expected patterns as in supervisory and advisory literature h). Proliferation data for each cell line was recorded (Table 3.1) and population doubling times (PDT) were extrapolated. The PDT of MCF-7 was 37 hours which is in line with the ATCC (American Type Culture Collection). MCF-7 TMX cells have an induced resistance, that is to say that they stem from a parent cell line of MCF-7 WT and slowly gain resistance after many passages. The PDT of MCF-7 TMX was 24 hours which is similar to that of MCF-7 cells examined in their 299th passage by Sutherland and colleagues (1983). The PDT of MDA-MB-231 which was 40 hours was also consistent with the ATCC. The discrepancy in doubling times between the breast cancer cells may harken to the school of understanding that directly correlates slower doubling times with increased tumorigenicity and aggressiveness as would be the case of MCF-7 WT and MDA-MB-231

however, *in vitro* morphology may not always defer the same traits in an *in vivo* model as would be the case of MDA-MB-231 which conveys invasive characteristics *in vitro* however in several xenograft assays has given rise to highly metastatic in *in vivo* models after direct introduction to the circulation (Kang *et al.*, 2003; Holliday & Speirs, 2011).

4.2 The Effect of Tamoxifen on Breast Cancer Cells

Tamoxifen is renowned the world over by researchers and clinicians as the gold standard treatment, adjuvant and preventative therapy of ER⁺ cancers (Cowell *et al.*, 2006). As an oestrogen receptor antagonist, it acts chiefly by halting or inhibiting the mitogenic processes by the competitive binding of the oestrogen receptor resulting in cytostatic or cytotoxic effect, especially in oestrogen dependent disease. The ED₅₀ is the median effective dose of a substance or chemical that elicits 50% of the desired effect (cell death). The ED₅₀ of tamoxifen was determined for each of the three cell lines investigated (Figures 3.4, 3.7 & 3.10) through their exposure to various doses of the drug over 48 hours.

The ED₅₀ of tamoxifen observed for MCF-7 WT cells as acquired from the MTT assay after 48 hours was low (relative to that of the other two cell lines) at 15.5µM; this response is insightful of tamoxifen's importance in hormonal therapy as an oestrogen receptor antagonist (Cowell *et al.*, 2006) and highlights the dependence of the MCF-7 WT cell line to oestrogen. In comparison, at the same drug dose of 15 µM, the MCF-7 TMX cell line with its meticulously acquired resistance to tamoxifen had a mean cell population of 80% with a relatively unchanged/statistically insignificant cell survival when exposed to concentrations of up to 12 µM of tamoxifen with its own ED₅₀ set at 18µM of tamoxifen. This change in character from its parent cell line, from its change in susceptibility to tamoxifen to its radically different mean cell volume (MCV) and PDT is not atypical of cell lines with induced resistance which are known to acquire all new phenotypes differing in DNA content and expression of intra and extracellular markers (Leung *et al.*, 2010). The response and ED₅₀ of the ER⁻ cell line MDA-MB-231 was similar to that of the tamoxifen resistant MCF-7 TMX cell line, yet disparate to the ER⁺ subject, highlighting the significance of

the use of tamoxifen in the inhibition and treatment of such cancers (Kang *et al.*, 2003; Cowell *et al.*, 2006; Cufí *et al.*, 2013)

Although primarily characterised and hailed for its cytostatic efficacy as an oestrogen receptor antagonist, in actuality, tamoxifen has been documented as exhibiting a duality of both antagonistic and agonistic effect on ER⁺ cancers. This paradoxical nature is why tamoxifen is called as a selective oestrogen receptor modulator (SERM). Research has shown that tamoxifen shares many of the same ER agonistic characteristics as its analogue oestrogen, in breast cancer cells effectively recapitulating a very similar gene expression profile including many transcription factors that ordinarily promote cell cycle progression such as fos, myc, myb, cdc25a (Hodges *et al.*, 2003) which may attribute to the positive response of MCF-7 WT observed in Figure 3. In 2003, Kisanga reported of the oestrogen receptor agonistic behaviour of tamoxifen on the expression of the sex hormone binding globulin (SHBG) in patients at higher relative clinical doses (the typical clinical titre tamoxifen being 1µM) of the drug which falls under the lower end of the dosage spectrum used where an agonistic response was observed which helps to support this narrative. All cell lines exhibited a dose dependent response to tamoxifen with the response from the tamoxifen resistant cell lines MDA-MB-231 and MCF-7 TMX responding later at higher doses; a narrative supported by other research on the dose and time specific response of the drug to ER⁻ cell lines (Zhang *et al.*, 1999; Zheng, Kallio and Härkönen, 2007; Zhu, 2013, Liu *et al.*, 2014). Interestingly, Cook and colleagues in 2014 when performing a knockdown of ERα on antioestrogen resistant LCC9 and susceptible LCC1 cell lines reported not only increased cell mortality in ER⁺ cell lines (highlighting their oestrogen dependence) but also an increased apoptosis in their antioestrogen resistant cell line thought to be most likely instigated by inhibition of certain survival mechanisms for which cytoplasmic ERα is thought to be responsible for. The marked response of the antioestrogen resistant cell lines MCF-7 TMX and the ER⁻ cell line MDA-MB-231 in the absence of functional oestrogen receptors is likely due to cytostatic/cytotoxic oestrogen receptor independent pathways (Liu *et al.*, 2014). Indeed, much research has been undergone to elucidate the role and nature of tamoxifen's ER independent pharmacology. The work of Zhen and colleagues in 2007 suggest that much of the immediate cytotoxic effects of tamoxifen at

pharmacological levels on the MCF-7 cell line linked tamoxifen exposure with sustained ERK (extracellular regulated kinase) activation which was prohibited by ERK inhibitors suggesting extracellular pathways at play even in oestrogen sensitive cell lines. Quite paradoxically, they proved that the presence of oestrogen receptors provides a semblance of resistance to tamoxifen in regard to the prevention of ERK phosphorylation and acute tamoxifen cytotoxicity, a trait which MDA-MB-231 does not have. As phenol red, the pH indicator present within the complete culturing medium is known to act a weak oestrogen; it is possible that through conveyed partial resistance to tamoxifen in the ER⁺ MCF-7 WT could have affected their immediate susceptibility to the drug at lower titres suggesting that the disparity in sensitivities between MCF-7 WT and the latter two cell lines investigated may have been (Berthois, Katzenellenbogen and Katzenellenbogen, 1986; Węsierska-Gądek *et al.*, 2006; Węsierska-Gądek *et al.*, 2007). Other studies have conveyed the significance of tamoxifen's ER independent cytotoxicity through the modulation of various other cell signalling proteins as well as oxidative stress (Nazarewicz *et al.*, 2007; Cho *et al.*, 2012), nevertheless the findings from the present study show an obvious and significant susceptibility of the ER⁺ MCF-7 WT to tamoxifen.

Resistance to tamoxifen both *in vitro* and *in vivo* is assumed to fall hand in hand with a marked rise in CD44⁺/CD24^{-low} cancer stem cells which are known to exhibit highly enhanced invasive properties and darken prognoses (Sheridan *et al.*, 2006; Hiscox *et al.*, 2012; Sun *et al.*, 2012). Untreated strains of MDA-MB-231 are known to exhibit comparatively proliferous amounts of CD44⁺/CD24^{-low} (Around 30% according to Sheridan *et al.*, 2006) which may be attributive of the disparate ED₅₀ values observed in the MTT assay between the three cell lines.

The Neutral Red (NR) viability staining assay served equally as both an accessory quantitative cell viability assay to the MTT test, but also in a qualitative capacity as a differential stain for the visual representation of the apparent changes in certain intracellular events, namely the lysosomes and other acidic cellular compartments (Fan *et al.*, 2006; Repetto, del Peso and Zurita, 2008). Through the differential staining of the lysosomes, it was possible to observe the documented lysosomotropic fate of tamoxifen exposure which is purported to perturb autophagic function and induce cell death (Codogno and

Meijer, 2005; Kohli *et al.*, 2013; Ashoor *et al.*, 2013). The NR control images from figures 3.16, 3.19 and 3.22 illustrated the latent presence of lysosomes within the three cell lines at rest. MDA exhibited the highest visual signal at rest highlighting the ever present role of autophagy in aggressive cancers (Hunakova *et al.*, 2009; Tu *et al.*, 2011). Both MCF-7 cell lines exhibited a rise in signal (Figures 3.16, 3.19) relative to control levels in response to tamoxifen demonstrating an increased lysosomotropic response between these two cell lines. The relative response to tamoxifen and gradual decline of NR retention in the MDA-MB-231 cell line in comparison to the two MCF-7 cell lines is indicative of cell death mediated by cytostatic or cytotoxic mechanisms independent of tamoxifen facilitated lysosomotropy. MCF-7 TMX (Figure 3.19) exhibited the highest positive response to tamoxifen exposure with NR signal suggesting a 50% increase in lysosome volume/capacity at 8 μ M compared to the relatively static NR expression from MCF-7 WT and the gradual decline from MDA-MB-231. This rampant rise in lysosomotropy in lieu of cell death suggests MCF-7 TMX's high affinity for autophagy as a mechanism for tamoxifen resistance. When comparing the disparity in percentage changes between MTT and Neutral Red signal in the MCF-7 cell line (Figures 3.4 and 3.16); cell viability appears to recede earlier, from about 10 μ M of tamoxifen dosage while the level of lysosomes represented by NR sequestration appears to be steadier for longer. This may be due to the fact that in lieu of cell population decline, an increase in lysosomotropic response to tamoxifen is being triggered in the surviving cells. Indeed, this hypothesis is further supported by Figures 3.29 and 3.30 in which NR signal between 8 and 16 μ M becomes visually more intense in the surviving cells. Indeed, a similar phenomenon may be observed in MCF-7 TMX between figures 3.7 and 3.19 which present an unwavering cell population/viability with a simultaneous increase of NR uptake. This correlation is similar to that observed by Fan and colleagues (2006) in an assay of a similar nature.

The use of Acridine Orange (AO) fluorescence staining (Figures within chapters 3.2.2.2, 3.2.2.5 and 3.2.2.9) for supplementary imagery of lysosomal activity served to further the support findings achieved through qualitative NR assessment by illustrating the lysosomotropic nature of tamoxifen. The increase in presence and intensity of the orange vesicles in using the

dichromatic stain were tantamount with that of neutral red intensity in the images taken serving to further exemplify this mechanism. In both stains, the higher dosages of tamoxifen (past the ED₅₀ for the respective cell lines) resulted in decrease of signal alluding to cell death being mediated now not by type II autophagic cell death but through other mechanisms linked to dose dependent cell necroptosis and necrosis (Bursch *et al.*, 1996; Fan *et al.*, 2006).

Caspase 3 is the terminal 'executor caspase' of the in the apoptotic cascade which is induced by the decrease in Bax:Bcl-2 ratio and whose up-regulation is linked with the irreversible upregulation of Type I apoptosis (Somai *et al.*, 2003). Tamoxifen has been shown to induce apoptosis in both ER⁺ and ER⁻ cancers from various origins through exposure to low levels of the drug in certain studies using lower levels of the drug relative to the ED₅₀ values investigated in the present study (Zartman *et al.*, 2004). Exposure to tamoxifen at the ED₅₀ for the three cell lines showed little change to the amount of caspase 3 expressed relative to the latent levels in the control. This may be due to the immediate cytotoxic effect of tamoxifen being caspase 3 independent; Kohli and colleagues in 2013 detailed a dose dependent rise in Caspase 3 up-regulation in ER⁺ malignant peripheral nerve sheath tumours however their findings showed that caspase inhibition did not protect the cells from apoptosis but rather that tamoxifen induced death was associated to autophagic induction which supports the narrative detailed in the present study from the neutral red and Acridine Orange assays and the rise in lysosomotropic activity within these breast cancer cell lines.

Contrary to expectations, treatment with tamoxifen presented a decrease in the presence of Annexin-V in all the cell lines. This could be as a result of the relatively high doses (compared to that of clinical treatment) necessary to examine the ED₅₀ values of the cell lines which, at the 48-hour time point may cause cells to engage in death mechanisms independent of Annexin-V. Indeed, Salami and colleagues in 2003 in the investigation of ER⁻ cell lines reported the existence of a dose-dependent peak value of Annexin-V expression after which a marked drop similar to that of the present study is observed.

4.3 The Effect of Chloroquine on Breast cancer cells

The synthetic quinolone chloroquine's therapeutic potential has been exploited over the past century from the treatment of malaria and rheumatism (Jamshidzadeh *et al.*, 2007; Teka *et al.*, 2008; Manic *et al.*, 2014; Wallace, *et al.*, 2015) to the more recent inquiry of its employment as a chemotherapeutic agent (Fan *et al.*, 2006). Its principal mechanism, even in that of the treatment of malaria, has been characterised by the abrogation of macroautophagy and subsequent cell death through accumulation and perturbation of lysosome synthesis; a primordial response seen in both *Plasmodium* and human species alike (Chinappi *et al.*, 2010; Sui *et al.*, 2013; Manic *et al.*, 2014; Choi *et al.*, 2014). As a direct result, CQ has been repositioned as a putative anti-cancer drug against breast cancer, as well as other aggressive cancers such as CD44⁺/CD24^{-/low} Cancer Stem Cells CSCs (Choi *et al.*, 2014), glioblastoma multiforme (Sotelo, 2006) and chronic myeloid leukaemia (Bellodi *et al.*, 2009).

In the present study, the overall effect of chloroquine on the viability of the three cell lines MCF-7 WT, MCF-7 TMX and MDA MB 231 was assessed with the MTT assay. There was a uniform dose-dependent response observed overall between the cells in response to exposure to chloroquine with the ED₅₀ value of MDA-MB-231 being the lowest at 44µM compared to the relatively higher ED₅₀ values of the MCF-7 cell lines which signifies the importance of autophagy in aggressive cancers as a primary form of resistance. The ED₅₀ values of MCF-7 WT and MCF-7 TMX, 52µM and 72µM respectively after 48 hours showing the susceptibility of these drugs in a dose dependent manner. MCF-7 TMX's greater apparent comparative tolerance to chloroquine compared to that of its parent cell line is perhaps anticipated given its nature as a drug resistant sub-group and suggests that its mechanism of intended tamoxifen resistance is not simply dependent on altered ER phenotype which is plausible given the exceptionally heterogeneous nature of MCF-7 and its sub-lines (Leung *et al.*, 2010).

The nature of chloroquine's lysosomotropic nature is even more evident given the findings from the present study using Neutral Red uptake analysis and Acridine Orange fluorescence microscopy. Through quantitative NR spectroscopy (Figures 3.17, 3.20 & 3.23) it is possible to visualise the how the cells mount a rapid lysosomotropic response to chloroquine from the lowest

doses. Both ER⁺ and ER⁻ wild-type breast cancer variants MCF-7 WT and MDA-MB-231 are seen to exhibit a similar severe response to low doses of chloroquine which, when compared to their similar responses from the MTT underlines the necessity of autophagy for their survival. The tamoxifen resistant MCF-7 TMX cell line's disparate initial NR response to chloroquine from the other two cell lines is compounded by its unique response in from the MTT assay. Although, as with the other two cell lines an increase in lysosomotrophy was apparent; MCF-7 TMX displayed a slighter, but sustained increase in over neutral red signal. The steeper decrease in MTT signal to the NR hints at an increased degree of lysosomotrophy in the tamoxifen resistant cell line, albeit less dramatic than in the latter lines. This is supported by the NR and AO images in subchapter 3.2 which show a dramatic increase in lysosomotrophy within each cell line compared to the relative senescence of the controls. Such response to chloroquine as seen in these images are a textbook response to the immediate effects of chloroquine which is plainly and beautifully displayed here and has been documented with familiarity in other cell lines (Fan *et al.*, 2006; Repetto *et al.*, 2008). Aside from autophagy, chloroquine has also of late been found to regulate cancer stem cells in triple negative breast cancers through the inhibition of Janus kinase 2 (JAK2) and DNA methyltransferase synthesis (Choi *et al.*, 2014; Manic *et al.*, 2014; Watson and Hughes, 2014). Autophagy independent cytotoxicity may also be apparent in this study as Fan and colleagues (2006) described reduced lysosomotrophy at higher concentrations of chloroquine when working on A549 lung cancer cells which is substantiated by the same reduction of lysosome signal in the three cell lines of the present study when subject to the same or higher levels of chloroquine. This may suggest that at higher (albeit clinically unfeasible) concentrations of chloroquine, cell cytotoxicity is being driven by as of yet unknown or poorly characterised autophagy independent cell death mechanism.

Choi and colleagues of the Houston Methodist Hospital (2014) described chloroquine as having a profoundly positive effect on the on the population of CD44⁺/CD24^{-/low} cancer stem cell population in triple negative breast cancers. As MDA-MB-231 has been previously characterised as having a relatively high population of such CSCs (>30%), it is fitting to assume this as an apt reason for why the MDA-MB-231 cell line in the present study had such a lower ED₅₀

dose response in comparison to the other two MCF-7 breast cancer cell lines (Choi et al., 2014).

As chloroquine has been highly characterised as being a facilitator of Type II autophagic cell death, it is interesting to note that the drug also appears to solicit a measurably high response in caspase-like activity when it came to performing the caspase 3 analysis after 48-hour incubation of the cell lines with ED₅₀ concentrations. Several publications have given inference to the overlap of specific apoptotic pathways including the activation of caspase 3 in certain cell lines, however many of the same articles have also established that the inhibition of caspase 3 had no effect on the rate or degree of cell death in these cell lines, leading to the consensus that the presence of caspase 3 by CQ to be incidental and not primary to cell death (Geng et al., 2010; Kim et al., 2010).

The marked upregulation Annexin-V expression in the present study for the cell lines MCF-7 WT and MCF-7 TMX is testimony to chloroquine's ability to facilitate cell death through not only autophagic apoptosis (as evidenced from both quantitative and qualitative Neutral Red investigation and Acridine Orange assay). Again the lack of any significant change in Annexin-V expression in the MDA-MB-231 cell line may be a result of the 48-hour time point which was chosen specifically as a snapshot to illustrate the processes occurring at the same time in the MTT, NR and AO experiments. Peak expression for MDA and the MCF-7 cell lines included may as inferred by Salami and Karami-Tehrani (2003) thus be at an earlier point in time.

Several other pathways have been characterised as being activated by chloroquine through mechanisms disparate from its characteristically described potentiation of Type II Cell death; chloroquine has been reported to affect breast cancers through the induction of mitochondrial damage through oxidative stress (Liang *et al.*, 2015), the normalisation of tumour vessels through the increased signalling of Notch1 in endothelial cells (Maes *et al.*, 2014) and immune response manipulation including rheumatism and lupus (Thomé *et al.*, 2013). It may be pertinent to add that all experiments in the present study were performed *in vitro*, and that due to the stark differences between the systemic and controlled environment, one must not conclude any findings *in vitro* would be directly corollary of a live model; indeed this is the case with the response of MDA-MB-231 and chloroquine, which the present study presents a clear and

favourable effects on cell viability, however in that of an *in vivo* mouse model study of the cell line with chloroquine by Tuomela and co-authors evidenced the contrary which, was explicated to be caused by some as of yet unestablished systemic response to chloroquine.

4.4 The Combined Effect of Chloroquine and Tamoxifen on Breast Cancer Cells

Due to the complex and often heterogeneous nature of cancers, the treatment of such diseases with single drugs focussed on a single receptor is commonly considered suboptimal as in many cases acquired resistance soon follows, leading to poor prognosis of the patient (Hiscox et al., 2012; Pourkavoos, 2012). Thus, the usage and development of combination modalities for the optimal treatment of breast cancers and other heterogeneous diseases such as diabetes, cardiovascular disease and HIV/AIDS is not only favourable, but necessary. Chloroquine has been at the forefront of much research in the concerted efforts of drug combination research, chiefly for its role in the abrogation of autophagy which has been found to be a central mechanism of drug resistance in many cell lines (Sui et al., 2013). It is the key premise of the present study that chloroquine may act in a potentiative manner to circumvent primary tamoxifen resistance and may thus translate as a promising therapeutic strategy for the improved treatment of breast cancers.

Through first obtaining the ED₅₀ dosage values from the two 48-hour treatment modalities of tamoxifen and chloroquine for each of the three cell lines MCF-7 WT, MCF-7 TMX and MDA-MB-231, the first initial combination studies were made (Figures, 3.13, 3.14 and 3.15). The initial experiment involved the combination of incremental fractions of tamoxifen (2-30µM) as prepared in earlier independent assay of the drug with the ED₅₀ dosage of Chloroquine (40µM). The rationale behind this decision was analogous to that of isobolic experimentation in which combined fractions of ED values add up to ED₁₀₀ (i.e. ED₂₅+ED₇₅ or ED₅₀+ED₅₀). Data from the dose-response graph was thus used to extrapolate the nature of drug-drug interaction. It was believed that a shift in the curve to the right would infer inhibitory pharmacokinetic interaction and a shift to the left would infer synergistic combination while no shift at all would infer additive effect (Meyerson, Went and Fultz, 2009; Prueksaritanont

et al., 2013). There was a unanimously positive response from all three cell lines with this initial combined treatment of tamoxifen with 40 μ M of chloroquine with ED₅₀ values dropping profoundly. In an additive response, one would expect the new ED₁₀₀ (that, is the minimum dose with which to kill all the cells) of tamoxifen with 40 μ M of chloroquine to fall at the current ED₅₀ values for each cell line; this, however is not the case with the ED₅₀ values for each cell line dropping to an unprecedented 1 μ M for MCF-7 WT and 2 μ M for MCF-7 TMX and MDA-MB-231 implying significant synergistic behaviour between the two drugs.

In an attempt to further establish the immediate cytotoxic effect of the two drugs in combination and better visualise any difference in response between the cell lines, a lesser concentration of chloroquine (10 μ M) was elected for use (Figures 3.6, 3.7 & 3.12). The results showed a drop in ED₅₀ values across the board, all curiously settling at 12 μ M of tamoxifen with the MDA-MB-231 cell line exhibiting the greatest fall from its previous ED₅₀ of 18.5 with MCF-7 TMX falling in line shortly after. The drop of the ED₅₀ values of both MCF-7 cell lines to a common figure suggests that chloroquine may serve to overcome primary resistance and restore sensitivity to tamoxifen in these cell lines in a similar fashion to findings published by Cufí and colleagues (2013) in their investigation into the combined effect of CQ with trastuzumab; an anti HER-2 monoclonal antibody through which they deduced that chloroquine mediated cell death may occur through the inhibition of autophagic resolution of autophagosomes formed in the presence of the herceptin drug (or in the case of the present study, tamoxifen) resulting in initiation of cell death through apoptosis. It has already been stated that, due to the largely unspecific nature of tamoxifen which has been documented as eliciting many (less well documented) oestrogen receptor independent pathways, an albeit lesser immediate response to the drug may be observed in conjunction with the ER⁻ MDA-MB-231 cell line. It is very likely that the response observed in the present study between MDA-MB-231 and the combination drug treatment may be similarly caused by chloroquine mediated sensitisation.

Results from the quantitative NR analysis of the three cell lines, as evidenced by Figures 3.18, 3.21 and 3.24 serve to further support this narrative of cell death facilitated through lysosomotropy and autophagic gridlock. There

is a similar delayed response observed between MFC-7 cell lines WT and TMX before a surge in signal which signifies the increased retention of the Neutral Red pigment within the cells as instigated by an increase in the size and volume of acidic compartments within the cells. The shared delay of 8 μ M of tamoxifen may indicate the critical dose of tamoxifen where lysosomotropic synergy with chloroquine is most apparent. This observation is further supported through further light and fluorescence imagery of the cells in Chapter 3.2 which present a visibly pronounced increase in NR and AO acidity from the cell lines in comparison with the single drug modalities. The orange colour from the AO stems from the dichromatic nature of the stain; upon entering lysosomes and becoming protonated in the low pH environment, the dye emits more strongly at 640nm contrasting against the green surrounding environment. The signal potency of the orange vesicles from the composite images of the combined treatment (Figures 3.61, 3.68 & 3.75) are comparable with that seen in treatments of 40 μ M is an indication which highlights the synergistic effect of the drug couplet on lysosomotropic events. Going back to the NR quantitative assay, as MCF-7 cell lines WT and TMX were both seen to share a similar delayed response before peaking; MDA-MB-231 was seen to exhibit a more immediate response to the drug combination (Figure 3.24). This may be attributed to MDA-MB-231's apparent heightened sensitivity to chloroquine as evidenced from its lower ED₅₀ in Figure 3.11 and may infer as to why the combination elicits such a dramatic drop in viability (as recorded from the ED₅₀) relative to the other cells lines.

Results from the Caspase 3 DEVD-Pna colorimetric analysis presented with a marked increase in Caspase-like activity across the board for each of the three cell lines after treatment with their respective tamoxifen-chloroquine ED₅₀ doses (Figure 3.25). It was stated before that in cell death mediated by both drugs independently, while Caspase 3 specific activity may be present in a dose dependent manner, the inhibition of caspase activity did not prevent cell death. That being said, the high presence of Caspase 3 activity in the combination assays confirms that while in the confines of the present study tamoxifen and chloroquine do not independently display Caspase 3 activity, in conjunction they elicit a high Caspase 3 up-regulation greater than the sum of both drugs individually. From these findings, one may thus infer that tamoxifen-chloroquine

combination treatment facilitates cell death through both Type 1 caspase mediated apoptosis and Type II autophagic apoptosis. The experiment however only provides a snapshot of events at the 48 hour time period and may not be representative of peak Caspase-3 expression in response to the drug modality.

Combination therapy yielded a visible, yet statistically insignificant increase in Annexin-V expression for all the cell lines investigated which may either result as stated before from Annexin-V's fleeting presence post peak expression (Salami and Karami-Tehrani, 2003) or due to the interplay of different cell death mechanisms resulting from this modality such as the marked increase of autophagic events evidenced from Acridine Orange study. Results from the Caspase-like activity analysis however would beg the former as these are both investigative procedures for the detection of Type I apoptosis.

4.5 Conclusion

The endogenous factors at play of the SERM tamoxifen on breast cancers are a topic of constant study and ones that have been further exemplified in the present study through the nature of its reaction with both ER⁺ and ER⁻ cancer cell lines alike albeit at disparate concentrations pertaining to oestrogen receptor status. The cytotoxic effects of tamoxifen were found not to be limited by mitochondrial apoptosis but also through the mediation of autophagic cell death which was visualised through both qualitative and quantitative Neutral Red assay and further investigation with Acridine Orange. Through independent treatment, the cytotoxic nature of chloroquine on breast cancers was elucidated and was found to have a significantly higher dose-response ratio than that of tamoxifen. It was deduced that the more aggressive oestrogen receptor negative cell line MDA-MB-231 had a significantly stronger response to chloroquine than the ER α ⁺ cell line and its tamoxifen resistant strain.

When used in conjunction, the tamoxifen-chloroquine treatment displayed an undisputed potentiation of cell death characterised by the chaotic perturbation of autophagic phenomena. This combination demonstrated that small doses of chloroquine in combination with the antioestrogen tamoxifen could elicit lysosomotropic effects only seen at doses of up to four times of as much chloroquine in single use. Through its unanimous display of cytotoxicity across all three cell lines, the treatment combination shows its efficacy in not only overcoming primary resistance as seen in the similar ED₅₀'s of MCF-7 WT and MCF-7 TMX, but through its high toxicity observed in MDA-MB-231 suggests collaborative potentiation through pathways endogenous to classical oestrogen receptor suppression. The evidence from this study suggests that further exploration of the nature of this relationship could yield clinical benefit in the resensitization and treatment of many forms of breast cancer.

Chapter Five

5.0 Further Studies

5.0 Further Studies

The results from the present study suggested significant potentiation of chloroquine on the efficacy of tamoxifen (as evident in the decrease in ED_{50}) on each the three breast cancer cell lines investigated, however, the favoured mechanism of cell death, and thus the feasibility of its clinical application pertaining to tolerance and side effects remains unclear. Thus, further study would be necessary to determine the effect of these cells on the favoured mode of cell death. In this initial investigation, the presence of annexin-V and capsase 3 activity as seen through ELISA and spectrophotometry served as a snapshot to match the 48-hour treatment examined quantitatively with MTT and Neutral Red analysis however it has been suggested that such a study represents the activity of metabolites at a time point that may not infer their peak activity which may have a large discrepancy due to the disparate nature of the cell lines (Arif *et al*, 2015) thus an appropriate time course would be necessary. Moreover, to discern between apoptotic and necrotic populations within sample, annexin-V flow cytometry with propidium iodide, which was not within the fiscal scope of the present study would have been favourable to the ELISA assay to visualise the disparate populations. Additionally, LDH (Lactate Dehydrogenase) assays

have been used in the independent analysis of necrosis in other chloroquine related potentiation study (Fan et al., 2006; Cufí et al., 2013) and would also be pertinent to any future investigation.

Qualitative analysis for the visualisation of the lysosomotropic phenomena that occurred in the present study were not specific to lysosomes but all acidic vesicles within the cell. LC3-II (microtubule associated protein light chain 3) immunocytochemistry, while dearer, would be the ideal choice in any future investigation of lysosome-specific activity (Mizushima and Yoshimori, 2007; Cufí et al., 2013). The utilisation of scanning electron microscopy would serve to better observe cell ultrastructure and document any fine morphological changes which may not have been obvious in the present study (Jaafar, Sharif and Murtey, 2012).

The resistance to tamoxifen of the cell line MCF-TMX, an offshoot of the parent line MCF-7 is one that was selectively induced. Chloroquine resistance in human disease has not yet been investigated and studies in the facilitation of chloroquine resistance and subsequent response to the drug panel of the present study may prove to an area of unique interest, especially pertaining to future prospects in clinical application.

The Bcl-2 (B-cell lymphoma/leukaemia 2) family plays a role in cell survival and oncogenesis (Cory, Huang and Adams, 2003). The gene encodes an integral outer mitochondrial membrane protein that prevents the apoptosis in certain cells such as lymphocytes and has been characterised in many types of cancers and attributed to their survival. In some studies, cell death by tamoxifen has been linked with a down-regulation of bcl-2 (Zhang et al., 1999; El-Sheemy et al., 2015) thus it may be of interest to investigate if the potentiative effect of tamoxifen and chloroquine combination is preceded by a further drop in Bcl-2.

The present study was used to assess the three cell lines after a 48-hour treatment period using drug concentrations standardised to give a visible effect after this time period and the results from which are pertinent to the immediate effect of the drugs over this time scale. However, clinical doses of tamoxifen would rarely exceed 0.2µM in serum and 2µM in tissue (Vaillant et al., 2013) and thus a protracted study at such a range of drug over a longer time scale may be warranted to appraise a clinically relevant study.

The handful of data that exists on the effects of radiation on cells resistant to hormonal therapy also implies that they are resistant to radiation. Chloroquine has already been reported to independently sensitise cells to radiation thus after some standardisation, it would be of interest to see whether the tamoxifen-chloroquine modality infers any further potentiation with radiation treatment.

As stated before, tamoxifen exposure in MCF-7 WT cells has been linked with an overexpression of CD44, negatively affecting their sensitivity to the drug and promoting resistance and aggressiveness over time (Sheridan et al., 2006; Hiscox et al., 2012). Chloroquine on the other hand has been seen to exact the opposite response and has been identified as a candidate for CD44⁺/CD22^{-/low} cancer stem cell treatment (Choi et al., 2014). As the present study has shown that tamoxifen-chloroquine combination treatment potentiates cell death in the three cell lines investigated, it would be applicable to investigate whether this response is accompanied by any changes in the CD44⁺/CD22^{-/low} population of the breast cancer cell lines.

Janus Kinase 2 has been found to be integral in the activation of the Stat 1 transcription signaling pathway expressed in breast cancers (Watson and Hughes, 2014). Moreover, chloroquine has been seen to perturb Jak2 activation, eliminating cancer stem cells. Thus the monitoring and comparison of differences Jak2 synthesis between treatment systems may serve to further support this narrative.

Another such mechanism to investigate is that of p53 oncogene up-regulation by chloroquine. p53 protein is tumor suppressor that potently inhibits cell growth through the halting of proliferation and apoptotic pathways (Vogelstein, Lane and Levine, 2000). Chloroquine has been found to stimulate the up-regulation of this protein and is believed that p53 mediated apoptosis is a key component of chloroquine facilitated cell death (Kim et al., 2010; Loehberg et al., 2012). Tamoxifen, on the other hand has been shown to not cause any notable effects on p53 levels, thus an investigation on the effect on the role of this protein in tamoxifen-chloroquine synergy would be of great interest as to further understand the nature of their relationship (Zhang et al., 1999).

References

6.0 References

References

Abcam.com, (2015). Annexin V detection protocol for apoptosis | Abcam. [online] Available at: <http://www.abcam.com/protocols/annexin-v-detection-protocol-for-apoptosis> [Accessed 8 Aug. 2015].

Alizart, M., Saunus, J., Cummings, M. and Lakhani, S. (2012). Molecular classification of breast carcinoma. *Diagnostic Histopathology*, 18(3), pp.97--103.

Antoniou, A. and Easton, D. (2006). Models of genetic susceptibility to breast cancer. *Oncogene*, 25(43), pp.5898-5905.

Ascenzi, P., Bocedi, A. and Marino, M. (2006). Structure–function relationship of estrogen receptor α and β : Impact on human health. *Molecular Aspects of Medicine*, 27(4), pp.299-402.

Ashoor, R., Yafawi, R., Jessen, B. and Lu, S. (2013). The Contribution of Lysosomotropism to Autophagy Perturbation. PLoS ONE, 8(11), p.e82481.

Azu, M., Jean, S., Piotrowski, J. and O’Hea, B. (2007). Effective methods for disclosing breast cancer diagnosis. The American Journal of Surgery, 194(4), pp.488-490.

Bellodi, C., Lidonnici, M., Hamilton, A., Helgason, G., Soliera, A., Ronchetti, M., Galavotti, S., Young, K., Selmi, T., Yacobi, R., Van Etten, R., Donato, N., Hunter, A., Dinsdale, D., Tirrò, E., Vigneri, P., Nicotera, P., Dyer, M., Holyoake, T., Salomoni, P. and Calabretta, B. (2009). Targeting autophagy potentiates tyrosine kinase inhibitor–induced cell death in Philadelphia chromosome–positive cells, including primary CML stem cells. Journal of Clinical Investigation, 119(5), pp.1109-1123.

Berthois, Y., Katzenellenbogen, J. and Katzenellenbogen, B. (1986). Phenol red in tissue culture media is a weak estrogen: implications concerning the study of estrogen-responsive cells in culture. Proceedings of the National Academy of Sciences, 83(8), pp.2496-2500.

Bhosle, J. and Hall, G. (2009). Principles of cancer treatment by chemotherapy. Surgery (Oxford), 27(4), pp.173-177.

Bozic, I., Reiter, J., Allen, B., Antal, T., Chatterjee, K., Shah, P., Moon, Y., Yaquibie, A., Kelly, N., Le, D., Lipson, E., Chapman, P., Diaz, L., Vogelstein, B. and Nowak, M. (2013). Evolutionary dynamics of cancer in response to targeted combination therapy. eLife, 2.

Brauch, H. and Jordan, V. (2009). Targeting of tamoxifen to enhance antitumour action for the treatment and prevention of breast cancer: The ‘personalised’ approach?. European Journal of Cancer, 45(13), pp.2274-2283.

Brown, V., Sridhar, T. and Symonds, R. (2011). Principles of chemotherapy and radiotherapy. *Obstetrics, Gynaecology & Reproductive Medicine*, 21(12), pp.339-345.

Burns, B., Geisler, J., Hatterman-Zogg, M., De Young, B. and Buller, R. (2003). Malignant mixed mullerian tumor of the ovary and bilateral breast cancer: an argument for BRCA3, or a coincidental cluster of unconnected cancers?. *Gynecologic Oncology*, 91(2), pp.426-428.

Bursch, W., Ellinger, A., Kienzl, H., Török, L., Pandey, S., Sikorska, M., Walker, R. and Hermann, R. (1996). Active cell death induced by the anti-estrogens tamoxifen and ICI 164 384 in human mammary carcinoma cells (MCF-7) in culture: the role of autophagy. *Carcinogenesis*, 17(8), pp.1595-1607.

Caldas, C. (2012). Cancer sequencing unravels clonal evolution. *Nature biotechnology*, 30(5), p.408.

Cancerresearchuk.org, (2015). Breast cancer research | Cancer Research UK. [online] Available at: <http://www.cancerresearchuk.org/about-cancer/type/breast-cancer/treatment/research/> [Accessed 9 May 2015].

Chen, D. and Hsiao, Y. (2008). Computer-aided Diagnosis in Breast Ultrasound. *Journal of Medical Ultrasound*, 16(1), pp.46-56.

Chinappi, M., Via, A., Marcatili, P. and Tramontano, A. (2010). On the Mechanism of Chloroquine Resistance in *Plasmodium falciparum*. *PLOS ONE*, [online] 5(11), p.e14064. Available at: <http://journals.plos.org/plosone/article?id=10.1371/journal.pone.0014064> [Accessed 7 Sep. 2015].

Cho, K., Yoon, Y., Choi, J., Lee, S. and Koh, J. (2012). Induction of Autophagy and Cell Death by Tamoxifen in Cultured Retinal Pigment Epithelial and Photoreceptor Cells. *Investigative Ophthalmology & Visual Science*, 53(9), p.5344.

Choi, D., Blanco, E., Kim, Y., Rodriguez, A., Zhao, H., Huang, T., Chen, C., Jin, G., Landis, M., Burey, L., Qian, W., Granados, S., Dave, B., Wong, H., Ferrari, M., Wong, S. and Chang, J. (2014). Chloroquine Eliminates Cancer Stem Cells Through Deregulation of Jak2 and DNMT1. *STEM CELLS*, 32(9), pp.2309-2323.

Chuthapisith, S., Eremin, J., El-Sheemy, M. and Eremin, O. (2006). Neoadjuvant chemotherapy in women with large and locally advanced breast cancer: Chemoresistance and prediction of response to drug therapy. *The Surgeon*, 4(4), pp.211-219.

Clemons, M., Danson, S. and Howell, A. (2002). Tamoxifen ('Nolvadex'): a review. *Cancer Treatment Reviews*, 28(4), pp.165-180.

Codogno, P. and Meijer, A. (2005). Autophagy and signaling: their role in cell survival and cell death. *Cell Death Differ*, 12, pp.1509-1518.

Compton, C. (2003). Colorectal Carcinoma: Diagnostic, Prognostic, and Molecular Features. *Mod Pathol*, 16(4), pp.376-388.

Cook, K., Warri, A., Soto-Pantoja, D., Clarke, P., Cruz, M., Zwart, A. and Clarke, R. (2014). Hydroxychloroquine Inhibits Autophagy to Potentiate Antiestrogen Responsiveness in ER+ Breast Cancer. *Clinical Cancer Research*, 20(12), pp.3222-3232.

Cooper, R. (1969). Combination chemotherapy in hormone resistant breast cancer. *Proceedings of the American Association for Cancer Research*, 10(15).

Cory, S., Huang, D. and Adams, J. (2003). The Bcl-2 family: roles in cell survival and oncogenesis. *Oncogene*, 22(53), pp.8590-8607.

Couse, J., Curtis Hewitt, S. and Korach, K. (2000). Receptor null mice reveal contrasting roles for estrogen receptor α and β in reproductive tissues. *The Journal of Steroid Biochemistry and Molecular Biology*, 74(5), pp.287-296.

Cowell, L., Graham, J., Bouton, A., Clarke, C. and O'Neill, G. (2006). Tamoxifen treatment promotes phosphorylation of the adhesion molecules, p130Cas/BCAR1, FAK and Src, via an adhesion-dependent pathway. *Oncogene*, 25(58), pp.7597-7607.

Cufí, S., Vazquez-Martin, A., Oliveras-Ferraro, C., Corominas-Faja, B., Cuyàs, E., López-Bonet, E., Martín-Castillo, B., Joven, J. and Menéndez, J. (2013). The anti-malarial chloroquine overcomes Primary resistance and restores sensitivity to Trastuzumab in HER2-positive breast cancer. *Scientific Reports*, 3.

Cullen, R., Maguire, T., McDermott, E., Hill, A., O'Higgins, N. and Duffy, M. (2001). Studies on oestrogen receptor- α and - β mRNA in breast cancer. *European Journal of Cancer*, 37(9), pp.1118-1122.

Curtis Hewitt, S., F Couse, J. and S Korach, K. (2000). *Breast Cancer Research*, 2(5), p.345.

Cyr, A. and Margenthaler, J. (2014). Molecular Profiling of Breast Cancer. *Surgical oncology clinics of North America*, 23(3), pp.451--462.

Da Silva, L. and Lakhani, S. (2010). Pathology of hereditary breast cancer. *Mod Pathol*, 23, pp.S46-S51.

Davies, E. (2012). Breast cancer. *Medicine*, 40(1), pp.5-9.

Davis, L., Katsu, Y., Iguchi, T., Lerner, D., Hirano, T. and Grau, E. (2010). Transcriptional activity and biological effects of mammalian estrogen receptor ligands on three hepatic estrogen receptors in Mozambique tilapia. *The Journal of Steroid Biochemistry and Molecular Biology*, 122(4), pp.272-278.

Dawson, S., Tsui, D., Murtaza, M., Biggs, H., Rueda, O., Chin, S., Dunning, M., Gale, D., Forshew, T., Mahler-Araujo, B., Rajan, S., Humphray, S., Becq, J., Halsall, D., Wallis, M., Bentley, D., Caldas, C. and Rosenfeld, N. (2013). Analysis of Circulating Tumor DNA to Monitor Metastatic Breast Cancer. *New England Journal of Medicine*, 368(13), pp.1199-1209.

DeVita, V. and Chu, E. (2008). A History of Cancer Chemotherapy. *Cancer Research*, 68(21), pp.8643-8653.

Diaz Jr, L., Williams, R., Wu, J., Kinde, I., Hecht, J., Berlin, J., Allen, B., Bozic, I., Reiter, J., Nowak, M., Kinzler, K., Oliner, K. and Vogelstein, B. (2012). The molecular evolution of acquired resistance to targeted EGFR blockade in colorectal cancers. *Nature*.

DiMasi, J., Hansen, R. and Grabowski, H. (2003). The price of innovation: new estimates of drug development costs. *Journal of Health Economics*, 22(2), pp.151-185.

El-Sheemy, M., Hussain, I., Rea, C. and Arif, K. (2015). The role of Nanog expression in tamoxifen-resistant breast cancer cells. *OTT*, p.1327.

English, M. (2010). Principles of chemotherapy. *Paediatrics and Child Health*, 20(3), pp.123-128.

Fan, C., Wang, W., Zhao, B., Zhang, S. and Miao, J. (2006). Chloroquine inhibits cell growth and induces cell death in A549 lung cancer cells. *Bioorganic & Medicinal Chemistry*, 14(9), pp.3218-3222.

Flobbe, K., Nelemans, P., Kessels, A., Beets, G., von Meyenfeldt, M. and van Engelshoven, J. (2002). The role of ultrasonography as an adjunct to mammography in the detection of breast cancer. *European Journal of Cancer*, 38(8), pp.1044-1050.

Froehlicher, M., Liedtke, A., Groh, K., López-Schier, H., Neuhauss, S., Segner, H. and Eggen, R. (2009). Estrogen receptor subtype $\beta 2$ is involved in neuromast development in zebrafish (*Danio rerio*) larvae. *Developmental Biology*, 330(1), pp.32-43.

Gan, S. and Patel, K. (2013). Enzyme Immunoassay and Enzyme-Linked Immunosorbent Assay. *J Investig Dermatol*, 133(9), p.e12.

Geng, Y., Kohli, L., Klocke, B. and Roth, K. (2010). Chloroquine-induced autophagic vacuole accumulation and cell death in glioma cells is p53 independent. *Neuro-Oncology*, [online] 12(5), pp.473-481. Available at: <http://www.ncbi.nlm.nih.gov/pmc/articles/PMC2940627/?report=classic> [Accessed 7 Oct. 2015].

Gharbi, M., Flegg, J., Hubert, V., Kendjo, E., Metcalf, J., Bertaux, L., Guérin, P. and Le Bras, J. (2013). Longitudinal study assessing the return of chloroquine susceptibility of *Plasmodium falciparum* in isolates from travellers returning from West and Central Africa, 2000–2011. *Malar J*, 12(1), p.35.

Ghosh, D., Griswold, J., Erman, M. and Pangborn, W. (2009). Structural basis for androgen specificity and oestrogen synthesis in human aromatase. *Nature*, 457(7226), pp.219-223.

Ginsburg, H. (2005). Should chloroquine be laid to rest?. *Acta Tropica*, 96(1), pp.16-23.

Goring, J. (2015). *Breast Cancer Grading*. 1st ed. [ebook] Glasgow: NHS Cancer Screening Programmes. Available at: https://www.gov.uk/government/uploads/system/uploads/attachment_data/file/465532/nhsbsp58-poster.pdf [Accessed 10 Jul. 2014].

Gougelet, A., Mueller, S., Korach, K. and Renoir, J. (2007). Oestrogen receptors pathways to oestrogen responsive elements: The transactivation function-1 acts as the keystone of oestrogen receptor (ER) β -mediated

transcriptional repression of ER α . The Journal of Steroid Biochemistry and Molecular Biology, 104(3-5), pp.110-122.

Gusterson, B. and Stein, T. (2012). Human breast development. Seminars in Cell & Developmental Biology, 23(5), pp.567-573.

Hardin, J., Bertoni, G., Kleinsmith, L. and Becker, W. (2012). Becker's world of the cell. Boston: Benjamin Cummings.

Hemminki, K. and Granström, C. (2002). Morphological types of breast cancer in family members and multiple primary tumours: is morphology genetically determined?. Breast Cancer Research, [online] 4(4), pp.1-6. Available at: <http://breast-cancer-research.com/content/4/4/R7> [Accessed 22 Feb. 2015].

Herynk, M. and Fuqua, S. (2004). Estrogen Receptor Mutations in Human Disease. Endocrine Reviews, 25(6), pp.869-898.

Hiscox, S., Baruha, B., Smith, C., Bellerby, R., Goddard, L., Jordan, N., Poghosyan, Z., Nicholson, R., Barrett-Lee, P. and Gee, J. (2012). Overexpression of CD44 accompanies acquired tamoxifen resistance in MCF7 cells and augments their sensitivity to the stromal factors, heregulin and hyaluronan. BMC Cancer, 12(1), p.458.

Hodges, L., Cook, J., Lobenhofer, E., Leping, L., Bennett, L., Bushel, P., Aldaz, C., Afshai, C. and Walker, C. (2003). Tamoxifen Functions As a Molecular Agonist Inducing Cell Cycle-Associated Genes in Breast Cancer Cells. Molecular Cancer Research, [online] 300(1). Available at: <http://mcr.aacrjournals.org/content/1/4/300.long> [Accessed 5 Sep. 2015].

Holliday, D. and Speirs, V. (2011). Choosing the right cell line for breast cancer research. Breast Cancer Research, 13(4), p.215.

Hu, Z., Fan, C., Oh, D., Marron, J., He, X., Qaqish, B., Livasy, C., Carey, L., Reynolds, E., Dressler, L., Nobel, A., Parker, J., Ewend, M., Sawyer, L., Wu, J.,

Liu, Y., Nanda, R., Tretiakova, M., Orrico, A., Dreher, D., Palazzo, J., Perreard, L., Nelson, E., Mone, M., Hansen, H., Mullins, M., Quackenbush, J., Ellis, M., Olopade, O., Bernard, P. and Perou, C. (2006). The molecular portraits of breast tumors are conserved across microarray platforms. *BMC Genomics*, 7(1), p.96.

HUNAKOVA, L., SEDLAKOVA, O., CHOLUJOVA, D., GRONESOVA, P., DURAJ, J. and SEDLAK, J. (2009). Modulation of markers associated with aggressive phenotype in MDA-MB-231 breast carcinoma cells by sulforaphane. *neo*, 56(6), pp.548-556.

Immunochemistry, (2013). Acridine Orange. [online] Available at: <http://www.immunochemistry.com/products/media/pdf/product-datasheet/Acridine-Orange-Stain-6130-Datasheet.pdf> [Accessed 25 May 2013].

Jaafar, H., Sharif, S. and Murtey, M. (2012). Distinctive features of advancing breast cancer cells and interactions with surrounding stroma observed under the scanning electron microscope. *Asian Pacific Journal of Cancer Prevention*, 13(4), pp.1305-1310.

Jalalian, A., Mashohor, S., Mahmud, H., Saripan, M., Ramli, A. and Karasfi, B. (2013). Computer-aided detection/diagnosis of breast cancer in mammography and ultrasound: a review. *Clinical Imaging*, 37(3), pp.420-426.

James, J., McMahon, M., Tennant, S. and Cornford, E. (2012). CT staging for breast cancer patients with poor prognostic tumours. *The Breast*, 21(6), pp.735-738.

Jamshidzadeh, A., Niknahad, H. and Kashafi, H. (2007). Cytotoxicity of chloroquine in isolated rat hepatocytes. - PubMed - NCBI. [online] Ncbi.nlm.nih.gov. Available at: <http://www.ncbi.nlm.nih.gov/pubmed/17265541> [Accessed 7 Aug. 2015].

Jiang, P., Zhao, Y., Deng, X., Mao, Y., Shi, W., Tang, Q., Li, Z., Zheng, Y., Yang, S. and Wei, Y. (2010). Antitumor and antimetastatic activities of chloroquine diphosphate in a murine model of breast cancer. *Biomedicine & Pharmacotherapy*, 64(9), pp.609-614.

Kang, Y., Siegel, P., Shu, W., Drobnjak, M., Kakonen, S., Cordon-Cardo, C., Guise, T. and Massagué, J. (2003). A multigenic program mediating breast cancer metastasis to bone. *Cancer Cell*, 3(6), pp.537-549.

Karhu, R., Laurila, E., Kallioniemi, A. and Syrjäkoski, K. (2006). Large genomic BRCA2 rearrangements and male breast cancer. *Cancer Detection and Prevention*, 30(6), pp.530-534.

Kim, E., Wustenberg, R., Rubsam, A., Schmitz-Salue, C., Warnecke, G., Bucker, E., Pettkus, N., Speidel, D., Rohde, V., Schulz-Schaeffer, W., Deppert, W. and Giese, A. (2010). Chloroquine activates the p53 pathway and induces apoptosis in human glioma cells. *Neuro-Oncology*, 12(4), pp.389-400.

Kim, E., Wustenberg, R., Rubsam, A., Schmitz-Salue, C., Warnecke, G., Bucker, E., Pettkus, N., Speidel, D., Rohde, V., Schulz-Schaeffer, W., Deppert, W. and Giese, A. (2010). Chloroquine activates the p53 pathway and induces apoptosis in human glioma cells. *Neuro-Oncology*, 12(4), pp.389-400.

Kisanga, E. (2004). Tamoxifen and Metabolite Concentrations in Serum and Breast Cancer Tissue during Three Dose Regimens in a Randomized Preoperative Trial. *Clinical Cancer Research*, 10(7), pp.2336-2343.

Kodama, E., Shigeta, S., Suzuki, T. and Clercq, E. (1996). Application of a gastric cancer cell line (MKN-28) for anti-adenovirus screening using the MTT method. *Antiviral Research*, 31(3), pp.159-164.

Kohli, L., Kaza, N., Coric, T., Byer, S., Brossier, N., Klocke, B., Bjornsti, M., Carroll, S. and Roth, K. (2013). 4-Hydroxytamoxifen Induces Autophagic Death through K-Ras Degradation. *Cancer Research*, 73(14), pp.4395-4405.

Kunath, F., Keck, B., Antes, G., Wullich, B. and Meerpohl, J. (2012). Tamoxifen for the management of breast events induced by non-steroidal antiandrogens in patients with prostate cancer: a systematic review. *BMC Medicine*, 10(1), p.96.

Kwan, M., Kushi, L., Weltzien, E., Maring, B., Kutner, S., Fulton, R., Lee, M., Ambrosone, C. and Caan, B. (2009). Epidemiology of breast cancer subtypes in two prospective cohort studies of breast cancer survivors. *Breast Cancer Research*, 11(3), p.R31.

Latrich, C., Stegerer, A., Häring, J., Schüler, S., Ortmann, O. and Treeck, O. (2013). Estrogen receptor β agonists affect growth and gene expression of human breast cancer cell lines. *Steroids*, 78(2), pp.195-202.

Lee, C. and Tannock, I. (2006). Inhibition of endosomal sequestration of basic anticancer drugs: influence on cytotoxicity and tissue penetration. *Br J Cancer*, 94(6), pp.863-869.

Leung, E., Kannan, N., Krissansen, G., Findlay, M. and Baguley, B. (2010). MCF-7 breast cancer cells selected for tamoxifen resistance acquire new phenotypes differing in DNA content, phospho-HER2 and PAX2 expression, and rapamycin sensitivity. *Cancer Biology & Therapy*, 9(9), pp.717-724.

Leung, K., Johannsson, G., Leong, G. and Ho, K. (2004). Estrogen Regulation of Growth Hormone Action. *Endocrine Reviews*, 25(5), pp.693-721.

Liang, D., Choi, D., Kaiparettu, B. and Chang, J. (2015). Effect of autophagy inhibitor, chloroquine in triple negative breast cancer through mitochondrial damage. *Journal of the American College of Surgeons*, 221(4), p.e51.

Lim, Y. (2006). Endoxifen, a Secondary Metabolite of Tamoxifen, and 4-OH-Tamoxifen Induce Similar Changes in Global Gene Expression Patterns in

MCF-7 Breast Cancer Cells. *Journal of Pharmacology and Experimental Therapeutics*, 318(2), pp.503-512.

Liu, C., Hung, M., Wang, D., Chu, P., Su, J., Teng, T., Huang, C., Chao, T., Wang, C., Shiau, C., Tseng, L. and Chen, K. (2014). Tamoxifen induces apoptosis through cancerous inhibitor of protein phosphatase 2A–dependent phospho-Akt inactivation in estrogen receptor–negative human breast cancer cells. *Breast Cancer Research*, 16(5), p.431.

Loehberg, C., Strissel, P., Dittrich, R., Strick, R., Dittmer, J., Dittmer, A., Fabry, B., Kalender, W., Koch, T., Wachter, D., Groh, N., Polier, A., Brandt, I., Lotz, L., Hoffmann, I., Koppitz, F., Oeser, S., Mueller, A., Fasching, P., Lux, M., Beckmann, M. and Schrauder, M. (2012). Akt and p53 are potential mediators of reduced mammary tumor growth by Chloroquine and the mTOR inhibitor RAD001. *Biochemical Pharmacology*, 83(4), pp.480-488.

Loprinzi, C., Zahasky, K., Sloan, J., Novotny, P. and Quella, S. (2000). Tamoxifen-Induced Hot Flashes. *Clinical Breast Cancer*, 1(1), pp.52-56.

Lykkesfeldt, A., Larsen, J., Christensen, I. and Briand, P. (1984). Effects of the antioestrogen tamoxifen on the cell cycle kinetics of the human breast cancer cell line, MCF-7. *Br J Cancer*, 49(6), pp.717-722.

MacLachlan, T. and El-Deiry, W. (2000). *Nature Medicine*, 6(12), pp.1318-1319.

Maes, H., Kuchnio, A., Peric, A., Moens, S., Nys, K., De Bock, K., Quaegebeur, A., Schoors, S., Georgiadou, M., Wouters, J., Vinckier, S., Vankelecom, H., Garmyn, M., Vion, A., Radtke, F., Boulanger, C., Gerhardt, H., Dejana, E., Dewerchin, M., Ghesquière, B., Annaert, W., Agostinis, P. and Carmeliet, P. (2014). Tumor Vessel Normalization by Chloroquine Independent of Autophagy. *Cancer Cell*, 26(2), pp.190-206.

Mandusic, V., Dimitrijevic, B., Nikolic-Vukosavljevic, D., Neskovic-Konstantinovic, Z., Kanjer, K. and Hamann, U. (2012). Different associations of estrogen receptor β isoforms, ER β 1 and ER β 2, expression levels with tumor size and survival in early- and late-onset breast cancer. *Cancer Letters*, 321(1), pp.73-79.

Manic, G., Obrist, F., Kroemer, G., Vitale, I. and Galluzzi, L. (2014). Chloroquine and hydroxychloroquine for cancer therapy. *Molecular & Cellular Oncology*. [online] Available at: <http://www.tandfonline.com/doi/full/10.4161/mco.29911> [Accessed 7 Sep. 2015].

Matsuoka, H., Tsubaki, M., Yamazoe, Y., Ogaki, M., Satou, T., Itoh, T., Kusunoki, T. and Nishida, S. (2009). Tamoxifen inhibits tumor cell invasion and metastasis in mouse melanoma through suppression of PKC/MEK/ERK and PKC/PI3K/Akt pathways. *Experimental Cell Research*, 315(12), pp.2022-2032.

Maycotte, P., Aryal, S., Cummings, C., Thorburn, J., Morgan, M. and Thorburn, A. (2012). Chloroquine sensitizes breast cancer cells to chemotherapy independent of autophagy. *Autophagy*, 8(2), pp.200-212.

McCubrey, J., Davis, N., Abrams, S., Montalto, G., Cervello, M., Libra, M., Nicoletti, F., D'Assoro, A., Cocco, L., Martelli, A. and others, (2014). Targeting breast cancer initiating cells: Advances in breast cancer research and therapy. *Advances in Biological Regulation*.

Meyerson, L., Went, G. and Fultz, T. (2009). Methods and Compositions for the Treatment of CNS-Related Conditions. US20100022659 A1.

Mizushima, N. and Yoshimori, T. (2007). How to Interpret LC3 Immunoblotting. *Autophagy*, 3(6), pp.542-545.

Mohamed, A., Soliman, H., Ismail, M., Ziada, D., Farid, T., Aref, A., Al Daly, M. and Abd Elmageed, Z. (2015). Evaluation of circulating ADH and MIC-1 as

diagnostic markers in Egyptian patients with pancreatic cancer. *Pancreatology*, 15(1), pp.34-39.

Moodley, S., Koorbanally, N., Moodley, T., Ramjugernath, D. and Pillay, M. (2014). The 3-(4,5-dimethylthiazol-2-yl)-2,5-diphenyl tetrazolium bromide (MTT) assay is a rapid, cheap, screening test for the in vitro anti-tuberculous activity of chalcones. *Journal of Microbiological Methods*, 104, pp.72-78.

Morrow, M., Waters, J. and Morris, E. (2011). MRI for breast cancer screening, diagnosis, and treatment. *The Lancet*, 378(9805), pp.1804-1811.

Munck, C., Gumpert, H., Wallin, A., Wang, H. and Sommer, M. (2014). Prediction of resistance development against drug combinations by collateral responses to component drugs. *Science Translational Medicine*, 6(262), pp.262ra156-262ra156.

Narod, S. (2006). Modifiers of risk of hereditary breast cancer. *Oncogene*, 25(43), pp.5832-5836.

Nathanson, K., Wooster, R. and Weber, B. (2001). *Nature Medicine*, 7(5), pp.552-556.

Nazarewicz, R., Zenebe, W., Parihar, A., Larson, S., Alidema, E., Choi, J. and Ghafourifar, P. (2007). Tamoxifen Induces Oxidative Stress and Mitochondrial Apoptosis via Stimulating Mitochondrial Nitric Oxide Synthase. *Cancer Research*, 67(3), pp.1282-1290.

Ncbi.nlm.nih.gov, (2015). RAD51 RAD51 recombinase [Homo sapiens (human)] - Gene - NCBI. [online] Available at: <http://www.ncbi.nlm.nih.gov/gene/5888> [Accessed 31 Mar. 2013].

Neve, R., Chin, K., Fridlyand, J., Yeh, J., Baehner, F., Fevr, T., Clark, L., Bayani, N., Coppe, J., Tong, F., Speed, T., Spellman, P., DeVries, S., Lapuk, A., Wang, N., Kuo, W., Stilwell, J., Pinkel, D., Albertson, D., Waldman, F.,

McCormick, F., Dickson, R., Johnson, M., Lippman, M., Ethier, S., Gazdar, A. and Gray, J. (2006). A collection of breast cancer cell lines for the study of functionally distinct cancer subtypes. *Cancer Cell*, 10(6), pp.515-527.

Newberne, J., Kuhn, W. and Elsea, J. (1966). Toxicologic studies on clomiphene. *Toxicology and Applied Pharmacology*, 9(1), pp.44-56.

Oldenburg, R., Meijers-Heijboer, H., Cornelisse, C. and Devilee, P. (2007). Genetic susceptibility for breast cancer: How many more genes to be found?. *Critical Reviews in Oncology/Hematology*, 63(2), pp.125-149.

Oliver, A., Freixenet, J., Martí, J., Pérez, E., Pont, J., Denton, E. and Zwiggelaar, R. (2010). A review of automatic mass detection and segmentation in mammographic images. *Medical Image Analysis*, 14(2), pp.87-110.

Ottini, L. (2014). Male breast cancer: a rare disease that might uncover underlying pathways of breast cancer. *Nature Reviews Cancer*, 14(10), pp.643-644.

Paid Clinical Trials - Clinical Trial News and Opinion, (2015). Anti-malaria Drug Quinine Heads the List of Breast Cancer Clinical Trials. [online] Available at: <http://www.paidclinicaltrials.org/media/anti-malaria-drug-quinine-heads-the-list-of-breast-cancer-clinical-trials/> [Accessed 10 May 2015].

Parnell, C. and Woll, P. (2003). Principles of cancer treatment by chemotherapy. *Surgery (Oxford)*, 21(11), pp.272-276.

Pearce, S. and Jordan, V. (2004). The biological role of estrogen receptors α and β in cancer. *Critical Reviews in Oncology/Hematology*, 50(1), pp.3-22.

Perou, C., Sørlie, T., Eisen, M., van de Rijn, M., Jeffrey, S., Rees, C., Pollack, J., Ross, D., Johnsen, H., Akslen, L., Fluge, Ø., Pergamenschikov, A., Williams, C., Zhu, S., Lønning, P., Børresen-Dale, A., Brown, P. and Botstein, D. (2000). Molecular portraits of human breast tumours. *Nature*, 406(6797), pp.747-752.

Persidis, A. (1999). Cancer multidrug resistance. *Nat. Biotechnol.*, 17(1), pp.94-95.

Platet, N., Cathiard, A., Gleizes, M. and Garcia, M. (2004). Estrogens and their receptors in breast cancer progression: a dual role in cancer proliferation and invasion. *Critical Reviews in Oncology/Hematology*, 51(1), pp.55-67.

Polat, K. and Güneş, S. (2007). Breast cancer diagnosis using least square support vector machine. *Digital Signal Processing*, 17(4), pp.694-701.

Pourkavoos, N. (2012). Unique Risks, Benefits, and Challenges of Developing Drug-Drug Combination Products in a Pharmaceutical Industrial Setting. *Combination Products in Therapy*, 2(1).

Prueksaritanont, T., Chu, X., Gibson, C., Cui, D., Yee, K., Ballard, J., Cabalu, T. and Hochman, J. (2013). Drug–Drug Interaction Studies: Regulatory Guidance and An Industry Perspective. *The AAPS Journal*, 15(3), pp.629-645.

Qadir, M., Kwok, B., Dragowska, W., To, K., Le, D., Bally, M. and Gorski, S. (2008). Macroautophagy inhibition sensitizes tamoxifen-resistant breast cancer cells and enhances mitochondrial depolarization. *Breast Cancer Res Treat*, 112(3), pp.389-403.

Rafnar, T., Benediktsdottir, K., Eldon, B., Gestsson, T., Saemundsson, H., Olafsson, K., Salvarsdottir, A., Steingrimsson, E. and Thorlacius, S. (2004). BRCA2, but not BRCA1, mutations account for familial ovarian cancer in Iceland: a population-based study. *European Journal of Cancer*, 40(18), pp.2788-2793.

Repetto, G., del Peso, A. and Zurita, J. (2008). Neutral red uptake assay for the estimation of cell viability/cytotoxicity. *Nat Protoc*, 3(7), pp.1125-1131.

Repetto, G., del Peso, A. and Zurita, J. (2008). Neutral red uptake assay for the estimation of cell viability/cytotoxicity. *Nat Protoc*, 3(7), pp.1125-1131.

Rieger, A., Nelson, K., Konowalchuk, J. and Barreda, D. (2011). Modified Annexin V/Propidium Iodide Apoptosis Assay For Accurate Assessment of Cell Death. *Journal of Visualized Experiments*, (50).

Riggins, R., Schrecengost, R., Guerrero, M. and Bouton, A. (2007). Pathways to tamoxifen resistance. *Cancer Letters*, 256(1), pp.1-24.

Robertson, I., Hand, F. and Kell, M. (2011). FDG-PET/CT in the staging of local/regional metastases in breast cancer. *The Breast*, 20(6), pp.491-494.

Robison, J., Perreard, L. and Bernard, P. (2004). State of the science: molecular classifications of breast cancer for clinical diagnostics. *Clinical biochemistry*, 37(7), pp.572--578.

Sansare, K., Khanna, V. and Karjodkar, F. (2011). Early victims of X-rays: a tribute and current perception. *Dentomaxillofacial Radiology*, 40(2), pp.123-125.

Saha, K., Raychaudhuri, G., Chattopadhyay, B. and Das, I. (2013). Comparative evaluation of six cytological grading systems in breast carcinoma. *Journal of Cytology*, 30(2), p.87.

Schwartz, G., Reis-Fihlo, J., Pusztai, L., Fentiman, I., Holland, R., Bartelink, H., Rutgers, E., Solin, L. and Palazzo, J. (2012). Adjuvant therapy in stage I carcinoma of the breast. *Cancer*, 118(8), pp.2031--2038.

Sheridan, C., Kishimoto, H., Fuchs, R., Mehrotra, S., Bhat-Nakshatri, P., Turner, C., Goulet, R., Badve, S. and Nakshatri, H. (2006). CD44+/CD24- breast cancer cells exhibit enhanced invasive properties: an early step necessary for metastasis. *Breast Cancer Research*, 8(5), p.R59.

Shyamala, G., Chou, Y., Louie, S., Guzman, R., Smith, G. and Nandi, S. (2002). Cellular expression of estrogen and progesterone receptors in mammary glands: regulation by hormones, development and aging. *The Journal of Steroid Biochemistry and Molecular Biology*, 80(2), pp.137-148.

Singh, M., Stringfellow, H., Paraskevaidis, E., Martin-Hirsch, P. and Martin, F. (2007). Tamoxifen: Important considerations of a multi-functional compound with organ-specific properties. *Cancer Treatment Reviews*, 33(2), pp.91-100.

Solomon, V. and Lee, H. (2009). Chloroquine and its analogs: A new promise of an old drug for effective and safe cancer therapies. *European Journal of Pharmacology*, 625(1-3), pp.220-233.

Soma, S., Chaouat, M., Jacob, D., Perrot, J., Rostne, W., Forgez, P. and Gompel, A. (2003). Antiestrogens are pro-apoptotic in normal human breast epithelial cells. *International Journal of Cancer*, 105(5), pp.607-612.

Sotelo, J. (2006). Adding Chloroquine to Conventional Treatment for Glioblastoma Multiforme. *Annals of Internal Medicine*, 144(5), p.337.

Sorlie, T., Perou, C., Tibshirani, R., Aas, T., Geisler, S., Johnsen, H., Hastie, T., Eisen, M., van de Rijn, M., Jeffrey, S., Thorsen, T., Quist, H., Matese, J., Brown, P., Botstein, D., Lonning, P. and Borresen-Dale, A. (2001). Gene expression patterns of breast carcinomas distinguish tumor subclasses with clinical implications. *Proceedings of the National Academy of Sciences*, 98(19), pp.10869-10874.

Sorlie, T., Tibshirani, R., Parker, J., Hastie, T., Marron, J., Nobel, A., Deng, S., Johnsen, H., Pesich, R., Geisler, S., Demeter, J., Perou, C., Lonning, P., Brown, P., Borresen-Dale, A. and Botstein, D. (2003). Repeated observation of breast tumor subtypes in independent gene expression data sets. *Proceedings of the National Academy of Sciences*, 100(14), pp.8418-8423.

Spellman, P. and Gray, J. (2011). A new treasure in the breast cancer gene hunt. *Nature Medicine*, 17(4), pp.422-423.

Sridhar, T. and Symonds, R. (2009). Principles of chemotherapy and radiotherapy. *Obstetrics, Gynaecology & Reproductive Medicine*, 19(3), pp.61-67.

Sui, X., Chen, R., Wang, Z., Huang, Z., Kong, N., Zhang, M., Han, W., Lou, F., Yang, J., Zhang, Q., Wang, X., He, C. and Pan, H. (2013). Autophagy and chemotherapy resistance: a promising therapeutic target for cancer treatment. *Cell Death Dis*, 4(10), pg. 838.

Sun, H., Jia, J., Wang, X., Ma, B., Di, L., Song, G. and Ren, J. (2012). CD44+/CD24- breast cancer cells isolated from MCF-7 cultures exhibit enhanced angiogenic properties. *Clin Transl Oncol*, 15(1), pp.46-54.

Swisher, E. (2004). Comment on "Malignant mixed Mullerian tumor of the ovary: an argument for BRCA3 or a coincidental cluster of unconnected cancer". *Gynecologic Oncology*, 95(3), pp.773-774.

Teka, H., Petros, B., Yamuah, L., Tesfaye, G., Elhassan, I., Muchohi, S., Kokwaro, G., Aseffa, A. and Engers, H. (2008). Chloroquine-resistant *Plasmodium vivax* malaria in Debre Zeit, Ethiopia. *Malar J*, 7(1), p.220.

Thomé, R., Lopes, S., Costa, F. and Verinaud, L. (2013). Chloroquine: Modes of action of an undervalued drug. *Immunology Letters*, 153(1-2), pp.50-57.

Travis, R. and Key, T. (2003). *Breast Cancer Research*, 5(5), p.239.

Tu, Y., Kaiparettu, B., Ma, Y. and Wong, L. (2011). Mitochondria of highly metastatic breast cancer cell line MDA-MB-231 exhibits increased autophagic properties. *Biochimica et Biophysica Acta (BBA) - Bioenergetics*, 1807(9), pp.1125-1132.

Tuomela, J., Sandholm, J. and Selander, K. (2013). Chloroquine has tumor-inhibitory and tumor-promoting effects in triple-negative breast cancer. *Oncology Letters*.

Vaillant, F., Merino, D., Lee, L., Breslin, K., Pal, B., Ritchie, M., Smyth, G., Christie, M., Phillipson, L., Burns, C., Mann, G., Visvader, J. and Lindeman, G. (2013). Targeting BCL-2 with the BH3 Mimetic ABT-199 in Estrogen Receptor-Positive Breast Cancer. *Cancer Cell*, 24(1), pp.120-129.

Vargo-Gogola, T. and Rosen, J. (2007). Modelling breast cancer: one size does not fit all. *Nature Reviews Cancer*, 7(9), pp.659-672.

Vogel, V. (2006). Effects of tamoxifen vs raloxifene on the risk of developing invasive breast cancer and other disease outcomes: the NSABP Study of Tamoxifen and Raloxifene (STAR) P-2 trial. *JAMA*, [online] 296(23), pp.2727-2741. Available at: <http://jama.jamanetwork.com/article.aspx?articleid=203040> [Accessed 15 Oct. 2015].

Vogelstein, B., Lane, D. and Levine, A. (2000). p53 : The Most Frequently Altered Gene in Human Cancers. *Nature*, 408(6810), pp.307-310.

Wallace, D., Furst, D. and Romain, P. (2015). Antimalarial drugs in the treatment of rheumatic disease. [online] Uptodate.com. Available at: <http://www.uptodate.com/contents/antimalarial-drugs-in-the-treatment-of-rheumatic-disease> [Accessed 7 Dec. 2015].

Watson, C. and Hughes, K. (2014). Breast cancer: the menacing face of Janus kinase. *Cell Death Differ*, 21(2), pp.185-186.

Weber, A. (2001). History of Head and Neck Radiology: Past, Present, and Future1. *Radiology*, 218(1), pp.15-24.

Węsierska-Gądek, J., Schreiner, T., Gueorguieva, M. and Ranftler, C. (2006). Phenol red reduces ROSC mediated cell cycle arrest and apoptosis in human MCF-7 cells. *Journal of Cellular Biochemistry*, 98(6), pp.1367-1379.

Węsierska-Gądek, J., Schreiner, T., Maurer, M., Waringer, A. and Ranftler, C. (2007). Phenol red in the culture medium strongly affects the susceptibility of human MCF-7 cells to roscovitine. *Cellular and Molecular Biology Letters*, 12(2).

Weigelt, B., Mackay, A., A'hern, R., Natrajan, R., Tan, D., Dowsett, M., Ashworth, A. and Reis-Filho, J. (2010). Breast cancer molecular profiling with single sample predictors: a retrospective analysis. *The Lancet Oncology*, 11(4), pp.339-349.

Wood, W. (2007). Breast surgery in advanced breast cancer: Local control in the presence of metastases. *The Breast*, 16, pp.63-66.

Xie, X., Yu, H., Wang, Y., Zhou, Y., Li, G., Ruan, Z., Li, F., Wang, X., Liu, H. and Zhang, J. (2014). Nicotinamide N-methyltransferase enhances the capacity of tumorigenesis associated with the promotion of cell cycle progression in human colorectal cancer cells. *Archives of Biochemistry and Biophysics*, 564, pp.52-66.

Yamaguchi, R., Tanaka, M., Yano, A., Tse, G., Yamaguchi, M., Koura, K., Kanomata, N., Kawaguchi, A., Akiba, J., Naito, Y., Ohshima, K. and Yano, H. (2012). Tumor-infiltrating lymphocytes are important pathologic predictors for neoadjuvant chemotherapy in patients with breast cancer. *Human Pathology*, 43(10), pp.1688-1694.

Youlden, D., Cramb, S., Dunn, N., Muller, J., Pyke, C. and Baade, P. (2012). The descriptive epidemiology of female breast cancer: An international comparison of screening, incidence, survival and mortality. *Cancer Epidemiology*, 36(3), pp.237-248.

Zaidi, A., McDonough, J., Klocke, B., Latham, C., Korsmeyer, S., Flavell, R., Schmidt, R. and Roth, K. (2001). Chloroquine-Induced Neuronal Cell Death Is p53 and Bcl-2 Family-Dependent But Caspase-Independent. *Journal of Neuropathology & Experimental Neurology*, 60(10), pp.937-945.

Zartman, J., Foreman, N., Donson, A. and Fleitz, J. (2004). Measurement of Tamoxifen-Induced Apoptosis in Glioblastoma by Cytometric Bead Analysis of Active Caspase-3. *J Neurooncol*, 67(1/2), pp.3-7.

Zhang, G., Kimijima, I., Onda, M., Kanno, M., Sato, H., Watanabe, T., Tsuchiya, A., Abe, R. and Takenoshita, S. (1999). Tamoxifen-induced Apoptosis in Breast Cancer Cells Relates to Down-Regulation of bcl-2, but not bax and bcl-XL, without Alteration of p53 Protein Levels. *Clinical Cancer Research*, [online] 2971(5). Available at: <http://clincancerres.aacrjournals.org/content/5/10/2971.full> [Accessed 5 Oct. 2015].

Zheng, A., Kallio, A. and Härkönen, P. (2007). Tamoxifen-Induced Rapid Death of MCF-7 Breast Cancer Cells Is Mediated via Extracellularly Signal-Regulated Kinase Signaling and Can Be Abrogated by Estrogen. *Endocrinology*, 148(6), pp.2764-2777.

Zhu, Q. (2013). Dose-dependent effect of tamoxifen in tamoxifen-resistant breast cancer cells via stimulation by the ERK1/2 and AKT signaling pathways. *Oncology Reports*, 29(4).

7.0 Appendices

7.0 Appendices

7.1 Appendix 1: 2way ANOVA with Dunnett's multiple comparisons test for all MTT Assays against Control

Within each row, compare columns (simple effects within rows)				
Number of families	1			
Number of comparisons per family	96			
Alpha	0.05			
Dunnett's multiple comparisons test	Mean Diff.	95% CI of diff.	Significant?	Summary
0				
Control vs. WT x T	0.0	-19.80 to 19.80	No	ns
Control vs. WT x TCQ	0.0	-19.80 to 19.80	No	ns
Control vs. TMX x T	0.0	-19.80 to 19.80	No	ns
Control vs. TMX x TCQ	0.0	-19.80 to 19.80	No	ns
Control vs. MDA x T	0.0	-19.80 to 19.80	No	ns
Control vs. MDA x TCQ	0.0	-19.80 to 19.80	No	ns
2				
Control vs. WT x T	1.736	-15.98 to 19.45	No	ns
Control vs. WT x TCQ	22.72	5.005 to 40.43	Yes	**
Control vs. TMX x T	-5.330	-23.04 to 12.38	No	ns
Control vs. TMX x TCQ	-3.468	-21.18 to 14.25	No	ns
Control vs. MDA x T	1.932	-15.78 to 19.65	No	ns
Control vs. MDA x TCQ	17.49	-0.2283 to 35.20	No	ns
4				
Control vs. WT x T	-5.385	-23.10 to 12.33	No	ns
Control vs. WT x TCQ	26.00	8.291 to 43.72	Yes	***
Control vs. TMX x T	-4.995	-22.71 to 12.72	No	ns
Control vs. TMX x TCQ	7.611	-10.10 to 25.32	No	ns
Control vs. MDA x T	4.650	-13.06 to 22.36	No	ns
Control vs. MDA x TCQ	18.71	0.9989 to 36.43	Yes	*
6				
Control vs. WT x T	-0.5273	-18.24 to 17.19	No	ns
Control vs. WT x TCQ	39.52	19.71 to 59.32	Yes	****
Control vs. TMX x T	-7.154	-24.87 to 10.56	No	ns
Control vs. TMX x TCQ	18.97	1.256 to 36.68	Yes	*
Control vs. MDA x T	2.682	-15.03 to 20.40	No	ns
Control vs. MDA x TCQ	16.20	-1.510 to 33.92	No	ns
8				
Control vs. WT x T	-3.081	-20.79 to 14.63	No	ns
Control vs. WT x TCQ	53.01	35.30 to 70.73	Yes	****
Control vs. TMX x T	-5.690	-23.40 to 12.02	No	ns
Control vs. TMX x TCQ	20.26	2.543 to 37.97	Yes	*
Control vs. MDA x T	5.985	-11.73 to 23.70	No	ns
Control vs. MDA x TCQ	21.44	3.727 to 39.15	Yes	**
10				

Control vs. WT x T	2.196	-15.52 to 19.91	No	ns
Control vs. WT x TCQ	58.02	40.31 to 75.74	Yes	****
Control vs. TMX x T	-2.121	-19.83 to 15.59	No	ns
Control vs. TMX x TCQ	28.51	10.79 to 46.22	Yes	****
Control vs. MDA x T	7.713	-10.00 to 25.43	No	ns
Control vs. MDA x TCQ	31.46	13.75 to 49.17	Yes	****
12				
Control vs. WT x T	17.12	-0.5918 to 34.84	No	ns
Control vs. WT x TCQ	71.96	54.25 to 89.67	Yes	****
Control vs. TMX x T	-2.575	-20.29 to 15.14	No	ns
Control vs. TMX x TCQ	57.00	39.28 to 74.71	Yes	****
Control vs. MDA x T	11.41	-6.301 to 29.13	No	ns
Control vs. MDA x TCQ	49.95	32.24 to 67.67	Yes	****
14				
Control vs. WT x T	32.30	14.58 to 50.01	Yes	****
Control vs. WT x TCQ	69.49	51.77 to 87.20	Yes	****
Control vs. TMX x T	5.180	-12.53 to 22.89	No	ns
Control vs. TMX x TCQ	65.92	48.20 to 83.63	Yes	****
Control vs. MDA x T	19.57	1.853 to 37.28	Yes	*
Control vs. MDA x TCQ	70.73	53.01 to 88.44	Yes	****
16				
Control vs. WT x T	56.19	38.48 to 73.90	Yes	****
Control vs. WT x TCQ	82.16	64.45 to 99.88	Yes	****
Control vs. TMX x T	23.95	6.239 to 41.67	Yes	***
Control vs. TMX x TCQ	65.90	48.19 to 83.61	Yes	****
Control vs. MDA x T	41.60	23.89 to 59.32	Yes	****
Control vs. MDA x TCQ	78.47	60.75 to 96.18	Yes	****
18				
Control vs. WT x T	64.84	47.13 to 82.56	Yes	****
Control vs. WT x TCQ	97.18	79.47 to 114.9	Yes	****
Control vs. TMX x T	51.20	33.48 to 68.91	Yes	****
Control vs. TMX x TCQ	92.94	75.23 to 110.7	Yes	****
Control vs. MDA x T	68.39	50.68 to 86.10	Yes	****
Control vs. MDA x TCQ	88.06	70.34 to 105.8	Yes	****
20				
Control vs. WT x T	85.21	67.49 to 102.9	Yes	****
Control vs. WT x TCQ	98.85	81.14 to 116.6	Yes	****
Control vs. TMX x T	85.88	68.17 to 103.6	Yes	****
Control vs. TMX x TCQ	97.37	79.66 to 115.1	Yes	****
Control vs. MDA x T	98.41	80.69 to 116.1	Yes	****
Control vs. MDA x TCQ	97.94	80.23 to 115.7	Yes	****
22				
Control vs. WT x T	98.28	80.57 to 116.0	Yes	****
Control vs. WT x TCQ	98.74	81.02 to 116.4	Yes	****
Control vs. TMX x T	99.73	82.01 to 117.4	Yes	****
Control vs. TMX x TCQ	99.57	81.86 to 117.3	Yes	****
Control vs. MDA x T	98.97	81.25 to 116.7	Yes	****
Control vs. MDA x TCQ	99.07	81.36 to 116.8	Yes	****
24				
Control vs. WT x T	99.09	81.38 to 116.8	Yes	****
Control vs. WT x TCQ	98.52	80.80 to 116.2	Yes	****
Control vs. TMX x T	99.10	81.39 to 116.8	Yes	****
Control vs. TMX x TCQ	99.06	81.35 to 116.8	Yes	****
Control vs. MDA x T	98.32	80.60 to 116.0	Yes	****

Control vs. MDA x TCQ	100.0	82.29 to 117.7	Yes	****
26				
Control vs. WT x T	99.90	82.19 to 117.6	Yes	****
Control vs. WT x TCQ	99.11	81.39 to 116.8	Yes	****
Control vs. TMX x T	99.53	81.81 to 117.2	Yes	****
Control vs. TMX x TCQ	99.79	82.07 to 117.5	Yes	****
Control vs. MDA x T	99.02	81.31 to 116.7	Yes	****
Control vs. MDA x TCQ	100.0	82.29 to 117.7	Yes	****
28				
Control vs. WT x T	99.68	81.97 to 117.4	Yes	****
Control vs. WT x TCQ	98.61	80.90 to 116.3	Yes	****
Control vs. TMX x T	99.52	81.80 to 117.2	Yes	****
Control vs. TMX x TCQ	100.0	82.29 to 117.7	Yes	****
Control vs. MDA x T	98.57	80.86 to 116.3	Yes	****
Control vs. MDA x TCQ	100.0	82.29 to 117.7	Yes	****
30				
Control vs. WT x T	100.0	82.29 to 117.7	Yes	****
Control vs. WT x TCQ	100.0	82.29 to 117.7	Yes	****
Control vs. TMX x T	100.0	82.29 to 117.7	Yes	****
Control vs. TMX x TCQ	100.0	82.29 to 117.7	Yes	****
Control vs. MDA x T	100.0	82.29 to 117.7	Yes	****
Control vs. MDA x TCQ	100.0	82.29 to 117.7	Yes	****

7.2 Appendix 2: 2way ANOVA with Tukey's multiple comparisons test for all MTT Assays; cross comparison

Within each row, compare columns (simple effects within rows)				
Number of families	1			
Number of comparisons per family	336			
Alpha	0.05			
Tukey's multiple comparisons test	Mean Diff.	95% CI of diff.	Significant?	Summary
0				

WT x T vs. WT x TCQ	0.0	-23.37 to 23.37	No	ns
WT x T vs. TMX x T	0.0	-23.37 to 23.37	No	ns
WT x T vs. TMX x TCQ	0.0	-23.37 to 23.37	No	ns
WT x T vs. MDA x T	0.0	-23.37 to 23.37	No	ns
WT x T vs. MDA x TCQ	0.0	-23.37 to 23.37	No	ns
WT x TCQ vs. Control	0.0	-26.13 to 26.13	No	ns
WT x TCQ vs. TMX x T	0.0	-23.37 to 23.37	No	ns
WT x TCQ vs. TMX x TCQ	0.0	-23.37 to 23.37	No	ns
WT x TCQ vs. MDA x T	0.0	-23.37 to 23.37	No	ns
WT x TCQ vs. MDA x TCQ	0.0	-23.37 to 23.37	No	ns
WT x TCQ vs. Control	0.0	-26.13 to 26.13	No	ns
TMX x T vs. TMX x TCQ	0.0	-23.37 to 23.37	No	ns
TMX x T vs. MDA x T	0.0	-23.37 to 23.37	No	ns
TMX x T vs. MDA x TCQ	0.0	-23.37 to 23.37	No	ns
TMX x T vs. Control	0.0	-26.13 to 26.13	No	ns
TMX x TCQ vs. MDA x T	0.0	-23.37 to 23.37	No	ns
TMX x TCQ vs. MDA x TCQ	0.0	-23.37 to 23.37	No	ns
TMX x TCQ vs. Control	0.0	-26.13 to 26.13	No	ns
MDA x T vs. MDA x TCQ	0.0	-23.37 to 23.37	No	ns
MDA x T vs. Control	0.0	-26.13 to 26.13	No	ns
MDA x TCQ vs. Control	0.0	-26.13 to 26.13	No	ns
2				
WT x T vs. WT x TCQ	20.98	-2.389 to 44.35	No	ns
WT x T vs. TMX x T	-7.066	-30.44 to 16.31	No	ns
WT x T vs. TMX x TCQ	-5.205	-28.58 to 18.17	No	ns
WT x T vs. MDA x T	0.1960	-23.18 to 23.57	No	ns
WT x T vs. MDA x TCQ	15.75	-7.622 to 39.12	No	ns
WT x T vs. Control	-1.736	-25.11 to 21.64	No	ns
WT x TCQ vs. TMX x T	-28.05	-51.42 to -4.677	Yes	**
WT x TCQ vs. TMX x TCQ	-26.19	-49.56 to -2.815	Yes	**
WT x TCQ vs. MDA x T	-20.79	-44.16 to 2.585	No	ns
WT x TCQ vs. MDA x TCQ	-5.233	-28.60 to 18.14	No	ns
WT x TCQ vs. Control	-22.72	-46.09 to 0.6531	No	ns
TMX x T vs. TMX x TCQ	1.861	-21.51 to 25.23	No	ns
TMX x T vs. MDA x T	7.262	-16.11 to 30.63	No	ns
TMX x T vs. MDA x TCQ	22.81	-0.5563 to 46.19	No	ns
TMX x T vs. Control	5.330	-18.04 to 28.70	No	ns
TMX x TCQ vs. MDA x T	5.401	-17.97 to 28.77	No	ns
TMX x TCQ vs. MDA x TCQ	20.95	-2.418 to 44.32	No	ns
TMX x TCQ vs. Control	3.468	-19.90 to 26.84	No	ns
MDA x T vs. MDA x TCQ	15.55	-7.818 to 38.92	No	ns
MDA x T vs. Control	-1.932	-25.30 to 21.44	No	ns
MDA x TCQ vs. Control	-17.49	-40.86 to 5.886	No	ns
4				
WT x T vs. WT x TCQ	31.39	8.017 to 54.76	Yes	****
WT x T vs. TMX x T	0.3894	-22.98 to 23.76	No	ns
WT x T vs. TMX x TCQ	13.00	-10.38 to 36.37	No	ns
WT x T vs. MDA x T	10.03	-13.34 to 33.41	No	ns
WT x T vs. MDA x TCQ	24.10	0.7257 to 47.47	Yes	*
WT x T vs. Control	5.385	-17.99 to 28.76	No	ns
WT x TCQ vs. TMX x T	-31.00	-54.37 to -7.628	Yes	****
WT x TCQ vs. TMX x TCQ	-18.39	-41.76 to 4.978	No	ns
WT x TCQ vs. MDA x T	-21.35	-44.73 to 2.017	No	ns
WT x TCQ vs. MDA x TCQ	-7.292	-30.66 to 16.08	No	ns

WT x TCQ vs. Control	-26.00	-49.38 to -2.633	Yes	**
TMX x T vs. TMX x TCQ	12.61	-10.77 to 35.98	No	ns
TMX x T vs. MDA x T	9.645	-13.73 to 33.02	No	ns
TMX x T vs. MDA x TCQ	23.71	0.3362 to 47.08	Yes	*
TMX x T vs. Control	4.995	-18.38 to 28.37	No	ns
TMX x TCQ vs. MDA x T	-2.961	-26.33 to 20.41	No	ns
TMX x TCQ vs. MDA x TCQ	11.10	-12.27 to 34.47	No	ns
TMX x TCQ vs. Control	-7.611	-30.98 to 15.76	No	ns
MDA x T vs. MDA x TCQ	14.06	-9.308 to 37.43	No	ns
MDA x T vs. Control	-4.650	-28.02 to 18.72	No	ns
MDA x TCQ vs. Control	-18.71	-42.08 to 4.659	No	ns
6				
WT x T vs. WT x TCQ	40.04	13.91 to 66.17	Yes	****
WT x T vs. TMX x T	-6.627	-30.00 to 16.74	No	ns
WT x T vs. TMX x TCQ	19.50	-3.875 to 42.87	No	ns
WT x T vs. MDA x T	3.210	-20.16 to 26.58	No	ns
WT x T vs. MDA x TCQ	16.73	-6.641 to 40.10	No	ns
WT x T vs. Control	0.5273	-22.84 to 23.90	No	ns
WT x TCQ vs. TMX x T	-46.67	-72.80 to -20.54	Yes	****
WT x TCQ vs. TMX x TCQ	-20.55	-46.68 to 5.583	No	ns
WT x TCQ vs. MDA x T	-36.83	-62.96 to -10.70	Yes	****
WT x TCQ vs. MDA x TCQ	-23.31	-49.44 to 2.817	No	ns
WT x TCQ vs. Control	-39.52	-65.65 to -13.39	Yes	****
TMX x T vs. TMX x TCQ	26.12	2.752 to 49.49	Yes	**
TMX x T vs. MDA x T	9.837	-13.53 to 33.21	No	ns
TMX x T vs. MDA x TCQ	23.36	-0.01383 to 46.73	No	ns
TMX x T vs. Control	7.154	-16.22 to 30.53	No	ns
TMX x TCQ vs. MDA x T	-16.29	-39.66 to 7.084	No	ns
TMX x TCQ vs. MDA x TCQ	-2.766	-26.14 to 20.61	No	ns
TMX x TCQ vs. Control	-18.97	-42.34 to 4.402	No	ns
MDA x T vs. MDA x TCQ	13.52	-9.851 to 36.89	No	ns
MDA x T vs. Control	-2.682	-26.05 to 20.69	No	ns
MDA x TCQ vs. Control	-16.20	-39.57 to 7.168	No	ns
8				
WT x T vs. WT x TCQ	56.09	32.72 to 79.46	Yes	****
WT x T vs. TMX x T	-2.609	-25.98 to 20.76	No	ns
WT x T vs. TMX x TCQ	23.34	-0.03423 to 46.71	No	ns
WT x T vs. MDA x T	9.066	-14.31 to 32.44	No	ns
WT x T vs. MDA x TCQ	24.52	1.150 to 47.89	Yes	*
WT x T vs. Control	3.081	-20.29 to 26.45	No	ns
WT x TCQ vs. TMX x T	-58.70	-82.07 to -35.33	Yes	****
WT x TCQ vs. TMX x TCQ	-32.76	-56.13 to -9.385	Yes	****
WT x TCQ vs. MDA x T	-47.03	-70.40 to -23.66	Yes	****
WT x TCQ vs. MDA x TCQ	-31.57	-54.94 to -8.200	Yes	****
WT x TCQ vs. Control	-53.01	-76.38 to -29.64	Yes	****
TMX x T vs. TMX x TCQ	25.95	2.575 to 49.32	Yes	**
TMX x T vs. MDA x T	11.67	-11.70 to 35.05	No	ns
TMX x T vs. MDA x TCQ	27.13	3.759 to 50.50	Yes	**
TMX x T vs. Control	5.690	-17.68 to 29.06	No	ns
TMX x TCQ vs. MDA x T	-14.27	-37.64 to 9.100	No	ns
TMX x TCQ vs. MDA x TCQ	1.185	-22.19 to 24.56	No	ns
TMX x TCQ vs. Control	-20.26	-43.63 to 3.115	No	ns
MDA x T vs. MDA x TCQ	15.46	-7.916 to 38.83	No	ns
MDA x T vs. Control	-5.985	-29.36 to 17.39	No	ns

MDA x TCQ vs. Control	-21.44	-44.81 to 1.930	No	ns
10				
WT x T vs. WT x TCQ	55.83	32.46 to 79.20	Yes	****
WT x T vs. TMX x T	-4.317	-27.69 to 19.05	No	ns
WT x T vs. TMX x TCQ	26.31	2.939 to 49.68	Yes	**
WT x T vs. MDA x T	5.517	-17.85 to 28.89	No	ns
WT x T vs. MDA x TCQ	29.26	5.893 to 52.64	Yes	***
WT x T vs. Control	-2.196	-25.57 to 21.18	No	ns
WT x TCQ vs. TMX x T	-60.15	-83.52 to -36.77	Yes	****
WT x TCQ vs. TMX x TCQ	-29.52	-52.89 to -6.146	Yes	***
WT x TCQ vs. MDA x T	-50.31	-73.68 to -26.94	Yes	****
WT x TCQ vs. MDA x TCQ	-26.56	-49.93 to -3.192	Yes	**
WT x TCQ vs. Control	-58.02	-81.39 to -34.65	Yes	****
TMX x T vs. TMX x TCQ	30.63	7.257 to 54.00	Yes	***
TMX x T vs. MDA x T	9.835	-13.54 to 33.21	No	ns
TMX x T vs. MDA x TCQ	33.58	10.21 to 56.95	Yes	****
TMX x T vs. Control	2.121	-21.25 to 25.49	No	ns
TMX x TCQ vs. MDA x T	-20.79	-44.16 to 2.578	No	ns
TMX x TCQ vs. MDA x TCQ	2.954	-20.42 to 26.33	No	ns
TMX x TCQ vs. Control	-28.51	-51.88 to -5.135	Yes	***
MDA x T vs. MDA x TCQ	23.75	0.3759 to 47.12	Yes	*
MDA x T vs. Control	-7.713	-31.08 to 15.66	No	ns
MDA x TCQ vs. Control	-31.46	-54.83 to -8.089	Yes	****
12				
WT x T vs. WT x TCQ	54.84	31.47 to 78.21	Yes	****
WT x T vs. TMX x T	-19.70	-43.07 to 3.674	No	ns
WT x T vs. TMX x TCQ	39.88	16.50 to 63.25	Yes	****
WT x T vs. MDA x T	-5.709	-29.08 to 17.66	No	ns
WT x T vs. MDA x TCQ	32.83	9.460 to 56.20	Yes	****
WT x T vs. Control	-17.12	-40.49 to 6.250	No	ns
WT x TCQ vs. TMX x T	-74.54	-97.91 to -51.17	Yes	****
WT x TCQ vs. TMX x TCQ	-14.96	-38.33 to 8.408	No	ns
WT x TCQ vs. MDA x T	-60.55	-83.92 to -37.18	Yes	****
WT x TCQ vs. MDA x TCQ	-22.01	-45.38 to 1.364	No	ns
WT x TCQ vs. Control	-71.96	-95.33 to -48.59	Yes	****
TMX x T vs. TMX x TCQ	59.57	36.20 to 82.94	Yes	****
TMX x T vs. MDA x T	13.99	-9.384 to 37.36	No	ns
TMX x T vs. MDA x TCQ	52.53	29.16 to 75.90	Yes	****
TMX x T vs. Control	2.575	-20.80 to 25.95	No	ns
TMX x TCQ vs. MDA x T	-45.59	-68.96 to -22.21	Yes	****
TMX x TCQ vs. MDA x TCQ	-7.045	-30.42 to 16.33	No	ns
TMX x TCQ vs. Control	-57.00	-80.37 to -33.63	Yes	****
MDA x T vs. MDA x TCQ	38.54	15.17 to 61.91	Yes	****
MDA x T vs. Control	-11.41	-34.78 to 11.96	No	ns
MDA x TCQ vs. Control	-49.95	-73.32 to -26.58	Yes	****
14				
WT x T vs. WT x TCQ	37.19	13.82 to 60.56	Yes	****
WT x T vs. TMX x T	-27.12	-50.49 to -3.744	Yes	**
WT x T vs. TMX x TCQ	33.62	10.25 to 56.99	Yes	****
WT x T vs. MDA x T	-12.73	-36.10 to 10.64	No	ns
WT x T vs. MDA x TCQ	38.43	15.06 to 61.80	Yes	****
WT x T vs. Control	-32.30	-55.67 to -8.925	Yes	****
WT x TCQ vs. TMX x T	-64.31	-87.68 to -40.93	Yes	****
WT x TCQ vs. TMX x TCQ	-3.570	-26.94 to 19.80	No	ns

WT x TCQ vs. MDA x T	-49.92	-73.29 to -26.55	Yes	****
WT x TCQ vs. MDA x TCQ	1.242	-22.13 to 24.61	No	ns
WT x TCQ vs. Control	-69.49	-92.86 to -46.11	Yes	****
TMX x T vs. TMX x TCQ	60.74	37.36 to 84.11	Yes	****
TMX x T vs. MDA x T	14.39	-8.985 to 37.76	No	ns
TMX x T vs. MDA x TCQ	65.55	42.18 to 88.92	Yes	****
TMX x T vs. Control	-5.180	-28.55 to 18.19	No	ns
TMX x TCQ vs. MDA x T	-46.35	-69.72 to -22.98	Yes	****
TMX x TCQ vs. MDA x TCQ	4.812	-18.56 to 28.18	No	ns
TMX x TCQ vs. Control	-65.92	-89.29 to -42.54	Yes	****
MDA x T vs. MDA x TCQ	51.16	27.79 to 74.53	Yes	****
MDA x T vs. Control	-19.57	-42.94 to 3.805	No	ns
MDA x TCQ vs. Control	-70.73	-94.10 to -47.36	Yes	****
16				
WT x T vs. WT x TCQ	25.97	2.604 to 49.35	Yes	**
WT x T vs. TMX x T	-32.24	-55.61 to -8.865	Yes	****
WT x T vs. TMX x TCQ	9.710	-13.66 to 33.08	No	ns
WT x T vs. MDA x T	-14.58	-37.96 to 8.786	No	ns
WT x T vs. MDA x TCQ	22.28	-1.092 to 45.65	No	ns
WT x T vs. Control	-56.19	-79.56 to -32.82	Yes	****
WT x TCQ vs. TMX x T	-58.21	-81.58 to -34.84	Yes	****
WT x TCQ vs. TMX x TCQ	-16.26	-39.64 to 7.106	No	ns
WT x TCQ vs. MDA x T	-40.56	-63.93 to -17.19	Yes	****
WT x TCQ vs. MDA x TCQ	-3.696	-27.07 to 19.68	No	ns
WT x TCQ vs. Control	-82.16	-105.5 to -58.79	Yes	****
TMX x T vs. TMX x TCQ	41.95	18.57 to 65.32	Yes	****
TMX x T vs. MDA x T	17.65	-5.720 to 41.02	No	ns
TMX x T vs. MDA x TCQ	54.52	31.14 to 77.89	Yes	****
TMX x T vs. Control	-23.95	-47.32 to -0.5815	Yes	*
TMX x TCQ vs. MDA x T	-24.29	-47.67 to -0.9237	Yes	*
TMX x TCQ vs. MDA x TCQ	12.57	-10.80 to 35.94	No	ns
TMX x TCQ vs. Control	-65.90	-89.27 to -42.53	Yes	****
MDA x T vs. MDA x TCQ	36.86	13.49 to 60.24	Yes	****
MDA x T vs. Control	-41.60	-64.98 to -18.23	Yes	****
MDA x TCQ vs. Control	-78.47	-101.8 to -55.10	Yes	****
18				
WT x T vs. WT x TCQ	32.34	8.969 to 55.71	Yes	****
WT x T vs. TMX x T	-13.65	-37.02 to 9.726	No	ns
WT x T vs. TMX x TCQ	28.10	4.726 to 51.47	Yes	**
WT x T vs. MDA x T	3.550	-19.82 to 26.92	No	ns
WT x T vs. MDA x TCQ	23.22	-0.1558 to 46.59	No	ns
WT x T vs. Control	-64.84	-88.21 to -41.47	Yes	****
WT x TCQ vs. TMX x T	-45.99	-69.36 to -22.61	Yes	****
WT x TCQ vs. TMX x TCQ	-4.243	-27.61 to 19.13	No	ns
WT x TCQ vs. MDA x T	-28.79	-52.16 to -5.419	Yes	***
WT x TCQ vs. MDA x TCQ	-9.124	-32.50 to 14.25	No	ns
WT x TCQ vs. Control	-97.18	-120.6 to -73.81	Yes	****
TMX x T vs. TMX x TCQ	41.74	18.37 to 65.11	Yes	****
TMX x T vs. MDA x T	17.20	-6.176 to 40.57	No	ns
TMX x T vs. MDA x TCQ	36.86	13.49 to 60.23	Yes	****
TMX x T vs. Control	-51.20	-74.57 to -27.82	Yes	****
TMX x TCQ vs. MDA x T	-24.55	-47.92 to -1.176	Yes	*
TMX x TCQ vs. MDA x TCQ	-4.882	-28.25 to 18.49	No	ns
TMX x TCQ vs. Control	-92.94	-116.3 to -69.57	Yes	****

MDA x T vs. MDA x TCQ	19.67	-3.705 to 43.04	No	ns
MDA x T vs. Control	-68.39	-91.76 to -45.02	Yes	****
MDA x TCQ vs. Control	-88.06	-111.4 to -64.69	Yes	****
20				
WT x T vs. WT x TCQ	13.64	-9.727 to 37.02	No	ns
WT x T vs. TMX x T	0.6737	-22.70 to 24.04	No	ns
WT x T vs. TMX x TCQ	12.16	-11.21 to 35.54	No	ns
WT x T vs. MDA x T	13.20	-10.17 to 36.57	No	ns
WT x T vs. MDA x TCQ	12.74	-10.63 to 36.11	No	ns
WT x T vs. Control	-85.21	-108.6 to -61.84	Yes	****
WT x TCQ vs. TMX x T	-12.97	-36.34 to 10.40	No	ns
WT x TCQ vs. TMX x TCQ	-1.480	-24.85 to 21.89	No	ns
WT x TCQ vs. MDA x T	-0.4460	-23.82 to 22.93	No	ns
WT x TCQ vs. MDA x TCQ	-0.9078	-24.28 to 22.46	No	ns
WT x TCQ vs. Control	-98.85	-122.2 to -75.48	Yes	****
TMX x T vs. TMX x TCQ	11.49	-11.88 to 34.86	No	ns
TMX x T vs. MDA x T	12.52	-10.85 to 35.90	No	ns
TMX x T vs. MDA x TCQ	12.06	-11.31 to 35.43	No	ns
TMX x T vs. Control	-85.88	-109.3 to -62.51	Yes	****
TMX x TCQ vs. MDA x T	1.034	-22.34 to 24.40	No	ns
TMX x TCQ vs. MDA x TCQ	0.5719	-22.80 to 23.94	No	ns
TMX x TCQ vs. Control	-97.37	-120.7 to -74.00	Yes	****
MDA x T vs. MDA x TCQ	-0.4618	-23.83 to 22.91	No	ns
MDA x T vs. Control	-98.41	-121.8 to -75.03	Yes	****
MDA x TCQ vs. Control	-97.94	-121.3 to -74.57	Yes	****
22				
WT x T vs. WT x TCQ	0.4546	-22.92 to 23.83	No	ns
WT x T vs. TMX x T	1.446	-21.92 to 24.82	No	ns
WT x T vs. TMX x TCQ	1.291	-22.08 to 24.66	No	ns
WT x T vs. MDA x T	0.6856	-22.69 to 24.06	No	ns
WT x T vs. MDA x TCQ	0.7901	-22.58 to 24.16	No	ns
WT x T vs. Control	-98.28	-121.7 to -74.91	Yes	****
WT x TCQ vs. TMX x T	0.9917	-22.38 to 24.36	No	ns
WT x TCQ vs. TMX x TCQ	0.8360	-22.54 to 24.21	No	ns
WT x TCQ vs. MDA x T	0.2310	-23.14 to 23.60	No	ns
WT x TCQ vs. MDA x TCQ	0.3354	-23.04 to 23.71	No	ns
WT x TCQ vs. Control	-98.74	-122.1 to -75.36	Yes	****
TMX x T vs. TMX x TCQ	-0.1558	-23.53 to 23.22	No	ns
TMX x T vs. MDA x T	-0.7608	-24.13 to 22.61	No	ns
TMX x T vs. MDA x TCQ	-0.6563	-24.03 to 22.71	No	ns
TMX x T vs. Control	-99.73	-123.1 to -76.36	Yes	****
TMX x TCQ vs. MDA x T	-0.6050	-23.98 to 22.77	No	ns
TMX x TCQ vs. MDA x TCQ	-0.5005	-23.87 to 22.87	No	ns
TMX x TCQ vs. Control	-99.57	-122.9 to -76.20	Yes	****
MDA x T vs. MDA x TCQ	0.1045	-23.27 to 23.48	No	ns
MDA x T vs. Control	-98.97	-122.3 to -75.60	Yes	****
MDA x TCQ vs. Control	-99.07	-122.4 to -75.70	Yes	****
24				
WT x T vs. WT x TCQ	-0.5754	-23.95 to 22.80	No	ns
WT x T vs. TMX x T	0.01167	-23.36 to 23.38	No	ns
WT x T vs. TMX x TCQ	-0.02642	-23.40 to 23.34	No	ns
WT x T vs. MDA x T	-0.7752	-24.15 to 22.60	No	ns
WT x T vs. MDA x TCQ	0.9088	-22.46 to 24.28	No	ns
WT x T vs. Control	-99.09	-122.5 to -75.72	Yes	****

WT x TCQ vs. TMX x T	0.5871	-22.78 to 23.96	No	ns
WT x TCQ vs. TMX x TCQ	0.5490	-22.82 to 23.92	No	ns
WT x TCQ vs. MDA x T	-0.1998	-23.57 to 23.17	No	ns
WT x TCQ vs. MDA x TCQ	1.484	-21.89 to 24.86	No	ns
WT x TCQ vs. Control	-98.52	-121.9 to -75.14	Yes	****
TMX x T vs. TMX x TCQ	-0.03809	-23.41 to 23.33	No	ns
TMX x T vs. MDA x T	-0.7868	-24.16 to 22.58	No	ns
TMX x T vs. MDA x TCQ	0.8971	-22.47 to 24.27	No	ns
TMX x T vs. Control	-99.10	-122.5 to -75.73	Yes	****
TMX x TCQ vs. MDA x T	-0.7487	-24.12 to 22.62	No	ns
TMX x TCQ vs. MDA x TCQ	0.9352	-22.44 to 24.31	No	ns
TMX x TCQ vs. Control	-99.06	-122.4 to -75.69	Yes	****
MDA x T vs. MDA x TCQ	1.684	-21.69 to 25.06	No	ns
MDA x T vs. Control	-98.32	-121.7 to -74.94	Yes	****
MDA x TCQ vs. Control	-100.0	-123.4 to -76.63	Yes	****
26				
WT x T vs. WT x TCQ	-0.7952	-24.17 to 22.58	No	ns
WT x T vs. TMX x T	-0.3746	-23.75 to 23.00	No	ns
WT x T vs. TMX x TCQ	-0.1157	-23.49 to 23.26	No	ns
WT x T vs. MDA x T	-0.8817	-24.25 to 22.49	No	ns
WT x T vs. MDA x TCQ	0.09859	-23.27 to 23.47	No	ns
WT x T vs. Control	-99.90	-123.3 to -76.53	Yes	****
WT x TCQ vs. TMX x T	0.4206	-22.95 to 23.79	No	ns
WT x TCQ vs. TMX x TCQ	0.6795	-22.69 to 24.05	No	ns
WT x TCQ vs. MDA x T	-0.08650	-23.46 to 23.28	No	ns
WT x TCQ vs. MDA x TCQ	0.8938	-22.48 to 24.26	No	ns
WT x TCQ vs. Control	-99.11	-122.5 to -75.74	Yes	****
TMX x T vs. TMX x TCQ	0.2589	-23.11 to 23.63	No	ns
TMX x T vs. MDA x T	-0.5071	-23.88 to 22.86	No	ns
TMX x T vs. MDA x TCQ	0.4732	-22.90 to 23.84	No	ns
TMX x T vs. Control	-99.53	-122.9 to -76.16	Yes	****
TMX x TCQ vs. MDA x T	-0.7660	-24.14 to 22.61	No	ns
TMX x TCQ vs. MDA x TCQ	0.2143	-23.16 to 23.59	No	ns
TMX x TCQ vs. Control	-99.79	-123.2 to -76.41	Yes	****
MDA x T vs. MDA x TCQ	0.9803	-22.39 to 24.35	No	ns
MDA x T vs. Control	-99.02	-122.4 to -75.65	Yes	****
MDA x TCQ vs. Control	-100.0	-123.4 to -76.63	Yes	****
28				
WT x T vs. WT x TCQ	-1.069	-24.44 to 22.30	No	ns
WT x T vs. TMX x T	-0.1663	-23.54 to 23.20	No	ns
WT x T vs. TMX x TCQ	0.3171	-23.05 to 23.69	No	ns
WT x T vs. MDA x T	-1.109	-24.48 to 22.26	No	ns
WT x T vs. MDA x TCQ	0.3171	-23.05 to 23.69	No	ns
WT x T vs. Control	-99.68	-123.1 to -76.31	Yes	****
WT x TCQ vs. TMX x T	0.9026	-22.47 to 24.27	No	ns
WT x TCQ vs. TMX x TCQ	1.386	-21.99 to 24.76	No	ns
WT x TCQ vs. MDA x T	-0.03975	-23.41 to 23.33	No	ns
WT x TCQ vs. MDA x TCQ	1.386	-21.99 to 24.76	No	ns
WT x TCQ vs. Control	-98.61	-122.0 to -75.24	Yes	****
TMX x T vs. TMX x TCQ	0.4834	-22.89 to 23.85	No	ns
TMX x T vs. MDA x T	-0.9424	-24.31 to 22.43	No	ns
TMX x T vs. MDA x TCQ	0.4834	-22.89 to 23.85	No	ns
TMX x T vs. Control	-99.52	-122.9 to -76.15	Yes	****
TMX x TCQ vs. MDA x T	-1.426	-24.80 to 21.95	No	ns

TMX x TCQ vs. MDA x TCQ	0.0	-23.37 to 23.37	No	ns
TMX x TCQ vs. Control	-100.0	-123.4 to -76.63	Yes	****
MDA x T vs. MDA x TCQ	1.426	-21.95 to 24.80	No	ns
MDA x T vs. Control	-98.57	-121.9 to -75.20	Yes	****
MDA x TCQ vs. Control	-100.0	-123.4 to -76.63	Yes	****
30				
WT x T vs. WT x TCQ	-1.987e-008	-23.37 to 23.37	No	ns
WT x T vs. TMX x T	-1.987e-008	-23.37 to 23.37	No	ns
WT x T vs. TMX x TCQ	-1.987e-008	-23.37 to 23.37	No	ns
WT x T vs. MDA x T	-1.987e-008	-23.37 to 23.37	No	ns
WT x T vs. MDA x TCQ	-1.987e-008	-23.37 to 23.37	No	ns
WT x T vs. Control	-100.0	-123.4 to -76.63	Yes	****
WT x TCQ vs. TMX x T	0.0	-23.37 to 23.37	No	ns
WT x TCQ vs. TMX x TCQ	0.0	-23.37 to 23.37	No	ns
WT x TCQ vs. MDA x T	0.0	-23.37 to 23.37	No	ns
WT x TCQ vs. MDA x TCQ	0.0	-23.37 to 23.37	No	ns
WT x TCQ vs. Control	-100.0	-123.4 to -76.63	Yes	****
TMX x T vs. TMX x TCQ	0.0	-23.37 to 23.37	No	ns
TMX x T vs. MDA x T	0.0	-23.37 to 23.37	No	ns
TMX x T vs. MDA x TCQ	0.0	-23.37 to 23.37	No	ns
TMX x T vs. Control	-100.0	-123.4 to -76.63	Yes	****
TMX x TCQ vs. MDA x T	0.0	-23.37 to 23.37	No	ns
TMX x TCQ vs. MDA x TCQ	0.0	-23.37 to 23.37	No	ns
TMX x TCQ vs. Control	-100.0	-123.4 to -76.63	Yes	****
MDA x T vs. MDA x TCQ	0.0	-23.37 to 23.37	No	ns
MDA x T vs. Control	-100.0	-123.4 to -76.63	Yes	****
MDA x TCQ vs. Control	-100.0	-123.4 to -76.63	Yes	****

7.3 Appendix 3: 2way ANOVA with Dunnett's multiple comparisons test for all MTT Assays against Control

Within each row, compare columns (simple effects within rows)				
Number of families	15			
Number of comparisons per family	6			
Alpha	0.05			
Dunnett's multiple comparisons test	Mean Diff.	95% CI of diff.	Significant?	Summary
0				
Control vs. WT x T	0.0	-37.88 to 37.88	No	ns
Control vs. WTxTCQ	0.0	-37.88 to 37.88	No	ns
Control vs. TMX x T	0.0	-37.88 to 37.88	No	ns
Control vs. TMX x TCQ	0.0	-37.88 to 37.88	No	ns
Control vs. MDA x T	0.0	-37.88 to 37.88	No	ns
Control vs. MDA x TCQ	0.0	-37.88 to 37.88	No	ns
2				
Control vs. WT x T	-4.709	-42.59 to 33.17	No	ns
Control vs. WTxTCQ	-26.78	-64.66 to 11.10	No	ns
Control vs. TMX x T	-26.44	-64.32 to 11.44	No	ns
Control vs. TMX x TCQ	0.8320	-37.05 to 38.71	No	ns
Control vs. MDA x T	-0.5747	-38.45 to 37.31	No	ns
Control vs. MDA x TCQ	-83.21	-121.1 to -45.33	Yes	****
4				
Control vs. WT x T	0.5978	-37.28 to 38.48	No	ns
Control vs. WTxTCQ	-22.26	-60.14 to 15.62	No	ns

Control vs. TMX x T	-24.79	-62.67 to 13.09	No	ns
Control vs. TMX x TCQ	-3.540	-41.42 to 34.34	No	ns
Control vs. MDA x T	13.77	-24.11 to 51.65	No	ns
Control vs. MDA x TCQ	-86.87	-124.7 to -48.99	Yes	****
6				
Control vs. WT x T	-4.854	-42.73 to 33.03	No	ns
Control vs. WTxTCQ	-30.12	-68.00 to 7.762	No	ns
Control vs. TMX x T	-40.11	-77.99 to -2.232	Yes	*
Control vs. TMX x TCQ	-27.69	-65.58 to 10.19	No	ns
Control vs. MDA x T	23.11	-14.77 to 60.99	No	ns
Control vs. MDA x TCQ	-83.28	-121.2 to -45.40	Yes	****
8				
Control vs. WT x T	-4.653	-42.53 to 33.23	No	ns
Control vs. WTxTCQ	-25.06	-67.41 to 17.29	No	ns
Control vs. TMX x T	-62.31	-100.2 to -24.43	Yes	***
Control vs. TMX x TCQ	-77.70	-115.6 to -39.82	Yes	****
Control vs. MDA x T	30.57	-7.306 to 68.45	No	ns
Control vs. MDA x TCQ	-86.00	-123.9 to -48.12	Yes	****
10				
Control vs. WT x T	-4.614	-42.49 to 33.27	No	ns
Control vs. WTxTCQ	-12.00	-49.88 to 25.88	No	ns
Control vs. TMX x T	-41.59	-79.47 to -3.708	Yes	*
Control vs. TMX x TCQ	-61.74	-99.62 to -23.86	Yes	***
Control vs. MDA x T	35.11	-2.772 to 72.99	No	ns
Control vs. MDA x TCQ	-70.56	-108.4 to -32.68	Yes	****
12				
Control vs. WT x T	-16.51	-54.39 to 21.37	No	ns
Control vs. WTxTCQ	6.216	-31.66 to 44.10	No	ns
Control vs. TMX x T	-33.00	-70.88 to 4.883	No	ns
Control vs. TMX x TCQ	-0.8876	-38.77 to 36.99	No	ns
Control vs. MDA x T	38.04	0.1580 to 75.92	Yes	*
Control vs. MDA x TCQ	-37.44	-75.32 to 0.4409	No	ns
14				
Control vs. WT x T	-3.096	-40.98 to 34.78	No	ns
Control vs. WTxTCQ	40.32	-2.030 to 82.67	No	ns
Control vs. TMX x T	-18.24	-56.12 to 19.64	No	ns
Control vs. TMX x TCQ	-1.370	-39.25 to 36.51	No	ns
Control vs. MDA x T	49.02	11.14 to 86.90	Yes	**
Control vs. MDA x TCQ	-2.012	-39.89 to 35.87	No	ns
16				
Control vs. WT x T	17.89	-19.99 to 55.77	No	ns
Control vs. WTxTCQ	78.29	40.41 to 116.2	Yes	****
Control vs. TMX x T	-18.75	-56.63 to 19.13	No	ns
Control vs. TMX x TCQ	25.41	-12.47 to 63.29	No	ns
Control vs. MDA x T	68.74	30.86 to 106.6	Yes	****
Control vs. MDA x TCQ	55.17	17.29 to 93.05	Yes	**
18				
Control vs. WT x T	34.42	-7.927 to 76.78	No	ns
Control vs. WTxTCQ	78.95	36.59 to 121.3	Yes	****
Control vs. TMX x T	5.003	-32.88 to 42.88	No	ns
Control vs. TMX x TCQ	56.68	18.80 to 94.56	Yes	***
Control vs. MDA x T	80.32	42.44 to 118.2	Yes	****
Control vs. MDA x TCQ	48.85	10.97 to 86.73	Yes	**

20				
Control vs. WT x T	61.26	23.38 to 99.14	Yes	***
Control vs. WTxTCQ	105.0	62.62 to 147.3	Yes	****
Control vs. TMX x T	20.13	-17.75 to 58.01	No	ns
Control vs. TMX x TCQ	87.80	49.92 to 125.7	Yes	****
Control vs. MDA x T	90.46	52.58 to 128.3	Yes	****
Control vs. MDA x TCQ	70.74	32.86 to 108.6	Yes	****
22				
Control vs. WT x T	56.86	18.98 to 94.74	Yes	***
Control vs. WTxTCQ	98.48	60.60 to 136.4	Yes	****
Control vs. TMX x T	92.97	55.09 to 130.9	Yes	****
Control vs. TMX x TCQ	100.0	62.12 to 137.9	Yes	****
Control vs. MDA x T	94.91	57.03 to 132.8	Yes	****
Control vs. MDA x TCQ	74.02	36.14 to 111.9	Yes	****
24				
Control vs. WT x T	64.84	26.96 to 102.7	Yes	****
Control vs. WTxTCQ	94.37	40.80 to 147.9	Yes	****
Control vs. TMX x T	95.91	58.03 to 133.8	Yes	****
Control vs. TMX x TCQ	100.0	62.12 to 137.9	Yes	****
Control vs. MDA x T	95.36	57.48 to 133.2	Yes	****
Control vs. MDA x TCQ	87.69	49.81 to 125.6	Yes	****
26				
Control vs. WT x T	76.36	38.48 to 114.2	Yes	****
Control vs. WTxTCQ	78.57	36.22 to 120.9	Yes	****
Control vs. TMX x T	95.91	58.03 to 133.8	Yes	****
Control vs. TMX x TCQ	100.0	62.12 to 137.9	Yes	****
Control vs. MDA x T	95.59	57.71 to 133.5	Yes	****
Control vs. MDA x TCQ	89.51	51.63 to 127.4	Yes	****
28				
Control vs. WT x T	64.93	27.05 to 102.8	Yes	****
Control vs. WTxTCQ	94.37	40.80 to 147.9	Yes	****
Control vs. TMX x T	100.0	62.12 to 137.9	Yes	****
Control vs. TMX x TCQ	100.0	62.12 to 137.9	Yes	****
Control vs. MDA x T	100.6	62.71 to 138.5	Yes	****
Control vs. MDA x TCQ	100.0	62.12 to 137.9	Yes	****

7.4 Appendix 3: 2way ANOVA with Tukey's multiple comparisons test for all MTT Assays; cross comparison

Within each row, compare columns (simple effects within rows)				
Number of families	15			
Number of comparisons per family	15			
Alpha	0.05			
Tukey's multiple comparisons test	Mean Diff.	95% CI of diff.	Significant?	Summary
0				
WT x T vs. WTxTCQ	0.0	-45.74 to 45.74	No	ns
WT x T vs. TMX x T	0.0	-45.74 to 45.74	No	ns
WT x T vs. TMX x TCQ	0.0	-45.74 to 45.74	No	ns
WT x T vs. MDA x T	0.0	-45.74 to 45.74	No	ns
WT x T vs. MDA x TCQ	0.0	-45.74 to 45.74	No	ns
WTxTCQ vs. TMX x T	0.0	-45.74 to 45.74	No	ns
WTxTCQ vs. TMX x TCQ	0.0	-45.74 to 45.74	No	ns
WTxTCQ vs. MDA x T	0.0	-45.74 to 45.74	No	ns
WTxTCQ vs. MDA x TCQ	0.0	-45.74 to 45.74	No	ns
TMX x T vs. TMX x TCQ	0.0	-45.74 to 45.74	No	ns
TMX x T vs. MDA x T	0.0	-45.74 to 45.74	No	ns
TMX x T vs. MDA x TCQ	0.0	-45.74 to 45.74	No	ns
TMX x TCQ vs. MDA x T	0.0	-45.74 to 45.74	No	ns
TMX x TCQ vs. MDA x TCQ	0.0	-45.74 to 45.74	No	ns
MDA x T vs. MDA x TCQ	0.0	-45.74 to 45.74	No	ns
2				
WT x T vs. WTxTCQ	-22.07	-67.81 to 23.68	No	ns
WT x T vs. TMX x T	-21.73	-67.47 to 24.02	No	ns
WT x T vs. TMX x TCQ	5.541	-40.20 to 51.28	No	ns
WT x T vs. MDA x T	4.134	-41.61 to 49.88	No	ns
WT x T vs. MDA x TCQ	-78.51	-124.2 to -32.76	Yes	****
WTxTCQ vs. TMX x T	0.3406	-45.40 to 46.08	No	ns
WTxTCQ vs. TMX x TCQ	27.61	-18.13 to 73.35	No	ns
WTxTCQ vs. MDA x T	26.20	-19.54 to 71.94	No	ns
WTxTCQ vs. MDA x TCQ	-56.44	-102.2 to -10.70	Yes	**
TMX x T vs. TMX x TCQ	27.27	-18.48 to 73.01	No	ns
TMX x T vs. MDA x T	25.86	-19.88 to 71.60	No	ns
TMX x T vs. MDA x TCQ	-56.78	-102.5 to -11.04	Yes	**
TMX x TCQ vs. MDA x T	-1.407	-47.15 to 44.34	No	ns

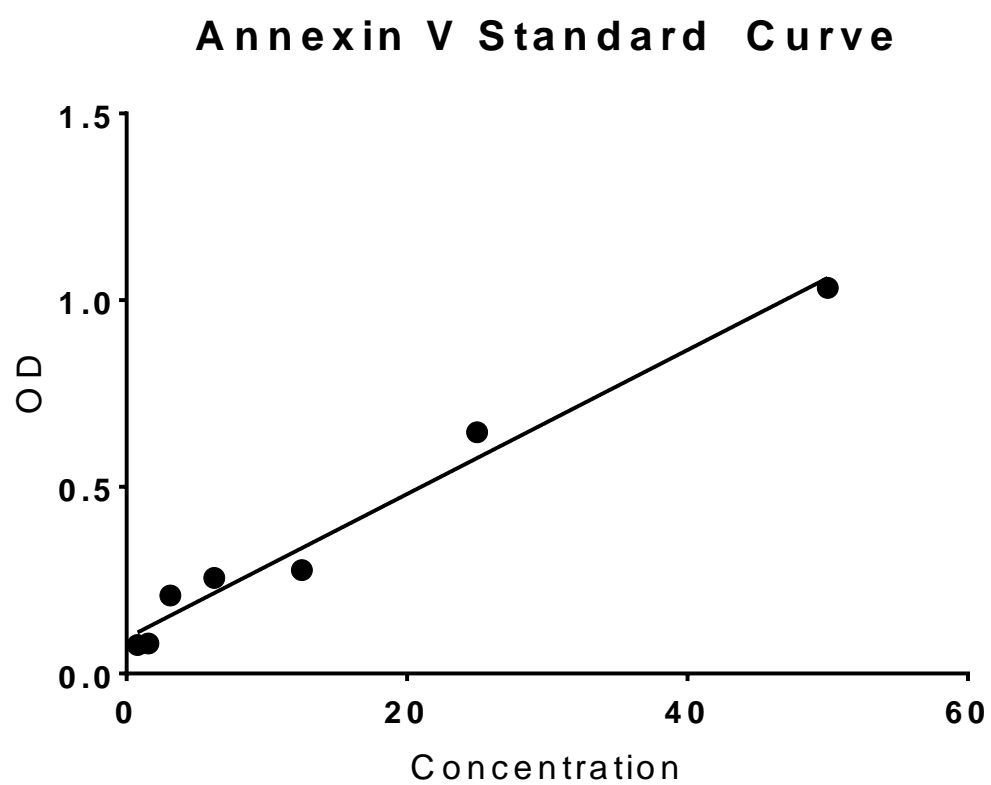
TMX x TCQ vs. MDA x TCQ	-84.05	-129.8 to -38.30	Yes	****
MDA x T vs. MDA x TCQ	-82.64	-128.4 to -36.90	Yes	****
4				
WT x T vs. WTxTCQ	-22.85	-68.60 to 22.89	No	ns
WT x T vs. TMX x T	-25.38	-71.13 to 20.36	No	ns
WT x T vs. TMX x TCQ	-4.138	-49.88 to 41.60	No	ns
WT x T vs. MDA x T	13.18	-32.57 to 58.92	No	ns
WT x T vs. MDA x TCQ	-87.47	-133.2 to -41.72	Yes	****
WTxTCQ vs. TMX x T	-2.530	-48.27 to 43.21	No	ns
WTxTCQ vs. TMX x TCQ	18.72	-27.03 to 64.46	No	ns
WTxTCQ vs. MDA x T	36.03	-9.713 to 81.77	No	ns
WTxTCQ vs. MDA x TCQ	-64.61	-110.4 to -18.87	Yes	***
TMX x T vs. TMX x TCQ	21.25	-24.50 to 66.99	No	ns
TMX x T vs. MDA x T	38.56	-7.183 to 84.30	No	ns
TMX x T vs. MDA x TCQ	-62.08	-107.8 to -16.34	Yes	**
TMX x TCQ vs. MDA x T	17.31	-28.43 to 63.06	No	ns
TMX x TCQ vs. MDA x TCQ	-83.33	-129.1 to -37.59	Yes	****
MDA x T vs. MDA x TCQ	-100.6	-146.4 to -54.90	Yes	****
6				
WT x T vs. WTxTCQ	-25.26	-71.01 to 20.48	No	ns
WT x T vs. TMX x T	-35.26	-81.00 to 10.48	No	ns
WT x T vs. TMX x TCQ	-22.84	-68.58 to 22.90	No	ns
WT x T vs. MDA x T	27.96	-17.78 to 73.71	No	ns
WT x T vs. MDA x TCQ	-78.43	-124.2 to -32.69	Yes	****
WTxTCQ vs. TMX x T	-9.994	-55.74 to 35.75	No	ns
WTxTCQ vs. TMX x TCQ	2.423	-43.32 to 48.17	No	ns
WTxTCQ vs. MDA x T	53.23	7.485 to 98.97	Yes	*
WTxTCQ vs. MDA x TCQ	-53.16	-98.91 to -7.421	Yes	*
TMX x T vs. TMX x TCQ	12.42	-33.33 to 58.16	No	ns
TMX x T vs. MDA x T	63.22	17.48 to 109.0	Yes	**
TMX x T vs. MDA x TCQ	-43.17	-88.91 to 2.572	No	ns
TMX x TCQ vs. MDA x T	50.80	5.062 to 96.55	Yes	*
TMX x TCQ vs. MDA x TCQ	-55.59	-101.3 to -9.844	Yes	**
MDA x T vs. MDA x TCQ	-106.4	-152.1 to -60.65	Yes	****
8				
WT x T vs. WTxTCQ	-20.41	-71.55 to 30.73	No	ns
WT x T vs. TMX x T	-57.66	-103.4 to -11.91	Yes	**
WT x T vs. TMX x TCQ	-73.04	-118.8 to -27.30	Yes	***
WT x T vs. MDA x T	35.23	-10.52 to 80.97	No	ns
WT x T vs. MDA x TCQ	-81.35	-127.1 to -35.61	Yes	****
WTxTCQ vs. TMX x T	-37.25	-88.39 to 13.90	No	ns
WTxTCQ vs. TMX x TCQ	-52.63	-103.8 to -1.492	Yes	*
WTxTCQ vs. MDA x T	55.64	4.494 to 106.8	Yes	*
WTxTCQ vs. MDA x TCQ	-60.94	-112.1 to -9.801	Yes	**
TMX x T vs. TMX x TCQ	-15.39	-61.13 to 30.36	No	ns
TMX x T vs. MDA x T	92.88	47.14 to 138.6	Yes	****
TMX x T vs. MDA x TCQ	-23.70	-69.44 to 22.05	No	ns
TMX x TCQ vs. MDA x T	108.3	62.53 to 154.0	Yes	****
TMX x TCQ vs. MDA x TCQ	-8.309	-54.05 to 37.43	No	ns
MDA x T vs. MDA x TCQ	-116.6	-162.3 to -70.84	Yes	****
10				
WT x T vs. WTxTCQ	-7.386	-53.13 to 38.36	No	ns
WT x T vs. TMX x T	-36.97	-82.72 to 8.769	No	ns
WT x T vs. TMX x TCQ	-57.12	-102.9 to -11.38	Yes	**

WT x T vs. MDA x T	39.72	-6.020 to 85.47	No	ns
WT x T vs. MDA x TCQ	-65.94	-111.7 to -20.20	Yes	***
WTxTCQ vs. TMX x T	-29.59	-75.33 to 16.16	No	ns
WTxTCQ vs. TMX x TCQ	-49.74	-95.48 to -3.994	Yes	*
WTxTCQ vs. MDA x T	47.11	1.366 to 92.85	Yes	*
WTxTCQ vs. MDA x TCQ	-58.56	-104.3 to -12.81	Yes	**
TMX x T vs. TMX x TCQ	-20.15	-65.89 to 25.59	No	ns
TMX x T vs. MDA x T	76.70	30.95 to 122.4	Yes	****
TMX x T vs. MDA x TCQ	-28.97	-74.71 to 16.77	No	ns
TMX x TCQ vs. MDA x T	96.85	51.10 to 142.6	Yes	****
TMX x TCQ vs. MDA x TCQ	-8.820	-54.56 to 36.92	No	ns
MDA x T vs. MDA x TCQ	-105.7	-151.4 to -59.92	Yes	****
12				
WT x T vs. WTxTCQ	22.73	-23.02 to 68.47	No	ns
WT x T vs. TMX x T	-16.49	-62.23 to 29.25	No	ns
WT x T vs. TMX x TCQ	15.62	-30.12 to 61.36	No	ns
WT x T vs. MDA x T	54.55	8.805 to 100.3	Yes	**
WT x T vs. MDA x TCQ	-20.93	-66.67 to 24.81	No	ns
WTxTCQ vs. TMX x T	-39.21	-84.96 to 6.530	No	ns
WTxTCQ vs. TMX x TCQ	-7.103	-52.85 to 38.64	No	ns
WTxTCQ vs. MDA x T	31.82	-13.92 to 77.57	No	ns
WTxTCQ vs. MDA x TCQ	-43.65	-89.40 to 2.088	No	ns
TMX x T vs. TMX x TCQ	32.11	-13.63 to 77.85	No	ns
TMX x T vs. MDA x T	71.04	25.29 to 116.8	Yes	***
TMX x T vs. MDA x TCQ	-4.442	-50.18 to 41.30	No	ns
TMX x TCQ vs. MDA x T	38.93	-6.817 to 84.67	No	ns
TMX x TCQ vs. MDA x TCQ	-36.55	-82.29 to 9.191	No	ns
MDA x T vs. MDA x TCQ	-75.48	-121.2 to -29.73	Yes	****
14				
WT x T vs. WTxTCQ	43.42	-7.725 to 94.56	No	ns
WT x T vs. TMX x T	-15.15	-60.89 to 30.60	No	ns
WT x T vs. TMX x TCQ	1.727	-44.02 to 47.47	No	ns
WT x T vs. MDA x T	52.11	6.369 to 97.85	Yes	*
WT x T vs. MDA x TCQ	1.085	-44.66 to 46.83	No	ns
WTxTCQ vs. TMX x T	-58.56	-109.7 to -7.422	Yes	*
WTxTCQ vs. TMX x TCQ	-41.69	-92.83 to 9.451	No	ns
WTxTCQ vs. MDA x T	8.694	-42.45 to 59.84	No	ns
WTxTCQ vs. MDA x TCQ	-42.33	-93.47 to 8.809	No	ns
TMX x T vs. TMX x TCQ	16.87	-28.87 to 62.62	No	ns
TMX x T vs. MDA x T	67.26	21.52 to 113.0	Yes	***
TMX x T vs. MDA x TCQ	16.23	-29.51 to 61.97	No	ns
TMX x TCQ vs. MDA x T	50.38	4.642 to 96.13	Yes	*
TMX x TCQ vs. MDA x TCQ	-0.6420	-46.38 to 45.10	No	ns
MDA x T vs. MDA x TCQ	-51.03	-96.77 to -5.284	Yes	*
16				
WT x T vs. WTxTCQ	60.41	14.66 to 106.1	Yes	**
WT x T vs. TMX x T	-36.64	-82.38 to 9.106	No	ns
WT x T vs. TMX x TCQ	7.522	-38.22 to 53.27	No	ns
WT x T vs. MDA x T	50.85	5.104 to 96.59	Yes	*
WT x T vs. MDA x TCQ	37.28	-8.460 to 83.03	No	ns
WTxTCQ vs. TMX x T	-97.04	-142.8 to -51.30	Yes	****
WTxTCQ vs. TMX x TCQ	-52.88	-98.63 to -7.140	Yes	*
WTxTCQ vs. MDA x T	-9.559	-55.30 to 36.18	No	ns
WTxTCQ vs. MDA x TCQ	-23.12	-68.87 to 22.62	No	ns

TMX x T vs. TMX x TCQ	44.16	-1.584 to 89.90	No	ns
TMX x T vs. MDA x T	87.48	41.74 to 133.2	Yes	****
TMX x T vs. MDA x TCQ	73.92	28.18 to 119.7	Yes	****
TMX x TCQ vs. MDA x T	43.32	-2.419 to 89.07	No	ns
TMX x TCQ vs. MDA x TCQ	29.76	-15.98 to 75.50	No	ns
MDA x T vs. MDA x TCQ	-13.56	-59.31 to 32.18	No	ns
18				
WT x T vs. WT x TCQ	44.52	-11.50 to 100.5	No	ns
WT x T vs. TMX x T	-29.42	-80.56 to 21.72	No	ns
WT x T vs. TMX x TCQ	22.25	-28.89 to 73.39	No	ns
WT x T vs. MDA x T	45.90	-5.243 to 97.04	No	ns
WT x T vs. MDA x TCQ	14.43	-36.71 to 65.57	No	ns
WT x TCQ vs. TMX x T	-73.94	-125.1 to -22.80	Yes	***
WT x TCQ vs. TMX x TCQ	-22.27	-73.41 to 28.87	No	ns
WT x TCQ vs. MDA x T	1.378	-49.76 to 52.52	No	ns
WT x TCQ vs. MDA x TCQ	-30.09	-81.23 to 21.05	No	ns
TMX x T vs. TMX x TCQ	51.67	5.931 to 97.42	Yes	*
TMX x T vs. MDA x T	75.32	29.58 to 121.1	Yes	****
TMX x T vs. MDA x TCQ	43.85	-1.893 to 89.59	No	ns
TMX x TCQ vs. MDA x T	23.65	-22.10 to 69.39	No	ns
TMX x TCQ vs. MDA x TCQ	-7.823	-53.57 to 37.92	No	ns
MDA x T vs. MDA x TCQ	-31.47	-77.21 to 14.27	No	ns
20				
WT x T vs. WT x TCQ	43.72	-7.424 to 94.86	No	ns
WT x T vs. TMX x T	-41.12	-86.87 to 4.620	No	ns
WT x T vs. TMX x TCQ	26.55	-19.20 to 72.29	No	ns
WT x T vs. MDA x T	29.20	-16.54 to 74.94	No	ns
WT x T vs. MDA x TCQ	9.485	-36.26 to 55.23	No	ns
WT x TCQ vs. TMX x T	-84.84	-136.0 to -33.70	Yes	****
WT x TCQ vs. TMX x TCQ	-17.17	-68.31 to 33.97	No	ns
WT x TCQ vs. MDA x T	-14.52	-65.66 to 36.63	No	ns
WT x TCQ vs. MDA x TCQ	-34.23	-85.38 to 16.91	No	ns
TMX x T vs. TMX x TCQ	67.67	21.93 to 113.4	Yes	***
TMX x T vs. MDA x T	70.33	24.58 to 116.1	Yes	***
TMX x T vs. MDA x TCQ	50.61	4.865 to 96.35	Yes	*
TMX x TCQ vs. MDA x T	2.655	-43.09 to 48.40	No	ns
TMX x TCQ vs. MDA x TCQ	-17.06	-62.80 to 28.68	No	ns
MDA x T vs. MDA x TCQ	-19.72	-65.46 to 26.03	No	ns
22				
WT x T vs. WT x TCQ	41.62	-4.122 to 87.36	No	ns
WT x T vs. TMX x T	36.11	-9.630 to 81.86	No	ns
WT x T vs. TMX x TCQ	43.14	-2.602 to 88.88	No	ns
WT x T vs. MDA x T	38.06	-7.687 to 83.80	No	ns
WT x T vs. MDA x TCQ	17.16	-28.58 to 62.91	No	ns
WT x TCQ vs. TMX x T	-5.509	-51.25 to 40.23	No	ns
WT x TCQ vs. TMX x TCQ	1.520	-44.22 to 47.26	No	ns
WT x TCQ vs. MDA x T	-3.566	-49.31 to 42.18	No	ns
WT x TCQ vs. MDA x TCQ	-24.46	-70.20 to 21.28	No	ns
TMX x T vs. TMX x TCQ	7.028	-38.71 to 52.77	No	ns
TMX x T vs. MDA x T	1.943	-43.80 to 47.69	No	ns
TMX x T vs. MDA x TCQ	-18.95	-64.69 to 26.79	No	ns
TMX x TCQ vs. MDA x T	-5.085	-50.83 to 40.66	No	ns
TMX x TCQ vs. MDA x TCQ	-25.98	-71.72 to 19.76	No	ns
MDA x T vs. MDA x TCQ	-20.89	-66.64 to 24.85	No	ns

24				
WT x T vs. WTxTCQ	29.53	-35.16 to 94.22	No	ns
WT x T vs. TMX x T	31.07	-14.67 to 76.81	No	ns
WT x T vs. TMX x TCQ	35.16	-10.59 to 80.90	No	ns
WT x T vs. MDA x T	30.52	-15.23 to 76.26	No	ns
WT x T vs. MDA x TCQ	22.85	-22.89 to 68.59	No	ns
WTxTCQ vs. TMX x T	1.543	-63.15 to 66.23	No	ns
WTxTCQ vs. TMX x TCQ	5.629	-59.06 to 70.32	No	ns
WTxTCQ vs. MDA x T	0.9882	-63.70 to 65.68	No	ns
WTxTCQ vs. MDA x TCQ	-6.677	-71.37 to 58.01	No	ns
TMX x T vs. TMX x TCQ	4.087	-41.66 to 49.83	No	ns
TMX x T vs. MDA x T	-0.5544	-46.30 to 45.19	No	ns
TMX x T vs. MDA x TCQ	-8.220	-53.96 to 37.52	No	ns
TMX x TCQ vs. MDA x T	-4.641	-50.38 to 41.10	No	ns
TMX x TCQ vs. MDA x TCQ	-12.31	-58.05 to 33.44	No	ns
MDA x T vs. MDA x TCQ	-7.665	-53.41 to 38.08	No	ns
26				
WT x T vs. WTxTCQ	2.217	-48.92 to 53.36	No	ns
WT x T vs. TMX x T	19.56	-26.18 to 65.30	No	ns
WT x T vs. TMX x TCQ	23.64	-22.10 to 69.39	No	ns
WT x T vs. MDA x T	19.24	-26.50 to 64.98	No	ns
WT x T vs. MDA x TCQ	13.16	-32.58 to 58.90	No	ns
WTxTCQ vs. TMX x T	17.34	-33.80 to 68.48	No	ns
WTxTCQ vs. TMX x TCQ	21.43	-29.71 to 72.57	No	ns
WTxTCQ vs. MDA x T	17.02	-34.12 to 68.16	No	ns
WTxTCQ vs. MDA x TCQ	10.94	-40.20 to 62.08	No	ns
TMX x T vs. TMX x TCQ	4.087	-41.66 to 49.83	No	ns
TMX x T vs. MDA x T	-0.3187	-46.06 to 45.42	No	ns
TMX x T vs. MDA x TCQ	-6.399	-52.14 to 39.34	No	ns
TMX x TCQ vs. MDA x T	-4.405	-50.15 to 41.34	No	ns
TMX x TCQ vs. MDA x TCQ	-10.49	-56.23 to 35.26	No	ns
MDA x T vs. MDA x TCQ	-6.080	-51.82 to 39.66	No	ns
28				
WT x T vs. WTxTCQ	29.44	-35.25 to 94.13	No	ns
WT x T vs. TMX x T	35.07	-10.67 to 80.81	No	ns
WT x T vs. TMX x TCQ	35.07	-10.67 to 80.81	No	ns
WT x T vs. MDA x T	35.66	-10.09 to 81.40	No	ns
WT x T vs. MDA x TCQ	35.07	-10.67 to 80.81	No	ns
WTxTCQ vs. TMX x T	5.629	-59.06 to 70.32	No	ns
WTxTCQ vs. TMX x TCQ	5.629	-59.06 to 70.32	No	ns
WTxTCQ vs. MDA x T	6.217	-58.47 to 70.91	No	ns
WTxTCQ vs. MDA x TCQ	5.629	-59.06 to 70.32	No	ns
TMX x T vs. TMX x TCQ	0.0	-45.74 to 45.74	No	ns
TMX x T vs. MDA x T	0.5881	-45.15 to 46.33	No	ns
TMX x T vs. MDA x TCQ	0.0	-45.74 to 45.74	No	ns
TMX x TCQ vs. MDA x T	0.5881	-45.15 to 46.33	No	ns
TMX x TCQ vs. MDA x TCQ	0.0	-45.74 to 45.74	No	ns
MDA x T vs. MDA x TCQ	-0.5881	-46.33 to 45.15	No	ns

7.5 Appendix 4: Annexin V Standard Curve



7.6 Preliminary Combination Graphs

MCF-7 WT with Tamoxifen combined with 10, 20, 30 and 40 μ M of CQ independently

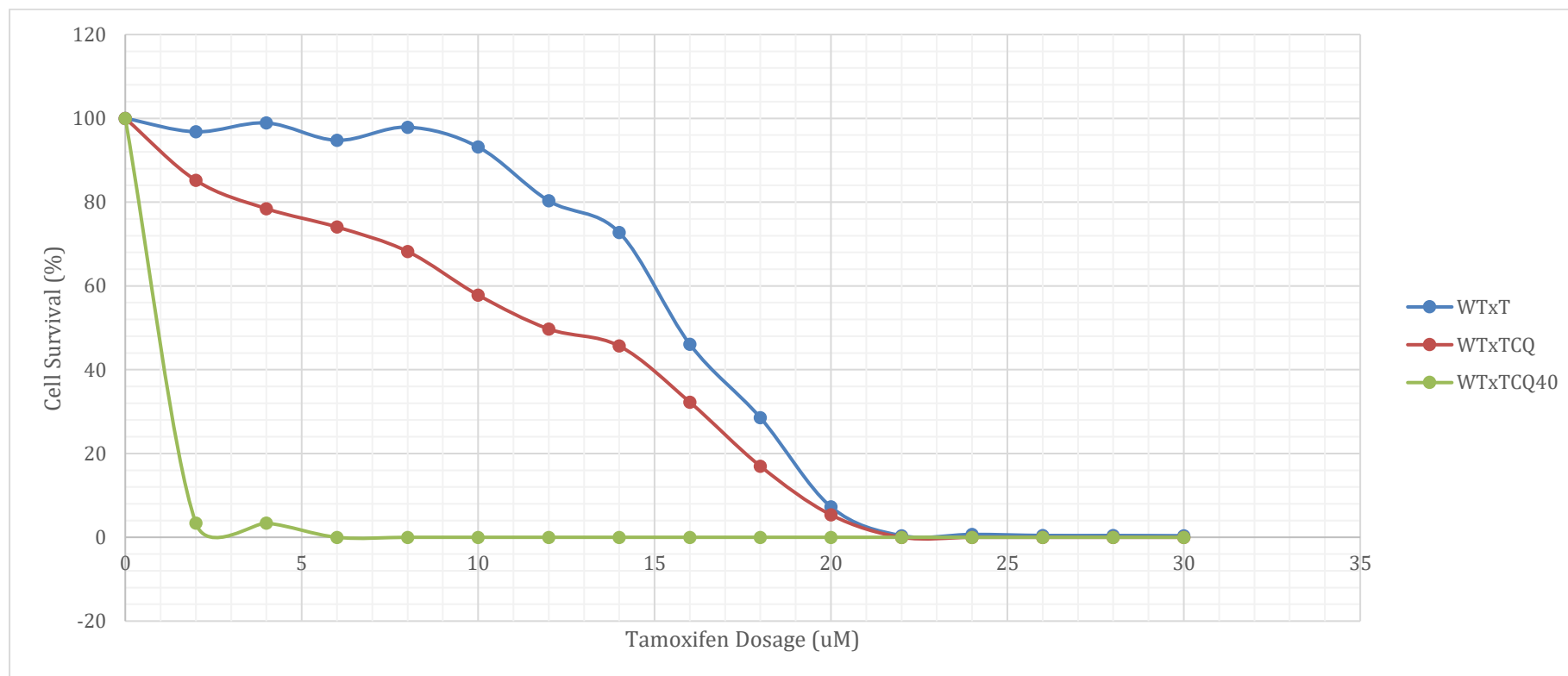


Figure 7.1: MTT cytotoxicity assay highlighting the difference in response in the combined effect of tamoxifen and chloroquine on MCF-7 WT with different doses of chloroquine (\pm SE, $n=3$). WTxT – No CQ, WTxTCQ – 10 μ M CQ, WTxTCQ40 – 40 μ M CQ. The ED_{50} concentrations read at 16 μ M of tamoxifen for WTxT, 12 μ M for WTxTCQ and 1 μ M for WTxTCQ40.

MTT MCF-7 TMX with Tamoxifen combined with 10, 20, 30 and 40µM of CQ independently

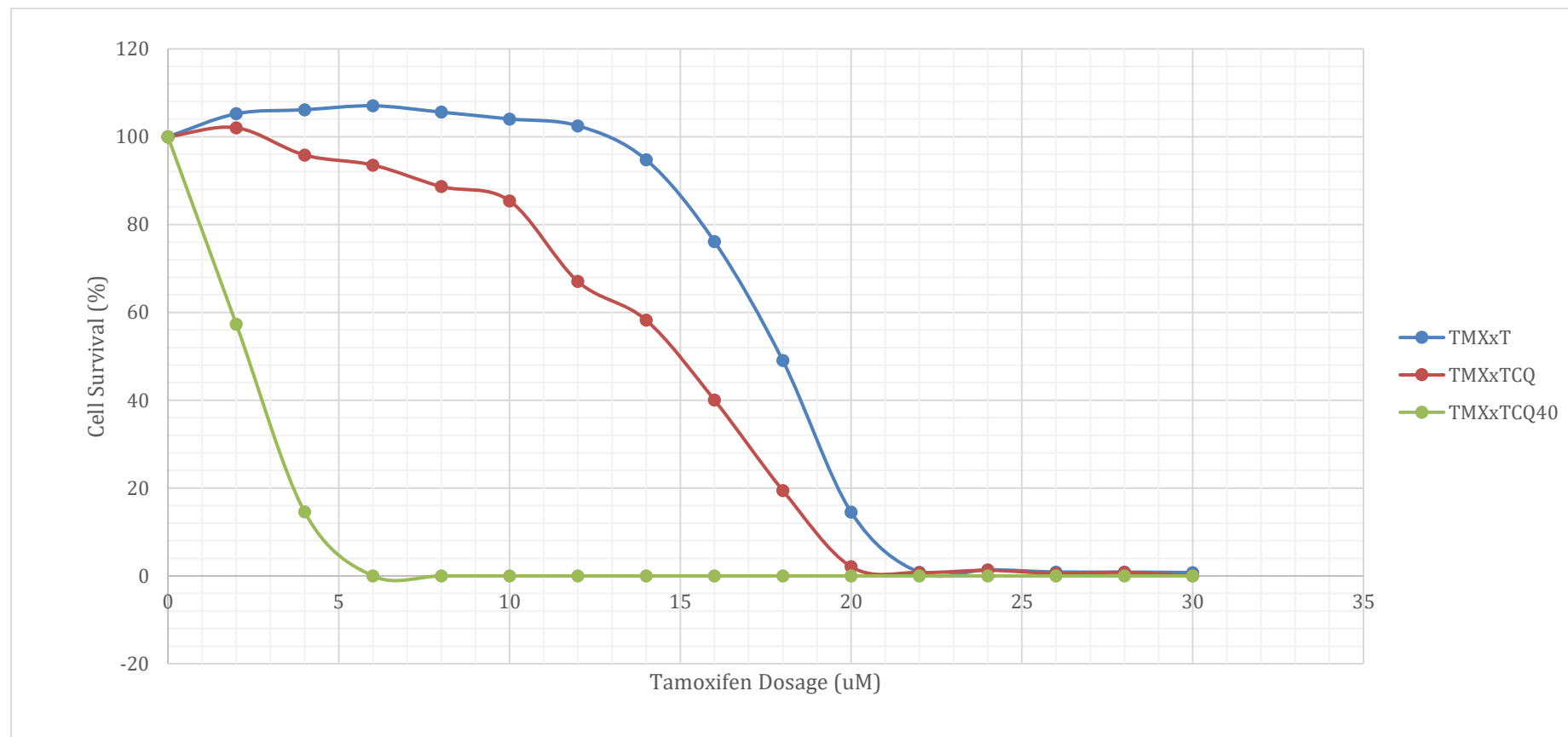


Figure 7.2: MTT cytotoxicity assay highlighting the difference in response in the combined effect of tamoxifen and chloroquine on MCF-7 TMX with different doses of Chloroquine (\pm SE, $n=3$). WTxT – No CQ, WTxTCQ – 10µM CQ, WTxTCQ40 – 40µM CQ. The ED_{50} concentration reads at 18µM of tamoxifen for TMXxT, 15µM for TMXxTCQ and 2.5µM for TMXxTCQ40.

MTT MDA-MB-231 with Tamoxifen combined with 10, 20, 30 and 40 μ M of CQ independently

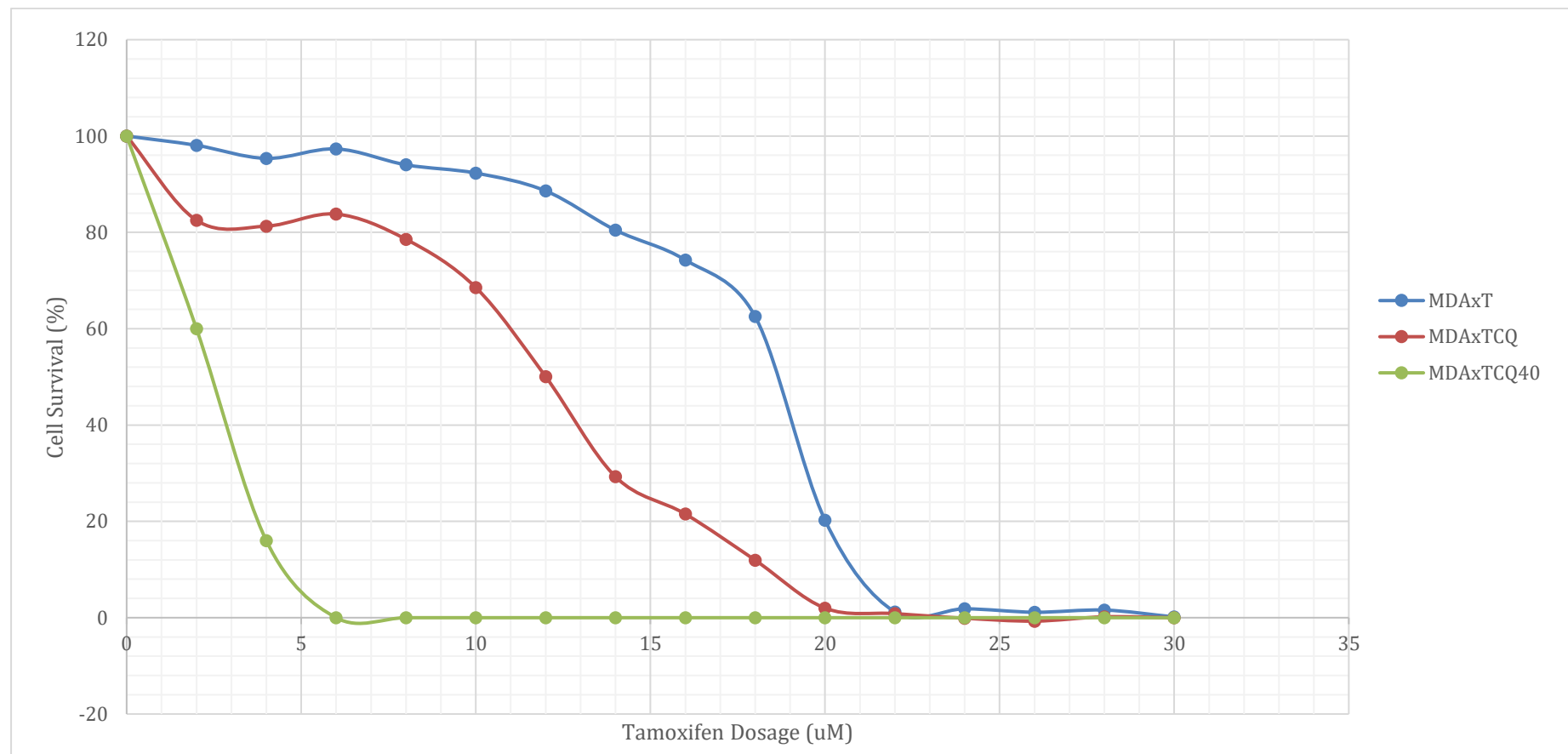


Figure 7.3: MTT cytotoxicity assay highlighting the difference in response in the combined effect of tamoxifen and chloroquine on MDA-MB-231 with different doses of Chloroquine. WTxT – No CQ, WTxTCQ – 10 μ M CQ, WTxTCQ40 – 40 μ M CQ. The ED_{50} concentration reads at 19 μ M of tamoxifen for MDAxT, 12 μ M for MDAxTCQ and 2.5 μ M for MDAxTCQ40.